Bathina, Chandra Sekhar, Role of catecholaminergic A2 neurons of nucleus of the solitary tract (NTS) in cardiovascular and respiratory adaptations to chronic intermittent hypoxia (CIH) in rats

Doctor of Philosophy (Biomedical Sciences), April 2014, 171 pp. , 3 tables, 28 figures, 211 references.

This study examined the role played by the catecholaminergic A2 neurons of the nucleus of the solitary tract (NTS) of adult male Sprague- Dawley rats in the increased mean arterial pressure (MAP) noticed following exposure to chronic intermittent hypoxia (CIH), a rodent model to simulate arterial hypoxemic conditions occurring in humans suffering from sleep apnea. In one study, we tested the hypothesis that tyrosine hydroxylase (TH) knockdown in NTS reduces the sustained elevation in MAP noticed in the rats exposed to CIH. Adult male Sprague-Dawley rats were implanted with radiotelemetry transmitters and adeno-associated viral constructs with a GFP reporter having either short hairpin RNA for TH (shRNA) or scrambled virus (scrambled) were injected into caudal NTS. shRNA through formation of RNA-induced silencing complex reduced the amount of TH levels in the NTS. Virus injected rats were exposed to 7 days CIH (alternating 6 min periods of 10% O2 and 4 min of 21% O2 from 8am to 4pm; from 4pm to 8am rats were exposed to 21% O2). CIH increased MAP and HR during the day in both the scrambled (n= 14, p<.001 MAP; p<.001HR) and shRNA (n=13, p<.001 MAP; p<.001 HR) groups. During the night MAP and HR remained elevated in the scrambled rats (p<0.001 MAP; p<0.001 HR) but not in the shRNA group. The number of TH-immunoreactive neurons was reduced by 20% in sections with GFP fluorescence; shRNA 28±1 cells/section compared to scrambled 35±1

cells/section (p=.005) without altering the number of dopamine β-hydroxylase (DBH) – immunoreactive neurons; shRNA 45±3 cells/section compared to scrambled 45±3 cells/section. Western blot analysis showed a reduction in TH protein levels of 30% and 10% in caudal and sub-postremal NTS respectively. Exposure to CIH increased MAP that persisted beyond the period of exposure to CIH. Knockdown of TH in the NTS reduces this persistent increase in MAP induced by exposure to CIH. This indicates that NTS A2 neurons play a role in the cardiovascular responses to CIH and suggests they may play a similar role in the pathology of sleep apnea in humans.

Experiments were also conducted to understand the molecular level changes occurring in the A2 neurons, following CIH exposure. mRNA expression changes occurring in the A2 neurons were analyzed by novel technique of laser capture microdissection (LCM) by labeling the A2 neurons using adeno-associated virus with TH promoter attached to green fluorescent protein (GFP). A2 neurons are found to express mRNA of angiotensin receptor subtypes AT1a and AT1b. Moreover, excitatory amino acids (EAAs) like glutamate released from chemoreceptor afferents during chronic intermittent hypoxia (CIH) are found to modulate the activity of the neurons in the region of NTS. The aim of this study was to assess the effect of CIH on the mRNA expression levels of AT1a, AT1b and EAAs receptor subunits in the A2 neurons. We utilized commercially available adeno associated virus (AAV) vector mediated delivery of green fluorescent protein (GFP) labeled tyrosine hydroxylase promoter (AAV-GFP-TH), which will incorporate into the TH genome and express GFP with the TH expression to label the A2 neurons. 7 virus injected rats were exposed to 7 days CIH (alternating 6 min periods of 10% O2 and 4 min of 21% O2 from 8am to 4pm; from 4pm to 8am rats were exposed to 21% O2). Laser capture microdissection was performed to capture the A2 neurons from caudal NTS. Total RNA

from these neurons was extracted and the gene expression for different genes were assessed by quantitative real time reverse transcription polymerase chain reaction and compared between the control and CIH rats using $2^{-\Delta\Delta ct}$ method. CIH is found to decrease AT1a ($p=0.002$; control - 1.08 ± 0.13, n=7; CIH – 0.48 ± 0.07, n= 6) and α-amino-3-hydroxy-5-methyl-4-isoxazolepropionate receptor (AMPA) receptor subunit GluR2 ($p=0.03$; control - 1.11 ± 0.24, n=7; CIH- 0.52 ± 0.12, n= 6) and increase transcription factor FosB ($p=0.03$; control - 1.14 ± 0.25, n=7; CIH- 1.97 ± 0.25, n= 5) mRNA expression levels in the A2 neurons. These results suggests that there is increase in activity of these neurons following CIH and a possibility of these neurons becoming more calcium permeable as GluR2 is found to resist calcium permeability. Western blot studies were also conducted from the whole NTS punches, to study the changes in protein levels of the genes studied using LCM. The changes in TH protein levels were not significant in both caudal and sub-postremal NTS ($P > 0.05$). GluR1 and GluR2 protein level changes were not significant in the caudal NTS, however, there was a significant decrease ($P < 0.05$) in GluR1 protein levels and significant increase ($P < 0.05$) in GluR2 protein levels in sub-postremal NTS

As the mRNA analysis of A2 neurons suggested, there might be changes occurring in the calcium permeability of A2 neurons following CIH, attempts were made to do calcium imaging studies on the A2 neurons. There was difficulty in the colocalization of GFP with the fura-2AM, the calcium imaging dye. So, calcium imaging was conducted on the NTS neurons of sham Sprague-Dawley rats and CIH exposed rats. 30 μM AMPA application caused a 340/380 ratio change of 0.17 ± 0.01 (n=5) in control rats and this change was significantly higher 0.55 ± 0.13 in CIH rats. The probability of neurons responding to AMPA application was considerably higher in CIH rats. CNQX treatment of the slices abolished the changes in intracellular calcium in neurons from both control and CIH rats, demonstrating that the responses noticed after AMPA

application were AMPA receptor mediated. Increases in intracellular calcium levels following 500 μM potassium chloride applications validate the fact that the neurons were viable. Further studies on quantifying the phosphorylated GluR1 and GluR2, subunits of AMPA receptors are required to explain the driving force behind this uniform increase in intracellular calcium levels of NTS neurons after CIH.

We conclude that the sustained hypertension observed during CIH can be prevented by TH knockdown and this mechanism might involve paraventricular nucleus (PVN) of forebrain, hypothalamo-pituitary adrenal axis (HPA axis) or intermediolateral cell column (IML) of spinal cord. A2 neurons also undergo molecular alterations that might increase their calcium influx in to the neuron and vise-versa.

ROLE OF CATECHOLAMINERGIC A2 NEURONS OF NUCLEUS OF THE SOLITARY TRACT (NTS) IN CARDIOVASCULAR AND RESPIRATORY ADAPTATIONS TO CHRONIC INTERMITTENT HYPOXIA (CIH) IN RATS

DISSERTATION

Presented to the Graduate Council of the

University of North Texas Health Science Center at Fort Worth

In Partial Fulfillment of the Requirements

For the Degree of

DOCTOR OF PHILOSOPHY

By

Chandra Sekhar Bathina, B.V.Sc., M.S

Fort Worth, Texas

April 2014

ABSTRACT

Obstructive sleep apnea is an increasingly recognized cause of cardiovascular disease. Repetitive, periodic cessation of breathing can lead to high blood pressure, daytime sleepiness and behavioral problems. To examine possible mechanisms that produce the high blood pressure, an animal model was used that mimics the pathology observed in sleep apnea patients. Rats were exposed to repeated periods of low oxygen (3 min of 10% O2 over a period of 10 min cycle and 21% O2 for the rest of the 10 min, 8 hours a day for 7 days) during the period of the day when the rats are asleep (8am - 4pm); Investigations have shown that a group of catecholaminergic neurons (A2) in a specific region of brain (NTS) are excited during hypoxia and play an important role in blood pressure regulation. Specific Aim 1: Viral construct were injected into the brain to decrease the activity of tyrosine hydroxylase (TH) in the A2 neurons. Blood pressure, heart rate, activity and respiratory frequency were measured to determine the role of the A2 neurons in driving the sustained increase in blood pressure following exposure to repeated periods of low oxygen. CIH increased MAP and HR during the day in both the scRNA (n= 14, $p<.001$ MAP; $p<.001$HR) and shRNA (n=13, $p<.001$ MAP; $p<.001$ HR) groups. During the night MAP and HR remained elevated in the scrambled rats ($p<0.001$ MAP; $p<0.001$ HR) but not in the shRNA group. Specific Aim 2: Viral constructs were injected into the rat's brain which labeled these A2 neurons and enabled their identification without immunohistochemistry. Using a laser capture instrument, only the labeled (A2) neurons were captured to perform RNA analyses to understand the molecular changes occurring in these neurons following exposure to repeated low oxygen levels. CIH is found to decrease AT1a ($p=0.002$; control - 1.08 ± 0.13, n=7; CIH – 0.48 ± 0.07, n= 6) and AMPA receptor subunit GluR2 ($p=0.03$; control - 1.11 ± 0.24, n=7; CIH- 0.52 ± 0.12, n= 6) and increase transcription factor FosB ($p=0.03$; control - 1.14 ± 0.25,

n=7; CIH- 1.97 ± 0.25, n= 5) mRNA. Specific Aim 3: Changes in the calcium levels of NTS neurons of rats exposed to periods of low oxygen were compared with that of the controls which are provided with room air. 30 μM AMPA application caused a 340/380 ratio change of 0.17 ± 0.01 (n=5) in control rats and this change was significantly higher 0.55 ± 0.13 in CIH rats. The probability of neurons responding to AMPA application was considerably higher in CIH rats. These results suggest that the A2 neurons might be undergoing molecular adaptations to play an important role in the sustained hypertension during CIH and the NTS neurons could display an increased intracellular calcium levels to cause molecular adaptations that could result in hypertension seen in CIH rats.

The project starts with a study in conscious animals (blood pressure, HR and RR) in Specific Aim 1 followed by a sub-cellular study (RNA analysis) in the Specific Aim 2 and ends with cellular level study (calcium level changes) in Specific Aim 3. The results of this project provided a better understanding of the mechanisms behind increased blood pressure in low oxygen supplied animals and sleep apnea patients.

ACKNOWLEDGEMENTS

I would never have completed my dissertation without the guidance of my major professor, committee members, help from friends and support from my family and wife.

I would like to express my deepest gratitude to my advisor, Dr. Steve Mifflin, for his excellent guidance, caring, patience and providing me with a good research environment. It is his intelligent advising that developed me into an independent researcher. It is my wish to carry forward at least part of his intellectual spirit in my future research endeavors. I sincerely thank my committee members Drs. Tom Cunningham, Ann Schreihofer, Rong Ma, Joseph Yuan and my university member Dr. Porunelloor Mathew for their invaluable suggestions and constructive criticism. I would particularly like to thank, Dr. Prashant Nedungadi, who taught me the way of research thinking and troubleshooting. I am indebted to the department of Integrative Physiology which has provided me the esteemed opportunity to be in the company of great researchers and scholars. I thank all the professors of this great department for their valuable lectures and seminars; those were all a wealth of knowledge and experience.

Over the years of my research in the lab, I had the company of some great people to work with; Mayurika, Kenta, Michelle, Yun, Qiong, Ashwini, Arthur, Annie, Melissa, Wendy and Joel, thank you all. Special thanks to Michelle for performing telemetry surgeries and Arthur for taking care of gas cylinders for my experiments.

“Behind every successful man there will be a woman”; I don’t know about others but, it is true in my case. I owe everything to my sweet wife, Anuradha who also helped me professionally by performing many experiments in this dissertation. She was always there cheering me up and stood by me through the good times and bad.

I am very indebted and thankful to my brother, Sudhakar Bathina, my mother Sai kumari Nimmagadda and my sister-in-law, Lakshmi Malladi for their never ending love and affection. What I have become today would not have been possible if not for their support.

I owe my deepest gratitude to all the rats that were part of this study. This research is funded by National institute of Health HL-088052

“I would like to dedicate this work to my wife, Anuradha and our little champion, who will arrive in June”.

ABBREVIATIONS

AAV	Adeno-associated virus
AMPA	α-amino-3-hydroxy-5-methyl-4-isoxazolepropionate
CIH	Chronic intermittent hypoxia
CPAP	Continuous positive airway pressure
CR	Chemoreceptors
EAA	Excitatory amino acid
GFP	Green fluorescent protein
HR	Heart rate
HPA	Hypothalamo-pituitary adrenal
IML	Intermediolateral cell column
LCM	Laser capture microdissection
MAP	Mean arterial pressure
NMDA	N-methyl D-aspartate
NTS	Nucleus of the solitary tract
OSA	Obstructive sleep apnea
PVN	Paraventricular nucleus
RF	Respiratory frequency
RVLM	Rostral ventro-lateral medulla
SNA	Sympathetic nerve activity
shRNA	Short hair-pin RNA
scRNA	Scrambled RNA
TH	Tyrosine hydroxylase

PUBLICATIONS

Koneru B*, **Bathina CS*,** Cherry B, Franzke M and Mifflin SW. Mineralocorticoid receptor in the nucleus of the solitary tract stimulates salt intake during 4th ventricular infusions of aldosterone **Am J Physiol Regul Integr Comp Physiol (* indicates co-first author).** 2013 Nov 20. PMID: 24259463

Bathina CS, Rajulapati A, Franzke M and Mifflin SW. Knockdown of tyrosine hydroxylase in the nucleus of the solitary tract reduces elevated blood pressure during chronic intermittent hypoxia. **Am J Physiol Regul Integr Comp Physiol.** 2013 Sep 18. PMID: 24049117

Nedungadi TP, Dutta M, **Bathina CS**, Caterina MJ and Cunningham JT. Expression and Distribution of TRPV2 in Rat Brain. **Exp Neurol**. 2012 Sep;237(1):223-37. 2012 PMID: 22750329

Nedungadi TP, Carreno FR, Walch JD, **Bathina CS** and Cunningham JT. Increased TRPV channel expression in the vasopressin magnocellular system in hepatic cirrhosis induced hyponatremia. **Journal of Neuroendocrinology**. 2011(*Accepted 17 Dec 2011*). PMID:22188460

Bathina CS, Rajulapati A, Nedungadi TP and Mifflin SW. laser capture microdissection reveals alterations in mRNA levels in NTS A2 neurons following exposure to chronic intermittent hypoxia. To be submitted to Am J Physiol Regul Integr Comp Physiol.

Nedungadi TP, **Bathina CS** and Mifflin SW. Knockdown of tyrosine hydroxylase in the nucleus of the solitary tract prevents attenuated body weight gain and blunts neuronal activation in the hypothalamus following chronic intermittent hypoxia (in preparation).

PRESENTATIONS AND ABSTRACTS

Oral Presentations

Bathina CS, Rajulapati A, Franzke M, Yamamoto K and Mifflin SW**.** Role of Catecholaminergic A2 neurons of nucleus of the solitary tract (NTS) in cardiovascular and respiratory adaptations to chronic intermittent hypoxia (CIH) in rats. Featured Topic: Neural Mechanisms In Cardiovascular Regulation, FASEB 2013, Gleneden Beach, OR

Nedungadi TP, **Bathina CS**, Mifflin SW and Cunningham JT. Role of hypothalamic peptides in chronic intermittent hypoxia associated metabolic dysfunction. Featured Topic: Neural Mechanisms In Cardiovascular Regulation, FASEB 2013, Gleneden Beach, OR

Bathina CS, Rajulapati A, Franzke M, Kenta Yamamoto, Tom Cunningham and Mifflin SW. Knockdown of tyrosine hydroxylase in the nucleus of the solitary tract reduces elevated blood pressure during chronic intermittent hypoxia. Invited talk; Featured Topic: Central Nervous System Modulation of Cardiorespiratory Responses to Hypoxia, EB 2013, Boston, MA.

Abstracts

Nedungadi TP*, **Bathina CS*** and Mifflin SW. Knockdown of tyrosine hydroxylase in the nucleus of the solitary tract prevents attenuated body weight gain and blunts neuronal activation in the hypothalamus following chronic intermittent hypoxia. Submitted to FASEB 2014, San Diego, CA.

Bathina CS, Rajulapati A, Franzke M, Yamamoto K and Mifflin SW**.** Role of Catecholaminergic A2 neurons of nucleus of the solitary tract (NTS) in cardiovascular and respiratory adaptations to chronic intermittent hypoxia (CIH) in rats. Neural Mechanisms In Cardiovascular Regulation, FASEB 2013, Gleneden Beach, OR

Nedungadi TP, **Bathina CS**, Mifflin SW and Cunningham JT. Role of hypothalamic peptides in chronic intermittent hypoxia associated metabolic dysfunction. Featured Topic: Neural Mechanisms In Cardiovascular Regulation, FASEB 2013, Gleneden Beach, OR

Nedungadi TP, **Bathina CS**, Kenta Yamamoto, Mifflin SW and Cunningham JT. Metabolic dysfunction in chronic intermittent hypoxia – role of hypothalamic peptides. Experimental Biology 2013, Boston, MA.

Bathina CS, Rajulapati A, Franzke M and Mifflin SW. Knockdown of tyrosine hydroxylase in the nucleus of the solitary tract reduces elevated blood pressure during chronic intermittent hypoxia. Experimental Biology 2013, Boston, MA.

Bathina CS, Rajulapati A and Mifflin SW. Angiotensin receptor subtype AT1a and AMPA receptor subunit GluR2 mRNA levels are reduced in A2 neurons of nucleus of the solitary tract following chronic intermittent hypoxia. Experimental Biology 2013, Boston, MA.

Yamamoto K, **Bathina CS**, Rajulapati A, Franzke M and Mifflin SW. Acute intermittent optogenetic stimulation of glutamatergic NTS neurons induces sympathetic long-term facilitation. Experimental Biology 2013, Boston, MA.

Koneru B*, **Bathina CS***, Cherry B, Franzke M and Mifflin SW. Mineralocorticoid receptor in the nucleus of the solitary tract stimulates salt intake during 4th ventricular infusions of aldosterone. **(* indicates co-first author)** Experimental Biology 2013, Boston, MA.

Bathina CS, Rajulapati A, Franzke M and Mifflin SW. Knockdown of tyrosine hydroxylase in the nucleus of the solitary tract reduces elevated blood pressure during chronic intermittent hypoxia. High Blood Pressure Council Research, Washington DC, 2012.

Koneru B*, **Bathina CS*,** Cherry B, Franzke M and Mifflin SW. Mineralocorticoid receptor in the nucleus of the solitary tract stimulates salt intake during 4th ventricular infusions of aldosterone **(* indicates co-first author)** High Blood Pressure Council Research, Washington DC, 2012.

Bathina CS and Mifflin SW. Adeno-associated virus mediated labeling of catecholaminergic A2 neurons in nucleus of solitary tract (NTS) of rats. Experimental Biology, San Diego, 2012. FASEB Journal.

Nagalla VK, **Bathina CS**, Mifflin SW. A new approach to identify tyrosine hydroxylase expressing neurons in the hindbrain. Research Appreciation Day, UNT Health Science Center, 2012.

Bathina CS, Kenta Yamamoto, Michelle Franzke and Mifflin SW. Effect of tyrosine hydroxylase knockdown in the nucleus of the solitary tract on the elevated blood pressure of rats during chronic intermittent hypoxia. Research Appreciation Day, UNT Health Science Center, 2012.

Bathina CS, Nedungadi TP, Cunningham JT, Mifflin SW. Angiotensin AT1 receptor subtypes AT1A and AT1B mRNAs are expressed in tyrosine hydroxylase immunoreactive (TH-ir) neurons in the rat caudal nucleus of the solitary track (NTS). Experimental Biology, Washington DC, 2011. FASEB Journal.

Bathina CS, Nedungadi TP, Cunningham JT, Mifflin SW. Angiotensin AT1 receptor subtypes AT1A and AT1B mRNAs are expressed in tyrosine hydroxylase immunoreactive (TH-ir) neurons in the rat caudal nucleus of the solitary tract (NTS). Research Appreciation Day, UNT Health Science Center, 2011.

Nedungadi TP, Carreno FR, **Bathina CS**, Walch JD, Niu X, Cunningham JT. Expression and regulation of TRPV2 in rat magnocellular neurosecretory cells. 9th World Congress on Neurohypophysial Hormones (WCNH 2011), Boston, 2011.

Nedungadi TP, Carreno FR, **Bathina CS**, Walch JD, Niu X, Cunningham JT. Expression and Distribution of TRPV2 in rat magnocellular neurosecretory cells. IInd Post-Doctoral Research Appreciation Day. UNT Health Science Center, Fortworth, TX, 2011.

Nedungadi TP, Carreno FR, **Bathina CS,** Niu X, Walch JD, Cunningham JT. Putative role of TRPV2 in central control of body fluid homeostasis. Research Appreciation Day, UNT Health Science Center, 2011.

TABLE OF CONTENTS

LIST OF TABLES

CHAPTER II

CHAPTER III

LIST OF FIGURES

CHAPTER II

Figure

CHAPTER III

Figure

CHAPTER IV

Figure

CHAPTER IV

Figure

APPENDIX A

Figure

CHAPTER I

Introduction

Obstructive sleep apnea (OSA) is characterized by frequent episodes of pause in respiratory airflow produced due to upper airway inspiratory collapse while sleeping, resulting in decreased oxygen saturation and arousal from sleep. OSA severity is quantified as the number of apneic and hypopneic episodes that occur in an hour and 'apnea:hypopnea index' of greater than 30 events per hour is noticed in severe cases (apnea-hypopnea index: 5-15 per hour in mild, 15-30 per hour in moderate and greater than 30 in severe cases) (59). An estimated 15 million Americans suffer from this disorder (77), with increased prevalence of 1.5-3 times more in men than in pre-menopausal women (35). Chemoreceptor activation by the resulting hypoxemia during nocturnal apneic episodes leads to increased sympathetic nerve activity (SNA) which contributes to increased arterial pressure (AP) (29, 65). This elevated SNA and AP persists even during the daytime when the patients are not experiencing apneic episodes (6). Reduction in this elevated SNA and AP upon treatment with continuous positive airway pressure (CPAP) (68, 73) has established the role of OSA as the driving force behind their cause. Adaptations occurring in neurons regulating SNA and AP due to the nighttime intermittent hypoxia might be one potential reason behind the elevated SNA during diurnal normoxia. Increased role of OSA in cardiovascular diseases and its prevalence in patients with insulin resistance, obesity, hypertension and dyslipidemias has led researchers to consider it as an OSA syndrome (10). The mechanism behind increased sympathetic outflow and the associated hypertension in patients of

OSA during wakefulness still remains vague. Neuronal adaptations resulting due to hypoxemic episodes of night are believed to be driving this diurnal AP elevation. The impact of this AP elevation can be understood from the Framingham study (3), which indicates that a decrease in diastolic pressure by 5-6 mmHg can lower the incidence reduces the risk of stroke by 35-40% and the risk of coronary artery disease by 20-25%. Equally important is the increased SNA, which is known to play a key role in insulin resistance, dyslipidemias, cardiac and renal failure (17, 36, 62).

Rodent model of chronic intermittent hypoxia (CIH): In a clinical setting, OSA patients usually present with arterial hypertension accompanied by ailments of metabolic syndrome (10). The initiation factor for this hypertension under OSA condition cannot be completely studied in humans, as patients seek treatment after months or years of OSA. For that reason, different animal models have been used to mimic the hypoxic episodes occurring in humans during OSA (27, 31, 38, 56). We used rodent model to study this CIH associated hypertension (39). In this study, adult male Sprague-Dawley rats were exposed to CIH during their nocturnal periods. CIH consists of alternating periods of 10% O_2 for 3 minutes followed by room air (21% O_2) starting from 8am to 4pm (8 hours) when the rats are asleep. From 4pm the rats are exposed to room air for the remainder of light period and throughout dark period (12hours light: 12 hours dark). Considering the number of hypoxic periods for one hour during CIH, this can be compared to mild level of sleep apnea in humans (59). Rats exposed for 7 days to this CIH protocol display an increase in the AP as seen in human patients of sleep apnea. In addition, the elevation in AP persists even during the dark phase during which rats are exposed to room air. This elevated AP (5-8 mmHg) was consistent with the magnitude fall noticed in the CPAP treated sleep apnea patients (4-10 mmHg) (68, 73). Hypoxia is associated with hypercapnia, during a sleep apneic

episode in humans. However, Fletcher's lab found that the MAP response to CIH was no different when it was associated with hypocapnia, eucapnia or hypercapnia (1). Studies have also shown that this increase in AP following CIH is mediated by elevated SNA (64). It is evident that the repeated hypoxic episodes caused an increased sympathetic outflow contributing to the AP elevation throughout the 24 hour period, as seen in patients with sleep apnea (65). This indicates that our CIH model is a good approach to study the mechanisms underlying elevated AP in OSA.

Role of arterial chemoreceptor activation in CIH induced hypertension: Stimulation of chemoreceptors activates TH-immunoreactive (TH-ir) and non-TH-ir neurons of NTS. Previously, it has been demonstrated that carotid sinus nerves (CSNs) sectioning prior to CIH exposure abolished the blood pressure elevation induced by CIH (19, 37). This emphasizes the essential role of carotid chemoreceptors in CIH induced increase in blood pressure. The arterial chemoreceptors synapse within the NTS (9, 14, 18) .

Neuronal adaptations in NTS: NTS is the primary site for the carotid body chemoreceptor afferent termination (14, 72) and neurons responding to the CR stimulations are found throughout the NTS (43). However, the important region of integration appears to be in the caudal aspects of the NTS, more precisely the commissural region caudal to the calamus scriptorius (43, 44, 57, 76, 80). Moreover, increased expression of transcription factors like c-fos, which is a neuronal marker for activation are demonstrated in this area following CIH (21). NTS neurons are excited by chemoreceptor afferents primarily by excitatory amino acid (EAA) receptors like NMDA (N-methyl D-aspartate) and non-NMDA subtypes (76, 80) along with other transmitter systems resulting in a variety of modulatory influences. The Catecholaminergic A2 neuron cell group is activated during hypoxia (5, 16, 69). Tyrosine hydroxylase (TH) is the

first enzyme in the synthesis of catecholamines and is the rate-limiting enzyme (46). A2 neurons are marked by the expression of TH (28).. Further, researchers have shown that chronic hypoxia increased TH expression within the A2 cell group (15, 67) and this increase was abolished after CSN sectioning (66). Therefore, the variations in TH expression observed in A2 group are not direct effects of tissue hypoxia, but are afferent chemoreceptor fiber mediated. Studies involving pharmacological reduction of central catecholamines did not affect ventilatory acclimatizations to hypoxia (42), suggesting the involvement of TH changes in the A2 group in non-respiratory components of the response to hypoxia. CIH induces changes in the synaptic activation of NTS neurons (32) as well as changes in the responses to exogenous application of AMPA and NMDA (12). However, none of these studies investigated the changes occurring in a specific phenotype of neurons, like A2. Retrograde and anterograde studies have revealed that A2 neurons project to wide array of forebrain nuclei like PVN (20, 58, 61, 75) and median preoptic nucleus (53). Hypoxia is a potent stimulus for the A2 neurons and responds with a variety of mechanisms including changes in ionic conductances, cellular ATP and free radical levels (13, 23, 24, 70) leading to increased firing from these neurons to the barosensitive neurons of RVLM (4, 22, 54) or through hypothalamo-pituitary adrenal axis (HPA) (39, 71) might cause an increased sympathetic nerve activity. Recent studies have found that cardiovascular response to activation of peripheral chemoreceptors is mediated through activation of PVN neurons (52, 55). One of the principal stimuli for PVN neuron activation is the projections from A2 neurons (74). Systemic hypoxia activated chemoreceptor afferents release glutamate at caudal NTS (32, 45) and act through AMPA and NMDA receptors (78-80).

FosB mediated neuronal plasticity: In response to chronic stressful stimuli like hypoxia, neurons exhibit changes in the neuronal function, termed as neuronal plasticity. Studies to

understand these changes in molecular mechanisms have led to the discovery of role played by activator protein 1 (AP-1) family of transcription factors (2, 30). In conditions of acute stress, AP-1 transcription factors are found to modulate gene expression (63). Studies by Nestler's group have shown that chronic stimuli like drug-addiction also modulate gene expression which is AP-1 transcription factor mediated (7, 34, 49). These transcription factors are heterodimeric proteins composed of fos and jun proteins binding to AP-1 regulatory site with sequence TGACTCA or TGACGTCA (25, 30). Several regions of CNS express basal levels of jun proteins (25, 26). Different Fos proteins vary in time course of expression and basal levels in CNS. c-Fos is found to have low basal expression in CNS and shows rapid and transient expression in response to synaptic activation or acute stress (11, 25, 26, 60). Chronic stimulation or stress causes expression of FosB and its more stable splice variant ΔFosB, which have a longer time course and stable expression (25, 41, 48, 51). A recent study from our group has demonstrated that CIH induces increased FosB expression in A2 and non-A2 neurons of NTS (33). Changes in FosB during CIH is an important finding because FosB/ΔFosB has been linked to neuronal adaptations and plasticity under conditions like drug addiction, epilepsy and long-term potentiation (8, 40, 41, 47, 48, 50, 51). This shows that, FosB is expressed in A2 neurons of NTS which are activated due to CIH and could mediate gene expression changes to alter neuronal function. Colocalization of FosB with TH-immunoreactive neurons (TH-ir) and non-TH-ir neurons helps in identifying NTS neurons which respond to CIH.

Based on this background, **we hypothesize that glutamate released from chemoreceptor afferents during CIH on catecholaminergic A2 and non-catecholaminergic neurons of caudal NTS causes intracellular calcium changes that increase their action potential discharge and initiate molecular alterations. This increases excitatory drive to the sites of**

sympatho-regulation like hypothalamic paraventricular nucleus PVN and RVLM contributing to the elevated AP and SNA induced by CIH.

To address the global hypothesis, 3 specific aims were developed to examine the changes occurring at the whole animal level, molecular level and at cellular level.

Specific aim 1: To assess the effect of TH knockdown in the catecholaminergic (A2) neurons on the cardiovascular and respiratory responses to CIH.

Adeno associated viral constructs with short hair-pin RNA for TH (AAV-TH-shRNA) were microinjected into the rat's caudal NTS region to suppress TH expression. All rats were telemetry instrumented to record blood pressures upon exposure to CIH and the respective controls under normoxia. **We hypothesized that TH knockdown would decrease the CIH induced sustained elevation in blood pressure.**

Specific aim 2: To determine the effect of CIH on the gene and protein expression of TH and glutamate receptor subunits in catecholaminergic (A2) neurons

We injected (AAV-GFP-TH promoter) to label the (A2) neurons of NTS, followed by laser capture microdissection (LCM) of only the labeled neurons to analyze for the gene and protein expression of respective genes under control and CIH conditions. **We hypothesized that CIH would induce an increase in the levels of TH and glutamate receptor subunits mRNA.**

Specific aim 3: To evaluate the changes in AMPA induced increase of intracellular calcium levels in NTS neurons following exposure to CIH.

Neurons in caudal NTS region of adult Sprague-Dawley rats were studied in an in vitro brain slice preparation for fura-2AM mediated calcium imaging in presence of AMPA. **We**

hypothesized that AMPA receptor mediated increase in intracellular calcium levels is enhanced in CIH exposed rats.

Summary of Results from Specific aims

The first specific aim was to determine the effect of TH knockdown on the sustained hypertension noticed in rats during CIH. AAV- TH - shRNA successfully reduced the TH-ir and TH protein levels in the NTS. TH knockdown abolished the sustained hypertension during the normoxic phase of CIH. The sustained elevation in the respiratory rate during the normoxic phase was also abolished by TH knockdown. FosB – ir was studied in the PVN and RVLM, to understand the upstream pathways that might lead to these changes to happen. PVN displayed a significant reduction in the FosB – ir, however, there was no change in the FosB –ir of RVLM. Therefore, it is concluded that A2 neurons contribute to the sustained hypertension part of CIH induced elevation in mean arterial pressure (MAP) through hypothalamo – pituitary adrenal axis or through intermediolateral cell column of spinal cord.

The second specific aim concentrated on the molecular changes that occur in the A2 neurons during CIH, which might lead to the sustained elevation in MAP. AAV – GFP – TH efficiently labeled the A2 neurons. Laser capture microdissection of the GFP labeled A2 neurons was successfully performed. A2 neurons displayed a significant reduction in the mRNA levels of AMPA receptor subunit GluR2 and angiotensin receptor subtype AT1A in CIH rats. FosB mRNA levels increased in the A2 neurons from CIH rats. No changes were noticed in the mRNA levels of TH and NMDA receptor subunits. Protein analysis from whole NTS punches showed that GluR1 levels decrease and GluR2 levels increase in CIH rats. These changes at molecular level made us conclude that A2 neurons might display an increase in intracellular calcium levels during CIH.

The third specific aim was to evaluate the increase in intracellular calcium levels of NTS neurons following CIH. 2nd specific aim made us hypothesize that A2 neurons might show an increase in intracellular calcium levels whereas the adjacent neurons of NTS might show a lower calcium influx in to the cell. However, GFP labeling appears to have hindered the fura uptake or into the neurons. Calcium imaging of the NTS neurons showed a higher calcium influx to AMPA in neurons from CIH rats, compared to neurons from control rats. Antagonist treatment of the slices abolished the calcium influx into the neurons. We conclude that NTS neurons display an increased calcium influx upon AMPA application and this influx is further enhanced in CIH rats. Further studies to quantify the posttranslational modifications in AMPA receptor subunits might explain the mechanism behind this increase in calcium influx in all the NTS neurons.

Significance and clinical relevance

This study shows that sustained hypertension during CIH can be abolished by just TH knockdown in A2 neurons rather than killing them. This is the first time that gene alterations occurring in a phenotypically defined neuronal population of NTS have been studied following CIH. Information from this study had lead to further understand the mechanism and role of A2 neurons in sustained hypertension during CIH which could result in a possible treatment for OSA patients.

References

1. **Bao G, Randhawa PM, and Fletcher EC**. Acute blood pressure elevation during repetitive hypocapnic and eucapnic hypoxia in rats. *J Appl Physiol* 82: 1071-1078, 1997.

2. **Baum MJ, Brown JJ, Kica E, Rubin BS, Johnson RS, and Papaioannou VE**. Effect of a null mutation of the c-fos proto-oncogene on sexual behavior of male mice. *Biol Reprod* 50: 1040-1048, 1994.

3. **Benjamin EJ, Wolf PA, D'Agostino RB, Silbershatz H, Kannel WB, and Levy D**. Impact of atrial fibrillation on the risk of death: the Framingham Heart Study. *Circulation* 98: 946-952, 1998.

4. **Blessing WW, Yu Y, and Nalivaiko E**. Medullary projections of rabbit carotid sinus nerve. *Brain Res* 816: 405-410, 1999.

5. **Buller KM, Smith DW, and Day TA**. NTS catecholamine cell recruitment by hemorrhage and hypoxia. *Neuroreport* 10: 3853-3856, 1999.

6. **Carlson JT, Hedner J, Elam M, Ejnell H, Sellgren J, and Wallin BG**. Augmented resting sympathetic activity in awake patients with obstructive sleep apnea. *Chest* 103: 1763-1768, 1993.

7. **Chao J, and Nestler EJ**. Molecular neurobiology of drug addiction. *Annu Rev Med* 55: 113-132, 2004.

8. **Chen J, Zhang Y, Kelz MB, Steffen C, Ang ES, Zeng L, and Nestler EJ**. Induction of cyclin-dependent kinase 5 in the hippocampus by chronic electroconvulsive seizures: role of [Delta]FosB. *J Neurosci* 20: 8965-8971, 2000.

9. **Claps A, and Torrealba F**. The carotid body connections: a WGA-HRP study in the cat. *Brain Res* 455: 123-133, 1988.

10. **Coughlin S, Calverley P, and Wilding J**. Sleep disordered breathing--a new component of syndrome x? *Obes Rev* 2: 267-274, 2001.

11. **Cunningham JT, Penny ML, and Murphy D**. Cardiovascular regulation of supraoptic neurons in the rat: synaptic inputs and cellular signals. *Prog Biophys Mol Biol* 84: 183-196, 2004.

12. **de Paula PM, Tolstykh G, and Mifflin S**. Chronic intermittent hypoxia alters NMDA and AMPA-evoked currents in NTS neurons receiving carotid body chemoreceptor inputs. *Am J Physiol Regul Integr Comp Physiol* 292: R2259-2265, 2007.

13. **Del Negro CA, Koshiya N, Butera RJ, Jr., and Smith JC**. Persistent sodium current, membrane properties and bursting behavior of pre-botzinger complex inspiratory neurons in vitro. *J Neurophysiol* 88: 2242-2250, 2002.

14. **Donoghue S, Felder RB, Jordan D, and Spyer KM**. The central projections of carotid baroreceptors and chemoreceptors in the cat: a neurophysiological study. *J Physiol* 347: 397-409, 1984.

15. **Dumas S, Pequignot JM, Ghilini G, Mallet J, and Denavit-Saubie M**. Plasticity of tyrosine hydroxylase gene expression in the rat nucleus tractus solitarius after ventilatory acclimatization to hypoxia. *Brain Res Mol Brain Res* 40: 188-194, 1996.

16. **Erickson JT, and Millhorn DE**. Hypoxia and electrical stimulation of the carotid sinus nerve induce Fos-like immunoreactivity within catecholaminergic and serotoninergic neurons of the rat brainstem. *J Comp Neurol* 348: 161-182, 1994.

17. **Esler M, Rumantir M, Wiesner G, Kaye D, Hastings J, and Lambert G**. Sympathetic nervous system and insulin resistance: from obesity to diabetes. *Am J Hypertens* 14: 304S-309S, 2001.

18. **Finley JC, and Katz DM**. The central organization of carotid body afferent projections to the brainstem of the rat. *Brain Res* 572: 108-116, 1992.

19. **Fletcher EC, Lesske J, Behm R, Miller CC, 3rd, Stauss H, and Unger T**. Carotid chemoreceptors, systemic blood pressure, and chronic episodic hypoxia mimicking sleep apnea. *J Appl Physiol* 72: 1978-1984, 1992.

20. **Geerling JC, Shin JW, Chimenti PC, and Loewy AD**. Paraventricular hypothalamic nucleus: axonal projections to the brainstem. *J Comp Neurol* 518: 1460-1499, 2010.

21. **Greenberg HE, Sica AL, Scharf SM, and Ruggiero DA**. Expression of c-fos in the rat brainstem after chronic intermittent hypoxia. *Brain Res* 816: 638-645, 1999.

22. **Guyenet PG**. Neural structures that mediate sympathoexcitation during hypoxia. *Respir Physiol* 121: 147-162, 2000.

23. **Haddad GG, and Jiang C**. O2 deprivation in the central nervous system: on mechanisms of neuronal response, differential sensitivity and injury. *Prog Neurobiol* 40: 277-318, 1993.

24. **Hammarstrom AK, and Gage PW**. Hypoxia and persistent sodium current. *Eur Biophys J* 31: 323-330, 2002.

25. **Herdegen T, and Leah JD**. Inducible and constitutive transcription factors in the mammalian nervous system: control of gene expression by Jun, Fos and Krox, and CREB/ATF proteins. *Brain Res Brain Res Rev* 28: 370-490, 1998.

26. **Herdegen T, and Zimmermann M**. Immediate early genes (IEGs) encoding for inducible transcription factors (ITFs) and neuropeptides in the nervous system: functional network for long-term plasticity and pain. *Prog Brain Res* 104: 299-321, 1995.

27. **Iturriaga R, Rey S, and Del Rio R**. Cardiovascular and ventilatory acclimatization induced by chronic intermittent hypoxia: a role for the carotid body in the pathophysiology of sleep apnea. *Biol Res* 38: 335-340, 2005.

28. **Kalia M, Fuxe K, and Goldstein M**. Rat medulla oblongata. II. Dopaminergic, noradrenergic (A1 and A2) and adrenergic neurons, nerve fibers, and presumptive terminal processes. *J Comp Neurol* 233: 308-332, 1985.

29. **Kara T, Narkiewicz K, and Somers VK**. Chemoreflexes--physiology and clinical implications. *Acta Physiol Scand* 177: 377-384, 2003.

30. **Karin M, Liu Z, and Zandi E**. AP-1 function and regulation. *Curr Opin Cell Biol* 9: 240-246, 1997.

31. **Katayama K, Smith CA, Henderson KS, and Dempsey JA**. Chronic intermittent hypoxia increases the CO2 reserve in sleeping dogs. *J Appl Physiol* 103: 1942-1949, 2007.

32. **Kline DD, Ramirez-Navarro A, and Kunze DL**. Adaptive depression in synaptic transmission in the nucleus of the solitary tract after in vivo chronic intermittent hypoxia: evidence for homeostatic plasticity. *J Neurosci* 27: 4663-4673, 2007.

33. **Knight WD, Little JT, Carreno FR, Toney GM, Mifflin SW, and Cunningham JT**. Chronic intermittent hypoxia increases blood pressure and expression of FosB/DeltaFosB in central autonomic regions. *Am J Physiol Regul Integr Comp Physiol* 301: R131-139, 2011.

34. **Koob GF, and Nestler EJ**. The neurobiology of drug addiction. *J Neuropsychiatry Clin Neurosci* 9: 482-497, 1997.

35. **Lee W, Nagubadi S, Kryger MH, and Mokhlesi B**. Epidemiology of Obstructive Sleep Apnea: a Population-based Perspective. *Expert review of respiratory medicine* 2: 349-364, 2008.

36. **Leimbach WN, Jr., Wallin BG, Victor RG, Aylward PE, Sundlof G, and Mark AL**. Direct evidence from intraneural recordings for increased central sympathetic outflow in patients with heart failure. *Circulation* 73: 913-919, 1986.

37. **Lesske J, Fletcher EC, Bao G, and Unger T**. Hypertension caused by chronic intermittent hypoxia--influence of chemoreceptors and sympathetic nervous system. *J Hypertens* 15: 1593-1603, 1997.

38. **Lin M, Ai J, Li L, Huang C, Chapleau MW, Liu R, Gozal D, Wead WB, Wurster RD, and Cheng ZJ**. Structural remodeling of nucleus ambiguus projections to cardiac ganglia following chronic intermittent hypoxia in C57BL/6J mice. *J Comp Neurol* 509: 103-117, 2008.

39. **Ma S, Mifflin SW, Cunningham JT, and Morilak DA**. Chronic intermittent hypoxia sensitizes acute hypothalamic-pituitary-adrenal stress reactivity and Fos induction in the rat locus coeruleus in response to subsequent immobilization stress. *Neuroscience* 154: 1639-1647, 2008.

40. **Madsen TM, Bolwig TG, and Mikkelsen JD**. Differential regulation of c-Fos and FosB in the rat brain after amygdala kindling. *Cell Mol Neurobiol* 26: 87-100, 2006.

41. **McClung CA, Ulery PG, Perrotti LI, Zachariou V, Berton O, and Nestler EJ**. DeltaFosB: a molecular switch for long-term adaptation in the brain. *Brain Res Mol Brain Res* 132: 146-154, 2004.

42. **McCrimmon DR, Dempsey JA, and Olson EB, Jr.** Effect of catecholamine depletion on ventilatory control in unanesthetized normoxic and hypoxic rats. *Journal of applied physiology: respiratory, environmental and exercise physiology* 55: 522-528, 1983.

43. **Mifflin SW**. Arterial chemoreceptor input to nucleus tractus solitarius. *Am J Physiol* 263: R368-375, 1992.

44. **Mifflin SW**. Inhibition of chemoreceptor inputs to nucleus of tractus solitarius neurons during baroreceptor stimulation. *Am J Physiol* 265: R14-20, 1993.

45. **Mizusawa A, Ogawa H, Kikuchi Y, Hida W, Kurosawa H, Okabe S, Takishima T, and Shirato K**. In vivo release of glutamate in nucleus tractus solitarii of the rat during hypoxia. *J Physiol* 478 (Pt 1): 55-66, 1994.

46. **Nagatsu T, Levitt M, and Udenfriend S**. Tyrosine Hydroxylase. The Initial Step in Norepinephrine Biosynthesis. *J Biol Chem* 239: 2910-2917, 1964.

47. **Nestler EJ**. Is there a common molecular pathway for addiction? *Nat Neurosci* 8: 1445-1449, 2005.

48. **Nestler EJ**. Molecular basis of long-term plasticity underlying addiction. *Nat Rev Neurosci* 2: 119-128, 2001.

49. **Nestler EJ**. Molecular mechanisms of drug addiction. *Neuropharmacology* 47 Suppl 1: 24-32, 2004.

50. **Nestler EJ**. Molecular neurobiology of addiction. *Am J Addict* 10: 201-217, 2001.

51. **Nestler EJ, Barrot M, and Self DW**. DeltaFosB: a sustained molecular switch for addiction. *Proc Natl Acad Sci U S A* 98: 11042-11046, 2001.

52. **Olivan MV, Bonagamba LG, and Machado BH**. Involvement of the paraventricular nucleus of the hypothalamus in the pressor response to chemoreflex activation in awake rats. *Brain Res* 895: 167-172, 2001.

53. **Otake K, Reis DJ, and Ruggiero DA**. Afferents to the midline thalamus issue collaterals to the nucleus tractus solitarii: an anatomical basis for thalamic and visceral reflex integration. *J Neurosci* 14: 5694-5707, 1994.

54. **Paton JF, Deuchars J, Li YW, and Kasparov S**. Properties of solitary tract neurones responding to peripheral arterial chemoreceptors. *Neuroscience* 105: 231-248, 2001.

55. **Reddy MK, Patel KP, and Schultz HD**. Differential role of the paraventricular nucleus of the hypothalamus in modulating the sympathoexcitatory component of peripheral and central chemoreflexes. *Am J Physiol Regul Integr Comp Physiol* 289: R789-797, 2005.

56. **Rey S, Tarvainen MP, Karjalainen PA, and Iturriaga R**. Dynamic time-varying analysis of heart rate and blood pressure variability in cats exposed to short-term chronic intermittent hypoxia. *Am J Physiol Regul Integr Comp Physiol* 295: R28-37, 2008.

57. **Rinaman L**. Hindbrain noradrenergic A2 neurons: diverse roles in autonomic, endocrine, cognitive, and behavioral functions. *Am J Physiol Regul Integr Comp Physiol* 300: R222-235, 2011.

58. **Rinaman L**. Oxytocinergic inputs to the nucleus of the solitary tract and dorsal motor nucleus of the vagus in neonatal rats. *J Comp Neurol* 399: 101-109, 1998.

59. **Ruehland WR, Rochford PD, O'Donoghue FJ, Pierce RJ, Singh P, and Thornton AT**. The new AASM criteria for scoring hypopneas: impact on the apnea hypopnea index. *Sleep* 32: 150-157, 2009.

60. **Rylski M, and Kaczmarek L**. Ap-1 targets in the brain. *Front Biosci* 9: 8-23, 2004.

61. **Sawchenko PE, Brown ER, Chan RK, Ericsson A, Li HY, Roland BL, and Kovacs KJ**. The paraventricular nucleus of the hypothalamus and the functional neuroanatomy of visceromotor responses to stress. *Prog Brain Res* 107: 201-222, 1996.

62. **Schlaich MP, Socratous F, Hennebry S, Eikelis N, Lambert EA, Straznicky N, Esler MD, and Lambert GW**. Sympathetic activation in chronic renal failure. *J Am Soc Nephrol* 20: 933-939, 2009.

63. **Schwarzschild MA, Cole RL, and Hyman SE**. Glutamate, but not dopamine, stimulates stress-activated protein kinase and AP-1-mediated transcription in striatal neurons. *J Neurosci* 17: 3455-3466, 1997.

64. **Silva AQ, and Schreihofer AM**. Altered sympathetic reflexes and vascular reactivity in rats after exposure to chronic intermittent hypoxia. *J Physiol* 589: 1463-1476, 2011.

65. **Somers VK, Dyken ME, Clary MP, and Abboud FM**. Sympathetic neural mechanisms in obstructive sleep apnea. *The Journal of clinical investigation* 96: 1897-1904, 1995.

66. **Soulier V, Cottet-Emard JM, Pequignot J, Hanchin F, Peyrin L, and Pequignot JM**. Differential effects of long-term hypoxia on norepinephrine turnover in brain stem cell groups. *J Appl Physiol* 73: 1810-1814, 1992.

67. **Soulier V, Dalmaz Y, Cottet-Emard JM, Kitahama K, and Pequignot JM**. Delayed increase of tyrosine hydroxylation in the rat A2 medullary neurons upon long-term hypoxia. *Brain Res* 674: 188-195, 1995.

68. **Suzuki M, Otsuka K, and Guilleminault C**. Long-term nasal continuous positive airway pressure administration can normalize hypertension in obstructive sleep apnea patients. *Sleep* 16: 545-549, 1993.

69. **Teppema LJ, Veening JG, Kranenburg A, Dahan A, Berkenbosch A, and Olievier C**. Expression of c-fos in the rat brainstem after exposure to hypoxia and to normoxic and hyperoxic hypercapnia. *J Comp Neurol* 388: 169-190, 1997.

70. **Toescu EC**. Hypoxia sensing and pathways of cytosolic Ca2+ increases. *Cell Calcium* 36: 187-199, 2004.

71. **Toney GM CJ, Mifflin SW**. Early neural adaptations to intermittent hypoxia: Triggers for the pathophysiology of sleep apnea. *In A Ally, TJ Maher, JM Wyss (Eds), (pp 75-96)* Recent

Advances in Cardiovascular Research: From Sleep to Exercise. Kerala, India: Transworld Research Network.: 2010.

72. **Torrealba F, and Claps A**. The carotid sinus connections: a WGA-HRP study in the cat. *Brain Res* 455: 134-143, 1988.

73. **Usui K, Bradley TD, Spaak J, Ryan CM, Kubo T, Kaneko Y, and Floras JS**. Inhibition of awake sympathetic nerve activity of heart failure patients with obstructive sleep apnea by nocturnal continuous positive airway pressure. *Journal of the American College of Cardiology* 45: 2008-2011, 2005.

74. **Valentine JD, Matta SG, and Sharp BM**. Nicotine-induced cFos expression in the hypothalamic paraventricular nucleus is dependent on brainstem effects: correlations with cFos in catecholaminergic and noncatecholaminergic neurons in the nucleus tractus solitarius. *Endocrinology* 137: 622-630, 1996.

75. **van der Kooy D, Koda LY, McGinty JF, Gerfen CR, and Bloom FE**. The organization of projections from the cortex, amygdala, and hypothalamus to the nucleus of the solitary tract in rat. *J Comp Neurol* 224: 1-24, 1984.

76. **Vardhan A, Kachroo A, and Sapru HN**. Excitatory amino acid receptors in commissural nucleus of the NTS mediate carotid chemoreceptor responses. *Am J Physiol* 264: R41-50, 1993.

77. **Wolk R, Shamsuzzaman AS, and Somers VK**. Obesity, sleep apnea, and hypertension. *Hypertension* 42: 1067-1074, 2003.

78. **Yen JC, Chan JY, and Chan SH**. Differential roles of NMDA and non-NMDA receptors in synaptic responses of neurons in nucleus tractus solitarii of the rat. *J Neurophysiol* 81: 3034-3043, 1999.

79. **Zhang J, and Mifflin SW**. Influences of excitatory amino acid receptor agonists on nucleus of the solitary tract neurons receiving aortic depressor nerve inputs. *J Pharmacol Exp Ther* 282: 639-647, 1997.

80. **Zhang W, and Mifflin SW**. Excitatory amino-acid receptors contribute to carotid sinus and vagus nerve evoked excitation of neurons in the nucleus of the tractus solitarius. *J Auton Nerv Syst* 55: 50-56, 1995.

CHAPTER II

KNOCKDOWN OF TYROSINE HYDROXYLASE IN THE NUCLEUS OF THE SOLITARY TRACT REDUCES ELEVATED BLOOD PRESSURE DURING CHRONIC INTERMITTENT HYPOXIA

Running Head: A2 neurons and intermittent hypoxia

Chandra Sekhar Bathina, Anuradha Rajulapati, Michelle Franzke,

Kenta Yamamoto, J. Thomas Cunningham and Steve Mifflin

Department of Integrative Physiology

Cardiovascular Research Institute

University of North Texas Health Science Center

Fort Worth, Texas – 76107

Published in Am J Physiol Regul Integr Comp Physiol 305: R1031–R1039, 2013.

First published September 18, 2013; doi:10.1152/ajpregu.00260.2013.

Abstract

Noradrenergic A2 neurons in NTS respond to stressors such as hypoxia. We hypothesize that tyrosine hydroxylase (TH) knockdown in NTS reduces cardiovascular responses to chronic intermittent hypoxia (CIH), a model of the arterial hypoxemia observed during sleep apnea in humans. Adult male Sprague-Dawley rats were implanted with radio telemetry transmitters and adeno-associated viral constructs with a GFP reporter having either short hairpin RNA (shRNA) for TH or scrambled virus (scRNA) were injected into caudal NTS. Virus injected rats were exposed to 7 days of CIH (alternating 6 min periods of 10% O2 and 4 min of 21% O2 from 8am-4pm; from 4pm-8am rats were exposed to 21% O2). CIH increased MAP and HR during the day in both the scRNA (n= 14, P <.001 MAP and HR) and shRNA (n=13, P <.001 MAP and HR) groups. During the night MAP and HR remained elevated in the scRNA rats (P <0.001 MAP and HR) but not in the shRNA group. TH immunoreactivity and protein were reduced in shRNA group. FosB/ΔFosB immunoreactivity was decreased in paraventricular nucleus (PVN) of shRNA group (P < 0.001). However, shRNA group did not show any change in the FosB/ΔFosB immunoreactivity in the rostral ventro-lateral medulla. Exposure to CIH increased MAP which persisted beyond the period of exposure to CIH. Knockdown of TH in the NTS reduced this CIH-induced persistent increase in MAP and reduced the transcriptional activation of PVN. This indicates that NTS A2 neurons play a role in the cardiovascular responses to CIH.

Keywords: A2 neurons, Nucleus of the solitary tract, Tyrosine hydroxylase and Chronic intermittent hypoxia.

Introduction

Sleep apnea is a condition where periodic, repetitive cessation of ventilation results in intermittent nocturnal episodes of arterial hypoxemia. This activates arterial chemoreceptors (CR) leading to increased sympathetic nerve activity (SNA), which contributes to increased arterial pressure (AP) (55). This elevated SNA and AP persist during the daytime when the patients are not experiencing apneic episodes (5). An estimated 15 million Americans suffer from various forms of sleep apnea (67).

The nucleus of the solitary tract (NTS) is the first integrative site of CR input termination within the central nervous system (11, 27) and neurons responding to CR activation are found throughout the NTS (35). However, chemoreceptor afferent integration appears to be more prevalent in the caudal aspects of the NTS, more precisely in the commissural region caudal to the calamus scriptorius (35, 36, 66) an area rich in catecholaminergic neurons, also known as A2 noradrenergic neurons. A2 neurons are activated by chemoreceptor afferents during systemic hypoxia and carotid sinus nerve stimulation (14). A2 neurons mediate responses to a variety of stressors (49) and project to sympatho-regulatory sites throughout the neuraxis (43, 49, 65). Among these regions is the paraventricular nucleus (PVN), which receives a major projection from A2 neurons (64), and studies have found that the cardiovascular response to activation of peripheral chemoreceptors involves activation of PVN neurons (42, 48). PVN projections to the rostral ventro-lateral medulla (RVLM) have been shown to contribute to the cardiovascular changes occurring during hypoxia exposure in rats (28).

To simulate the hypoxemia that occurs during sleep apnea, a number of labs have chronically exposed rats to intermittent hypoxia (CIH) which results in a persistently elevated AP (18, 29), as seen in humans with sleep apnea. The mechanisms involved in the genesis of hypertension

induced by sleep apnea and CIH appear to involve a sequence of events starting with increased arterial chemoreceptor function (16, 30), stimulation and activation of neurons of CNS (4, 14, 29, 61) leading to augmented SNA (2, 17). Studies have used accumulation of FosB or its more stable splice variant ΔFosB, a member of activator protein (AP)-1 transcription factor family, as a marker for chronic or intermittent activation of CNS neurons (23, 41) following CIH (29). The goal of these studies was to test the hypothesis that depletion of tyrosine hydroxylase (TH) in A2 neurons would attenuate the elevated AP observed during 7 day exposure to CIH by reducing the transcriptional activation of neurons in sympatho-regulatory sites like PVN and RVLM.

Materials and Methods

Animals: Experiments were conducted on adult male Sprague-Dawley rats (250–350g, Charles River Laboratories, Inc., Wilmington, MA, USA). Rats were housed in a thermostatically regulated room (23°c) with 12hour light: 12 hour dark cycle (12L:12D, on at 7 AM, off at 7 PM). 1 week of acclimatization period was provided for the rats before performing any procedures. Rats were provided with food and water *ad libitum*. All experimental procedures were approved by the Institutional Animal Care and Use Committee (IACUC) of the University of North Texas Health Science Center.

Telemetry implantation: Mean arterial pressure (MAP), heart rate (HR) and respiratory frequency (RF) were monitored in conscious rats using a radio telemetry system (DSI, St. Paul, MN, USA). Under 2% isoflurane inhalation anesthesia and aseptic conditions, all rats were implanted with an abdominal aortic catheter attached to a CA11PA-C40 radio-telemetry transmitter. The transmitter was secured to the abdominal muscle.

NTS microinjections: Rats were randomly divided into 2 groups: a group injected with an adeno-associated virus with a GFP reporter and short hairpin RNA for TH (shRNA; n=15), a

group injected with an adeno-associated virus (AAV) with a GFP reporter and scrambled RNA, which is a control for the shRNA virus (scRNA; n=14). The viral constructs were commercially available (Genedetect, New Zealand) and synthesized at titer 1.0 x 10^{12} genomic particles/ml using recently published sequences (63). After 1 week of recovery from telemetry implantation surgery, under 2% isoflurane inhalation anesthesia, rats were placed in a stereotaxic frame and a limited occipital craniotomy conducted to expose the caudal medulla region. Three 100nl injections of either shRNA or scRNA were performed with glass micropipette (tip diameter, 50 μm) using a pneumatic picopump (PV 800, WPI, Sarasota, FL, USA) over a 5 minute period, at the calamus scriptorius and bilaterally at 0.5 mm rostral and 0.5 mm lateral to calamus to cover the caudal NTS. Due to technical difficulties, telemetry data was recorded from 13 rats in shRNA group.

Chronic intermittent hypoxia exposure: One week after the AAV injections, rats were transferred to a commercially available hypoxia chamber system where O_2 concentration was varied using 100% N_2, 100% O_2 and a computerized system (Oxycycler, Biospherix, NY, USA). 7 days of baseline MAP, HR and RF were recorded during which the chambers were maintained at 21% O_2. This was followed by a 7 day exposure to CIH, as described previously (70). Setting the cycles at 9% O_2 for 6 min and 21% O_2 for 4 min resulted in an O_2 concentration of 10% for 3 of the 6 min. The rats were exposed to the CIH during the light phase, which coincides with their sleeping period, from 8am to 4pm (8 hours). From 4pm-8am the rats were exposed to 21% O_2. Following the last day of CIH exposure the rats were euthanized and the brains were collected for either immunohistochemistry or western blotting.

Immunohistochemistry: Rats were anesthetized with thiobutabarbital (100mg/kg i.p Inactin; Sigma, St. Louis, MO), on morning of the day following the last CIH exposure and perfused

transcardially with phosphate buffered saline followed by 4% paraformaldehyde. Brains were then postfixed for 1-2 hours before cryoprotecting in 30% sucrose at 4°C. Three sets of coronal 40-μm sections were collected and stored in cryoprotectant at -20°C until processed for immunohistochemistry. Separate sets of serial sections from the brainstem were processed either for TH- dopamine β-hydroxylase (DBH) double labeling or FosB-TH double labeling. Forebrain sections containing the PVN were processed only for FosB. For TH-DBH double labeling, the sections were processed with a primary antibody cocktail of rabbit anti-TH (1: 1,000, AB152; Millipore, Billerica, MA, USA) and mouse anti-DBH (1: 1,000, , MAB308; Millipore, Billerica, MA, USA) followed by a secondary antibody cocktail with CY3-labeled anti-rabbit (1: 250, 711-165-152; Jackson Immunoresearch, PA, USA) and AMCA- labeled anti-mouse (1: 100, 715-156-150; Jackson Immunoresearch, PA, USA). For FosB-TH double labeling, a separate set of brainstem, sections were first processed for FosB using a goat anti-FosB primary antibody (1: 5,000, sc-48-G, Santa Cruz Biotechnology, Santa Cruz, CA, USA) and a biotinylated horse anti-goat IgG (1:200, BA-9500; Vector labs Burlingame, CA, USA). Next the sections were reacted with an avidin-peroxidase conjugate (Vectastain ABC kit, PK-4000; Vector labs, Burlingame, CA, USA) and PBS containing 0.04% 3,3' –diaminobenzidine hydrochloride and 0.04% nickel ammonium sulfate for 10-11 min . After rinsing, these FosB stained brainstem sections were processed with mouse anti-TH primary antibody(1: 1,000, MAB318; Millipore, Billerica, MA, USA) and a CY3-labeled donkey anti-mouse secondary antibody (1: 250, 715-165-150; Jackson ImmunoResearch, PA, USA). Forebrain serial sections were only stained for FosB as described above. The FosB primary antibody used in this study does not discriminate ΔFosB from FosB; therefore the immunoreactivity will be referred to as FosB/ΔFosB.

Imaging and Cell counts: Imaging of TH-DBH immunoreactive neurons and GFP expression in the NTS was performed using an Olympus IX-2 DSU confocal microscope (Olympus, Tokyo, Japan) equipped for epifluorescence. Sections double labeled for TH-DBH were used to count the number of TH and DBH immunoreactive neurons and to construct the images in figure 2 and 3. FosB immunolabeled forebrain sections were used to count the number of FosB/ΔFosB immunoreactive neurons in PVN and for images in figure 5. Sections double labeled for TH-FosB were used to count FosB/ΔFosB immunoreactivity in RVLM and also to acquire images for figure 6 using Olympus microscope (BX41) equipped for epifluorescence and an Olympus DP70 digital camera with DP manager software (version 2.2.1). ImageJ software (v 1.44, NIH, Bethesda, MD, USA) was used to count the number of TH, DBH (shRNA, n=9 and scRNA, n= 8), FosB/ΔFosB in PVN and RVLM (shRNA, n=7 and scRNA, n= 7) immunoreactive neurons in 9 to 10 sections bilaterally for NTS and RVLM; 5 to 6 sections for PVN (2 to 3 sections per rat/ subnuclei dp, mp, lp and lm) from each rat and the average number of immunoreactive neurons per section calculated for each rat. The regions of interest were identified using the rat brain stereotaxic atlas (45) and within the regions, the counts were conducted in areas as previously described (29).

Western blot: 6 rats each from shRNA and scRNA groups were anesthetized with thiobutabarbital (100mg/kg i.p Inactin; Sigma, St. Louis, MO) and decapitated quickly. The brain stem was removed and snap frozen in isopentane on dry ice and placed in a brain matrix (Stoelting, Wood Dale, IL, USA) to cut 1- mm thick slices. Caudal and sub-postremal NTS regions were dissected from the frozen sections and subjected to sonication in modified radioimmunoprecipitation buffer supplemented with protease and phosphatase inhibitors followed by centrifugation at 10,000g at 4° C to obtain a clear supernatant of protein. Bradford

assay was conducted to determine the total protein concentration. 50 µg of tissue lysate per sample were loaded onto sodium dodecyl sulphate (SDS) - 10% acrylamide gel and electrophorosed before transferring to polyvinylidene fluoride (PVDF) membrane. The membrane was then blocked with 5% (wt/vol) nonfat milk in Tris-buffered saline 0.05% (vol/ vol) Tween 20 (TBS-Tween; 50 mM Tris base, 200 mM NaCl, 0.05% Tween 20) followed by overnight incubation with primary antibodies against TH (1: 1,000 mouse anti-TH, MAB318; Millipore, Billerica, MA, USA) and/or (Glyceraldehyde-3-phosphate dehydrogenase) GAPDH (1:1,000, mouse anti-GAPDH, MAB374; Millipore). Peroxidase-Conjugated AffiniPure sheep anti-mouse IgG (1:5,000, A5906; Sigma Aldrich, St. Louis, MO, USA) was used as a secondary antibody. Immunoreactive bands were detected by enhanced chemiluminescence (ECL reagents, Amersham, Piscataway, NJ, USA) by acquiring digital gel images using Syngene G-box (Frederick, MD, USA). ImageJ software was used to analyze the densitometry of immunoreactive bands.

Telemetry data analysis: MAP (sampled at 250 Hz), HR and RF were recorded for 10 s every 10 minutes as previously described (29, 70). Pulse interval and fluctuations obtained from the AP waveform were used to calculate HR and RF respectively (Dataquest, DSI, MN, USA). MAP, HR and RF were averaged for every hour in the 24hr period and the 1 hour averages averaged during the light phase (period of exposure) during CIH (8am to 4pm) and during the dark period (7pm to 7am).

Statistical analysis: All data are presented as mean ± SE. Effects of CIH on MAP, HR and RF during different periods of the day (light with CIH and dark with normoxia) in shRNA and scRNA were determined by 2-way ANOVA with repeated measures (SigmaPlot, Systat Software, Inc. San Jose, CA). Fisher LSD post hoc test was used to identify significant

difference among mean values. One way ANOVA was used to determine any differences between the control day baseline averages of the 3 parameters between 2 groups, differences between the scRNA and shRNA groups TH-ir cell counts, DBH cell counts, FosB/ΔFosB immunoreactivity in PVN and RVLM and western blot means values. P – value < 0.05 was considered statistically significant.

Results

Responses to CIH in conscious rats: Figure 1 shows the average changes from baseline MAP, HR and RF in the light period (A, C and E) and the dark period (B, D and F) in conscious rats during CIH. Seven days of control baseline values were recorded in both groups of rats. The average baseline values during the control period of MAP (mmHg), HR (beats/min) and RF (breaths/min) during light phase and dark phase are presented in Table 1. There was no significant difference between the average control days MAP and RF of shRNA and scRNA groups during light or dark phase. However, HR was greater in shRNA compared to scRNA (P < 0.001) during both the light and dark phases.

The average of MAP absolute values of each CIH day during light phase, when compared to the baseline values in the Table 1, were significantly higher on all days of CIH except day 1 in both shRNA and scRNA groups (P < 0.05). In the dark phase of CIH, MAP of all the 7 days were significantly higher in scRNA group, but were only significantly elevated on days 2 and 5 in shRNA group when compared to their respective baseline values. When the changes in MAP were compared, the shRNA treated rats showed a significantly reduced CIH-induced increase in MAP compared to scRNA treated rats during the dark phase (Figure 1B; P < 0.05).

HR on all the days of CIH was significantly higher when compared to the baseline in both scRNA and shRNA groups, during the light phase ($P < 0.05$). This elevation in HR persisted into the normoxic dark phase on all CIH days except day 1 in the scRNA group, but not in the shRNA group. The differences in HR between the groups were not significantly different (P= 0.127) (Figure 1D).

All the days in the scRNA group and the shRNA group, except day 1, showed a significant increase in RF during light phase on CIH days, compared to the baseline. During the dark phase, all the days in scRNA treated rats showed an increased RF compared to the baseline, whereas, only days 2 and 5 showed an increase in the shRNA group. Changes in RF during dark phase of CIH days in the shRNA group were significantly lower when compared to the scRNA group (Figure 1F; $P < 0.05$).

AAV-TH- shRNA reduces the number of TH- immunoreactive NTS neurons: Figure 2 illustrates that the shRNA construct reduced the number of TH- immunoreactive neurons in NTS without altering the DBH immunoreactivity. The arrows in the Figure 2 e, f, g and h point out to the neurons where virus infected cells showed no TH immunoreactivity, but the DBH was intact. The number of TH-immunoreactive neurons was reduced by 20% in sections with GFP fluorescence in shRNA group; shRNA 28.6±1.5 cells/section compared to scRNA 35.5±1.4 cells/section (*P*-value: 0.005). The number of DBH-immunoreactive neurons was not different between groups (shRNA: 43.8±2.4 cells/section; scRNA: 45.4±2.4 cells/section). The scrambled RNA treatments did not alter the TH immunoreactivity in the virus infected (GFP-expressing) neurons (Figure 3). There was no apparent difference in the reduction of TH-ir by the shRNA comparing sub-postremal and caudal regions of NTS.

Caudal and sub-postremal regions showed a reduced TH protein levels in shRNA group: Counting TH-ir cells is a binary measure, a cell either possess TH-ir or it does not, and cannot discern partial reductions in the TH content of individual neurons. To confirm TH knockdown as indicated by counting cells with TH–ir, we performed western blots. In the shRNA group, TH levels in caudal (*P*-value: 0.005; n=6 in both groups) and sub-postremal (*P*- value: 0.02; n=5, shRNA, n=6, scRNA) NTS, were reduced by 30% and 10% respectively compared to scRNA group (Figure 4).

shRNA group showed a reduced FosB/ΔFosB staining in different regions of PVN: There was a significant reduction in the number of FosB/ΔFosB – positive cells in the PVN of the shRNA group when compared to the scRNA injected group (*P*- value: 0.006; shRNA: 14 ± 1; scRNA: 34 ± 6, n=8 in both groups). Further analysis of different regions of PVN displayed a reduction in FosB/ΔFosB – positive cells in dorsal parvocellular (dp; *P*- value: <0.001; shRNA: 14 ± 1; scRNA: 35 ± 2), medial parvocellular (mp; *P*- value: <0.001; shRNA: 15 ± 1; scRNA: 48 ± 3) and lateral parvocellular (lp; *P*- value: <0.001; shRNA: 15 ± 1; scRNA: 33 ± 2) subnuclei. There was little to no FosB/ΔFosB staining in the posterior magnocellular region in either group (lm; shRNA: 3 ± 1; scRNA: 5 ± 1) with no difference between them (Figure 5).

No change in FosB/ΔFosB staining between the groups in RVLM: A moderate increase in the number of FosB/ΔFosB – positive cells in the RVLM of the shRNA group when compared to the scRNA group (*P*- value: 0.07; shRNA: 19 ± 3; scRNA: 12 ± 2) was not significant. While the FosB/ΔFosB staining in RVLM was intermingled with TH-positive neurons, the increase in FosB/ΔFosB staining was not associated with significant colocalization of FosB/ΔFosB with TH (shRNA: 1.8 ± 0.3; scRNA: 1.6 ± 0.2) (Figure 6).

Discussion

Sleep apnea is an increasingly recognized contributor to cardiovascular disease and mortality. Sleep apnea patients have elevated blood pressures during both the day and the night, indicating that the effects of sleep apnea persist beyond the actual exposure to nighttime apneas. The model of CIH used in the present study replicates this aspect of the sleep apnea phenotype. It is interesting to note that CIH induces a persistent increase in MAP in the absence of hypercapnia, which accompanies the hypoxia in sleep apnea patients. In fact, due to the increases in ventilation during intermittent hypoxia (IH) in CIH models, the hypoxia is accompanied by hypocapnia. Previous studies in human (8, 54, 68) and rodents (15, 62) indicate that IH- induced increases in MAP and/or SNA are independent of end-tidal CO_2, being the same whether the subject is hypocapnic, isocapnic or hypercapnic. The present study provides new insights that suggest catecholaminergic A2 neurons in the NTS are major contributors to the CIH-induced persistent increase in MAP.

A2 neurons are activated by a variety of stressors, including systemic hypoxia (14). A2 projections to sympatho-regulatory sites within the CNS (49) suggesting that A2 neurons play a role in the cardiovascular and sympathetic responses to systemic hypoxia. A 7 day exposure to IH produced no change in TH enzymatic activity or protein level in the brainstem; however this study did not examine specific areas within the brainstem (20). Chronic hypoxia increased TH expression within the A2 cell group (13, 57) and this increase was abolished after carotid sinus nerve section (56). Therefore, the variations in TH expression observed in A2 group are not solely the direct effect of tissue hypoxia, but are dependent upon afferent chemoreceptor inputs to NTS. A2 neurons also play a role in the hypothalamic-pituitary-adrenal (HPA) axis reactivity as they are found to express glucocorticoid receptors (19, 22) and project to regions important in

regulation of HPA axis function (49). Our group has shown that CIH sensitizes HPA axis reactivity (31) and since glucocorticoids have shown to increase arterial pressure in response to acute stress (51, 52), a hyper-reactive stress response may also contribute to the CIH induced increase in MAP. Exposure to CIH has been reported to increase the plasma corticosterone levels (71); however in that study plasma was collected for measurement of corticosterone at sacrifice so the elevated corticosterone level may reflect enhanced stress reactivity.

In this study, we reduced TH levels in A2 neurons using adeno-associated virus (AAV) vector delivery of short-hairpin RNAs-directed towards TH and observed MAP, HR and RF during exposure to CIH. This approach has been used to reduce TH levels in specific regions of the brain in mice (26) and rat (63). Genetic models are widely used to uncover the molecular mechanisms of a disease, but the use of transgenic and knockout models is limited by developmental effects, genetic compensation and lack of regional specificity. The use of shRNA to knockdown genes of interest in the whole brain (44) and in specific regions (26, 50, 69) has provided a useful adjunct approach to the use of genetic models. Unlike saporin toxin studies (10, 60) the use of shRNA reduces TH levels and does not kill the A2 neurons. To address concerns about the toxicity of these viral constructs and possible knock down of other genes, a previously used construct (63) at a safe titer (> 1 X 10^{12} genomic particles/ml) was used. In addition, immunohistochemistry was performed for DBH, which like TH, is also specific for catecholaminergic neurons. Figure 2 and 3 illustrate that the viral constructs are not toxic and do not suppress DBH levels. Uniform sized bands for the housekeeping gene GAPDH in the western blots in both shRNA and scrambled groups also suggest no nonspecific changes in protein levels.

Our finding of a CIH-induced persistent increase in respiratory frequency was surprising as central catecholaminergic neurons are considered to exert a weak, tonic inhibition of ventilation (34). However, the cited study produced a global reduction in neuronal catecholaminergic content and more selective and site-specific reductions in neuronal catecholamine content might produce different results. It has been suggested that CIH-induced hypertension might be due to increased respiratory drive to sympathoexcitatory neurons in the brainstem (37).

Previous studies from our group have shown that within the first week of exposure CIH increased MAP during the light phase, when the rats are exposed to the intermittent hypoxia, and the increase in MAP persisted into the normoxic dark phase (7, 24, 29). The results of this study demonstrate that TH knockdown in A2 neurons decreased the persistent increase in MAP and RF during the normoxic dark phase. These results demonstrate that A2 neurons contribute to the cardiovascular and respiratory responses to intermittent hypoxia without altering baseline blood pressure.

Consistent with this finding of a reduced response to CIH, a physiological stress, are the results of a recent study that found that injections of DBH-saporin into caudal NTS reduced the number of catecholaminergic neurons and reduced chronic stress-induced elevations in dark phase blood pressure (10). This study and others have shown increases or no change in baseline blood pressure following lesion of A2 neurons with either DBH-saporin (10, 60) or after silencing of A2 neurons by over-expressing potassium channels (12). Our results indicate no change in baseline blood pressure in shRNA injected rats. This may be result of a more modest reduction in TH in our study, however such modest reductions could represent a degree of knock down that might happen physiologically. It could also reflect the fact that the shRNA does not kill the A2

neurons. The contribution of A2 neurons to baseline blood pressure is important to understand and requires further study.

To define potential sites in the CNS that might be involved in the reduction in MAP during normoxic dark phase of CIH following decreased TH levels in NTS, we examined FosB/ΔFosB in sympatho-regulatory sites like PVN and RVLM. Increased expression of FosB during CIH is an important finding because FosB/ΔFosB has been linked to neuronal adaptations and plasticity under conditions such as drug addiction, epilepsy and long-term potentiation (6, 32, 33, 38-41). The present results confirm our previous studies (29) demonstrating increased levels of FosB/ΔFosB in CNS neurons following CIH which may mediate changes in gene expression that alter neuronal function. PVN neurons have been shown to increase levels of FosB/ΔFosB immunoreactivity following exposure to CIH (29). PVN parvocellular neurons project to RVLM (46, 47, 53, 58) and intermediolateral cell column of spinal cord (47, 53, 58, 59), the location of sympathetic preganglionic neurons. The reduction in the number of FosB/ΔFosB immunoreactive neurons in the dorsal parvocellular (dp), medial parvocellular (mp) and lateral parvocellular (lp) (Figure. 5) in the shRNA rats, when compared to scRNA rats, indicates that TH knockdown in the NTS reduced the transcriptional activation of PVN, most likely by reducing A2 neuron excitation of PVN neurons (49). This indicates that the sympathetic drive from the PVN (9, 21) might have been decreased, causing the reduction in the CIH-induced persistent increase in MAP during the normoxic dark phase.

The observation that shRNA knockdown of TH in the NTS was not associated with a change in the FosB/ΔFosB immunoreactivity in RVLM (Figure. 6) was not expected as decreased MAP was expected to be associated with decreased transcriptional activation of RVLM. However, A2 neurons do not project directly to the RVLM (3, 25). Optogenetic stimulation of

catecholaminergic neurons in RVLM in the rat increases SNA and blood pressure (1). Non-catecholaminergic neurons in RVLM serve a variety of functions (e.g., thermoregulation, respiration, cardiovascular). The reduced activity of PVN parvocellular neurons and their projections to the intermediolateral cell column of spinal cord might be the driving force behind the reduction in the dark phase MAP elevation observed after reductions in TH in the caudal NTS.

Perspectives and significance

This study shows that it is plausible to knockdown TH using viral vectors without affecting the cell vitality and other protein expression. These results suggest that activation of NTS A2 neurons during CIH mediates the increased sympathetic outflow that has been shown to underlie CIH-induced persistent hypertension. The observations that FosB was not different between treatment groups in the RVLM and that the increase in blood pressure during the light phase was also not different between groups raises the possibility that PVN sympathoexcitatory neurons might have a greater contribution to the dark phase elevation in baseline blood pressure, while the RVLM might be more involved during the light phase exposures to hypoxia."

Grants

Funded by National institute of Health HL-088052

Conflict of Interest

None

References

1. **Abbott SB, Stornetta RL, Socolovsky CS, West GH, and Guyenet PG**. Photostimulation of channelrhodopsin-2 expressing ventrolateral medullary neurons increases sympathetic nerve activity and blood pressure in rats. *J Physiol* 587: 5613-5631, 2009.

2. **Bao G, Metreveli N, Li R, Taylor A, and Fletcher EC**. Blood pressure response to chronic episodic hypoxia: role of the sympathetic nervous system. *J Appl Physiol* 83: 95-101, 1997.

3. **Blessing WW, Hedger SC, Joh TH, and Willoughby JO**. Neurons in the area postrema are the only catecholamine-synthesizing cells in the medulla or pons with projections to the rostral ventrolateral medulla (C1-area) in the rabbit. *Brain Res* 419: 336-340, 1987.

4. **Buller KM, Smith DW, and Day TA**. NTS catecholamine cell recruitment by hemorrhage and hypoxia. *Neuroreport* 10: 3853-3856, 1999.

5. **Carlson JT, Hedner J, Elam M, Ejnell H, Sellgren J, and Wallin BG**. Augmented resting sympathetic activity in awake patients with obstructive sleep apnea. *Chest* 103: 1763-1768, 1993.

6. **Chen J, Zhang Y, Kelz MB, Steffen C, Ang ES, Zeng L, and Nestler EJ**. Induction of cyclin-dependent kinase 5 in the hippocampus by chronic electroconvulsive seizures: role of [Delta]FosB. *J Neurosci* 20: 8965-8971, 2000.

7. **Cunningham JT, Knight WD, Mifflin SW, and Nestler EJ**. An Essential role for DeltaFosB in the median preoptic nucleus in the sustained hypertensive effects of chronic intermittent hypoxia. *Hypertension* 60: 179-187, 2012.

8. **Cutler MJ, Swift NM, Keller DM, Wasmund WL, Burk JR, and Smith ML**. Periods of intermittent hypoxic apnea can alter chemoreflex control of sympathetic nerve activity in humans. *Am J Physiol Heart Circ Physiol* 287: H2054-2060, 2004.

9. **Dampney RA, and Horiuchi J**. Functional organisation of central cardiovascular pathways: studies using c-fos gene expression. *Prog Neurobiol* 71: 359-384, 2003.

10. **Daubert DL, McCowan M, Erdos B, and Scheuer DA**. Nucleus of the solitary tract catecholaminergic neurons modulate the cardiovascular response to psychological stress in rats. *J Physiol* 590: 4881-4895, 2012.

11. **Donoghue S, Felder RB, Jordan D, and Spyer KM**. The central projections of carotid baroreceptors and chemoreceptors in the cat: a neurophysiological study. *J Physiol* 347: 397-409, 1984.

12. **Duale H, Waki H, Howorth P, Kasparov S, Teschemacher AG, and Paton JF**. Restraining influence of A2 neurons in chronic control of arterial pressure in spontaneously hypertensive rats. *Cardiovasc Res* 76: 184-193, 2007.

13. **Dumas S, Pequignot JM, Ghilini G, Mallet J, and Denavit-Saubie M**. Plasticity of tyrosine hydroxylase gene expression in the rat nucleus tractus solitarius after ventilatory acclimatization to hypoxia. *Brain Res Mol Brain Res* 40: 188-194, 1996.

14. **Erickson JT, and Millhorn DE**. Hypoxia and electrical stimulation of the carotid sinus nerve induce Fos-like immunoreactivity within catecholaminergic and serotoninergic neurons of the rat brainstem. *J Comp Neurol* 348: 161-182, 1994.

15. **Fletcher EC, and Bao G**. Effect of episodic eucapnic and hypocapnic hypoxia on systemic blood pressure in hypertension-prone rats. *J Appl Physiol* 81: 2088-2094, 1996.

16. **Fletcher EC, Lesske J, Behm R, Miller CC, 3rd, Stauss H, and Unger T**. Carotid chemoreceptors, systemic blood pressure, and chronic episodic hypoxia mimicking sleep apnea. *J Appl Physiol* 72: 1978-1984, 1992.

17. **Fletcher EC, Lesske J, Culman J, Miller CC, and Unger T**. Sympathetic denervation blocks blood pressure elevation in episodic hypoxia. *Hypertension* 20: 612-619, 1992.

18. **Fletcher EC, Lesske J, Qian W, Miller CC, 3rd, and Unger T**. Repetitive, episodic hypoxia causes diurnal elevation of blood pressure in rats. *Hypertension* 19: 555-561, 1992.

19. **Fuxe K, Cintra A, Agnati LF, Harfstrand A, Wikstrom AC, Okret S, Zoli M, Miller LS, Greene JL, and Gustafsson JA**. Studies on the cellular localization and distribution of glucocorticoid receptor and estrogen receptor immunoreactivity in the central nervous system of the rat and their relationship to the monoaminergic and peptidergic neurons of the brain. *J Steroid Biochem* 27: 159-170, 1987.

20. **Gozal E, Shah ZA, Pequignot JM, Pequignot J, Sachleben LR, Czyzyk-Krzeska MF, Li RC, Guo SZ, and Gozal D**. Tyrosine hydroxylase expression and activity in the rat brain: differential regulation after long-term intermittent or sustained hypoxia. *J Appl Physiol* 99: 642-649, 2005.

21. **Guyenet PG**. The sympathetic control of blood pressure. *Nat Rev Neurosci* 7: 335-346, 2006.

22. **Harfstrand A, Fuxe K, Cintra A, Agnati LF, Zini I, Wikstrom AC, Okret S, Yu ZY, Goldstein M, Steinbusch H, and et al.** Glucocorticoid receptor immunoreactivity in monoaminergic neurons of rat brain. *Proc Natl Acad Sci U S A* 83: 9779-9783, 1986.

23. **Herdegen T, and Leah JD**. Inducible and constitutive transcription factors in the mammalian nervous system: control of gene expression by Jun, Fos and Krox, and CREB/ATF proteins. *Brain Res Brain Res Rev* 28: 370-490, 1998.

24. **Hinojosa-Laborde C, and Mifflin SW**. Sex differences in blood pressure response to intermittent hypoxia in rats. *Hypertension* 46: 1016-1021, 2005.

25. **Hirooka Y, Polson JW, Potts PD, and Dampney RA**. Hypoxia-induced Fos expression in neurons projecting to the pressor region in the rostral ventrolateral medulla. *Neuroscience* 80: 1209-1224, 1997.

26. **Hommel JD, Sears RM, Georgescu D, Simmons DL, and DiLeone RJ**. Local gene knockdown in the brain using viral-mediated RNA interference. *Nat Med* 9: 1539-1544, 2003.

27. **Housley GD, Martin-Body RL, Dawson NJ, and Sinclair JD**. Brain stem projections of the glossopharyngeal nerve and its carotid sinus branch in the rat. *Neuroscience* 22: 237-250, 1987.

28. **Kc P, Balan KV, Tjoe SS, Martin RJ, Lamanna JC, Haxhiu MA, and Dick TE**. Increased vasopressin transmission from the paraventricular nucleus to the rostral medulla augments cardiorespiratory outflow in chronic intermittent hypoxia-conditioned rats. *J Physiol* 588: 725-740, 2010.

29. **Knight WD, Little JT, Carreno FR, Toney GM, Mifflin SW, and Cunningham JT**. Chronic intermittent hypoxia increases blood pressure and expression of FosB/DeltaFosB in central autonomic regions. *Am J Physiol Regul Integr Comp Physiol* 301: R131-139, 2011.

30. **Lesske J, Fletcher EC, Bao G, and Unger T**. Hypertension caused by chronic intermittent hypoxia--influence of chemoreceptors and sympathetic nervous system. *J Hypertens* 15: 1593-1603, 1997.

31. **Ma S, Mifflin SW, Cunningham JT, and Morilak DA**. Chronic intermittent hypoxia sensitizes acute hypothalamic-pituitary-adrenal stress reactivity and Fos induction in the rat locus coeruleus in response to subsequent immobilization stress. *Neuroscience* 154: 1639-1647, 2008.

32. **Madsen TM, Bolwig TG, and Mikkelsen JD**. Differential regulation of c-Fos and FosB in the rat brain after amygdala kindling. *Cell Mol Neurobiol* 26: 87-100, 2006.

33. **McClung CA, Ulery PG, Perrotti LI, Zachariou V, Berton O, and Nestler EJ**. DeltaFosB: a molecular switch for long-term adaptation in the brain. *Brain Res Mol Brain Res* 132: 146-154, 2004.

34. **McCrimmon DR, Dempsey JA, and Olson EB, Jr.** Effect of catecholamine depletion on ventilatory control in unanesthetized normoxic and hypoxic rats. *Journal of applied physiology: respiratory, environmental and exercise physiology* 55: 522-528, 1983.

35. **Mifflin SW**. Arterial chemoreceptor input to nucleus tractus solitarius. *Am J Physiol* 263: R368-375, 1992.

36. **Mifflin SW**. Inhibition of chemoreceptor inputs to nucleus of tractus solitarius neurons during baroreceptor stimulation. *Am J Physiol* 265: R14-20, 1993.

37. **Moraes DJ, Zoccal DB, and Machado BH**. Medullary respiratory network drives sympathetic overactivity and hypertension in rats submitted to chronic intermittent hypoxia. *Hypertension* 60: 1374-1380, 2012.

38. **Nestler EJ**. Is there a common molecular pathway for addiction? *Nat Neurosci* 8: 1445-1449, 2005.

39. **Nestler EJ**. Molecular basis of long-term plasticity underlying addiction. *Nat Rev Neurosci* 2: 119-128, 2001.

40. **Nestler EJ**. Molecular neurobiology of addiction. *Am J Addict* 10: 201-217, 2001.

41. **Nestler EJ, Barrot M, and Self DW**. DeltaFosB: a sustained molecular switch for addiction. *Proc Natl Acad Sci U S A* 98: 11042-11046, 2001.

42. **Olivan MV, Bonagamba LG, and Machado BH**. Involvement of the paraventricular nucleus of the hypothalamus in the pressor response to chemoreflex activation in awake rats. *Brain Res* 895: 167-172, 2001.

43. **Otake K, Reis DJ, and Ruggiero DA**. Afferents to the midline thalamus issue collaterals to the nucleus tractus solitarii: an anatomical basis for thalamic and visceral reflex integration. *J Neurosci* 14: 5694-5707, 1994.

44. **Pardridge WM**. shRNA and siRNA delivery to the brain. *Adv Drug Deliv Rev* 59: 141-152, 2007.

45. **Paxinos G, Watson CR, and Emson PC**. AChE-stained horizontal sections of the rat brain in stereotaxic coordinates. *J Neurosci Methods* 3: 129-149, 1980.

46. **Pyner S, and Coote JH**. Identification of an efferent projection from the paraventricular nucleus of the hypothalamus terminating close to spinally projecting rostral ventrolateral medullary neurons. *Neuroscience* 88: 949-957, 1999.

47. **Pyner S, and Coote JH**. Identification of branching paraventricular neurons of the hypothalamus that project to the rostroventrolateral medulla and spinal cord. *Neuroscience* 100: 549-556, 2000.

48. **Reddy MK, Patel KP, and Schultz HD**. Differential role of the paraventricular nucleus of the hypothalamus in modulating the sympathoexcitatory component of peripheral and central chemoreflexes. *Am J Physiol Regul Integr Comp Physiol* 289: R789-797, 2005.

49. **Rinaman L**. Hindbrain noradrenergic A2 neurons: diverse roles in autonomic, endocrine, cognitive, and behavioral functions. *Am J Physiol Regul Integr Comp Physiol* 300: R222-235, 2011.

50. **Salahpour A, Medvedev IO, Beaulieu JM, Gainetdinov RR, and Caron MG**. Local knockdown of genes in the brain using small interfering RNA: a phenotypic comparison with knockout animals. *Biol Psychiatry* 61: 65-69, 2007.

51. **Scheuer DA, Bechtold AG, Shank SS, and Akana SF**. Glucocorticoids act in the dorsal hindbrain to increase arterial pressure. *Am J Physiol Heart Circ Physiol* 286: H458-467, 2004.

52. **Scheuer DA, Bechtold AG, and Vernon KA**. Chronic activation of dorsal hindbrain corticosteroid receptors augments the arterial pressure response to acute stress. *Hypertension* 49: 127-133, 2007.

53. **Shafton AD, Ryan A, and Badoer E**. Neurons in the hypothalamic paraventricular nucleus send collaterals to the spinal cord and to the rostral ventrolateral medulla in the rat. *Brain Res* 801: 239-243, 1998.

54. **Smith ML, and Pacchia CF**. Sleep apnoea and hypertension: role of chemoreflexes in humans. *Exp Physiol* 92: 45-50, 2007.

55. **Somers VK, Dyken ME, Clary MP, and Abboud FM**. Sympathetic neural mechanisms in obstructive sleep apnea. *The Journal of clinical investigation* 96: 1897-1904, 1995.

56. **Soulier V, Cottet-Emard JM, Pequignot J, Hanchin F, Peyrin L, and Pequignot JM**. Differential effects of long-term hypoxia on norepinephrine turnover in brain stem cell groups. *J Appl Physiol* 73: 1810-1814, 1992.

57. **Soulier V, Dalmaz Y, Cottet-Emard JM, Kitahama K, and Pequignot JM**. Delayed increase of tyrosine hydroxylation in the rat A2 medullary neurons upon long-term hypoxia. *Brain Res* 674: 188-195, 1995.

58. **Stocker SD, Cunningham JT, and Toney GM**. Water deprivation increases Fos immunoreactivity in PVN autonomic neurons with projections to the spinal cord and rostral ventrolateral medulla. *Am J Physiol Regul Integr Comp Physiol* 287: R1172-1183, 2004.

59. **Swanson LW, and Kuypers HG**. The paraventricular nucleus of the hypothalamus: cytoarchitectonic subdivisions and organization of projections to the pituitary, dorsal vagal complex, and spinal cord as demonstrated by retrograde fluorescence double-labeling methods. *J Comp Neurol* 194: 555-570, 1980.

60. **Talman WT, Dragon DN, Jones SY, Moore SA, and Lin LH**. Sudden death and myocardial lesions after damage to catecholamine neurons of the nucleus tractus solitarii in rat. *Cell Mol Neurobiol* 32: 1119-1126, 2012.

61. **Teppema LJ, Veening JG, Kranenburg A, Dahan A, Berkenbosch A, and Olievier C**. Expression of c-fos in the rat brainstem after exposure to hypoxia and to normoxic and hyperoxic hypercapnia. *J Comp Neurol* 388: 169-190, 1997.

62. **Toney GM CJ, Mifflin SW**. Early neural adaptations to intermittent hypoxia: Triggers for the pathophysiology of sleep apnea. *In A Ally, TJ Maher, JM Wyss (Eds), (pp 75-96)* Recent Advances in Cardiovascular Research: From Sleep to Exercise. Kerala, India: Transworld Research Network.: 2010.

63. **Ulusoy A, Sahin G, Bjorklund T, Aebischer P, and Kirik D**. Dose optimization for long-term rAAV-mediated RNA interference in the nigrostriatal projection neurons. *Mol Ther* 17: 1574-1584, 2009.

64. **Valentine JD, Matta SG, and Sharp BM**. Nicotine-induced cFos expression in the hypothalamic paraventricular nucleus is dependent on brainstem effects: correlations with cFos in catecholaminergic and noncatecholaminergic neurons in the nucleus tractus solitarius. *Endocrinology* 137: 622-630, 1996.

65. **van der Kooy D, Koda LY, McGinty JF, Gerfen CR, and Bloom FE**. The organization of projections from the cortex, amygdala, and hypothalamus to the nucleus of the solitary tract in rat. *J Comp Neurol* 224: 1-24, 1984.

66. **Vardhan A, Kachroo A, and Sapru HN**. Excitatory amino acid receptors in commissural nucleus of the NTS mediate carotid chemoreceptor responses. *Am J Physiol* 264: R41-50, 1993.

67. **Wolk R, Shamsuzzaman AS, and Somers VK**. Obesity, sleep apnea, and hypertension. *Hypertension* 42: 1067-1074, 2003.

68. **Xie A, Skatrud JB, Crabtree DC, Puleo DS, Goodman BM, and Morgan BJ**. Neurocirculatory consequences of intermittent asphyxia in humans. *J Appl Physiol* 89: 1333-1339, 2000.

69. **Xue B, Beltz TG, Yu Y, Guo F, Gomez-Sanchez CE, Hay M, and Johnson AK**. Central interactions of aldosterone and angiotensin II in aldosterone- and angiotensin II-induced hypertension. *Am J Physiol Heart Circ Physiol* 300: H555-564, 2011.

70. **Yamamoto K, Eubank W, Franzke M, and Mifflin S**. Resetting of the sympathetic baroreflex is associated with the onset of hypertension during chronic intermittent hypoxia. *Auton Neurosci* 173: 22-27, 2013.

71. **Zoccal DB, Bonagamba LG, Antunes-Rodrigues J, and Machado BH**. Plasma corticosterone levels is elevated in rats submitted to chronic intermittent hypoxia. *Auton Neurosci* 134: 115-117, 2007.

Table 1. Average baseline values of physiological parameters in shRNA and scRNA groups

	Light phase		Dark Phase	
	scRNA	**shRNA**	**scRNA**	**shRNA**
MAP	100.9 ± 3.4	100.9 ± 2.3	104.1 ± 4.2	104.9 ± 2.7
HR	311.0 ± 6.1 *	320.5 ± 5.4	363.3 ± 7.6 *	378.4 ± 6.3
RF	95.4 ± 1.3	95.0 ± 1.5	94.4 ± 4.5	96.4 ± 2.9

* - significantly different from respective phase HR of shRNA

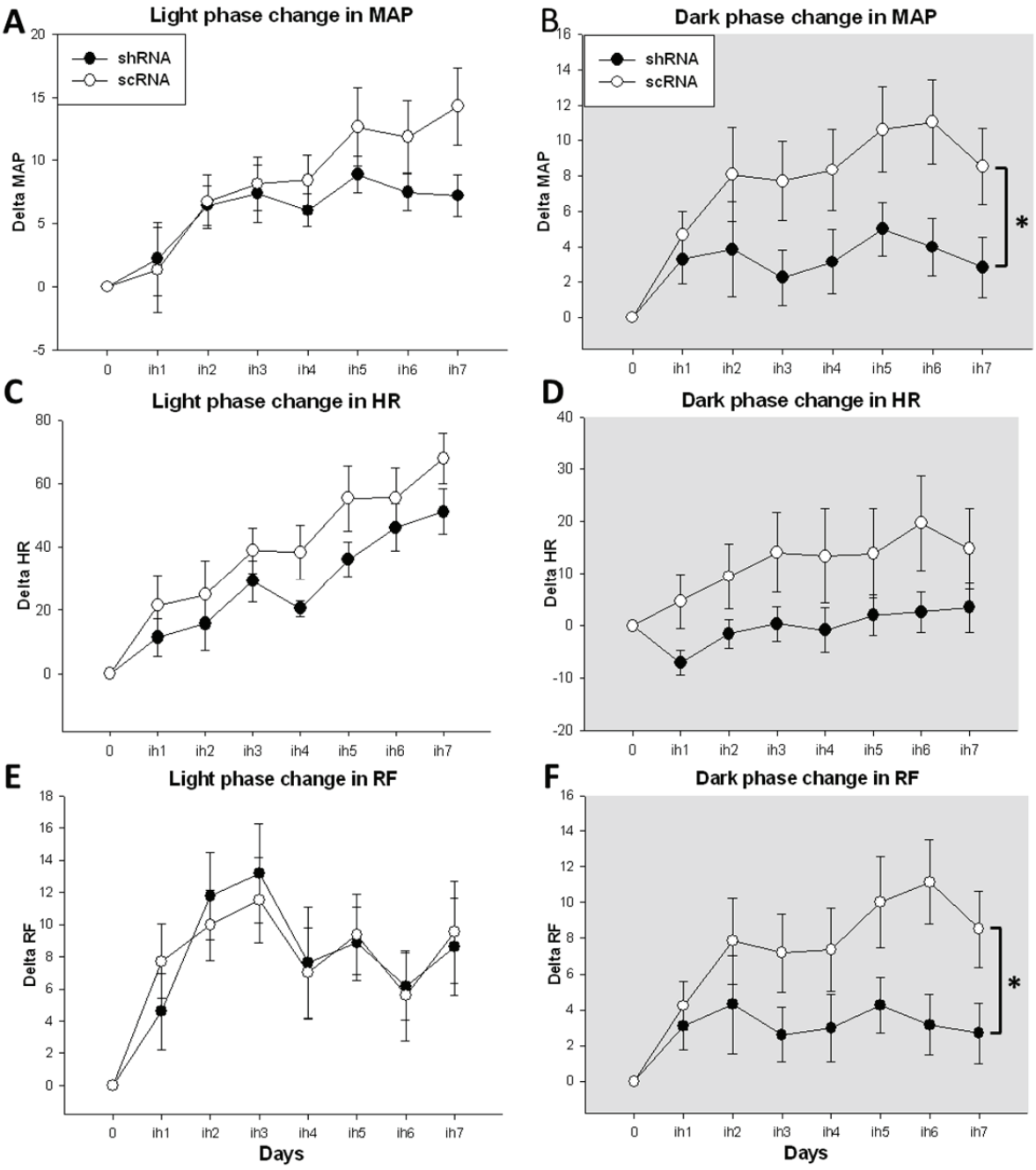
A
Light phase change in MAP
shRNA
scRNA
Delta MAP
20
15
10
5
0
-5
0
ih1
ih2
ih3
ih4
ih5
ih6
ih7
B
Dark phase change in MAP
shRNA
scRNA
Delta MAP
16
14
12
10
8
6
4
2
0
*
C
Light phase change in HR
Delta HR
80
60
40
20
0
D
Dark phase change in HR
Delta HR
40
30
20
10
0
-10
-20
E
Light phase change in RF
Delta RF
18
16
14
12
10
8
6
4
2
0
Days
F
Dark phase change in RF
Delta RF
Days

Figure 1. Graphs are presented as differences from baseline with the baseline absolute values represented as zero. 7 days of CIH are presented on x-axis as ih1 to ih7. **A**. CIH caused a significant elevation in MAP starting day 2 in both shRNA and scrambled virus injected groups, when compared to their baseline, during light phase **B.** Sustained hypertension during normoxic dark phase has been significantly reduced in shRNA virus injected rats **C.** CIH significantly increased the HR in both the virus injected groups **D**. During the dark phase, shRNA moderately decreased the HR elevation noticed in scRNA group. **E**. Light phase RF significantly increased in shRNA and scRNA viruses injected groups. **F**. This elevation in RF was significantly decreased by shRNA. (shRNA; n=13 and scRNA; n=14); * – shRNA group significantly different from scRNA group. *P*-value < 0.05 was considered significant.

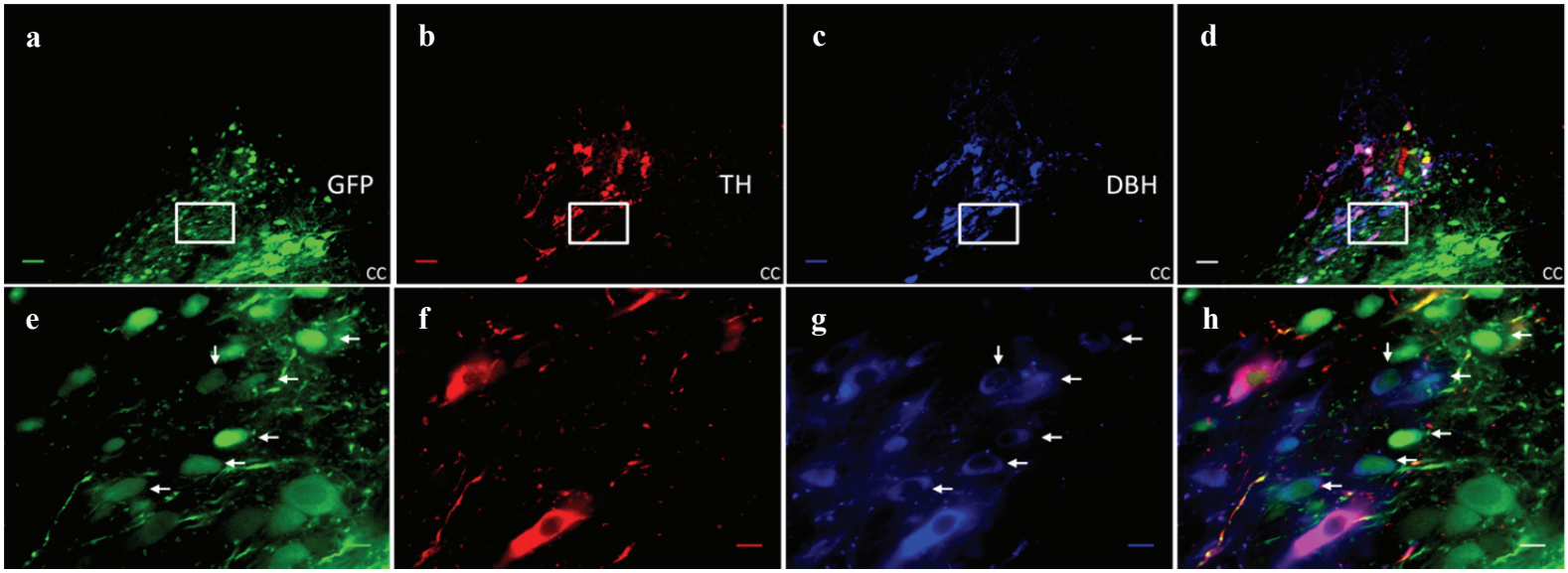

Figure 2. shRNA selective knockdown of TH in A2 neurons (a) GFP staining showing the AAV-TH-ShRNA infected cells in the NTS. (b) Red colored Cy3 labeled A2 neurons expressing TH (c) AMCA labeled blue colored DBH positive cells (d) Superimposed image of a, b and c. e, f, g and h are the high magnification images of the area in box of a, b, c and d respectively. Arrows point at the cells where in shRNA successfully knocked down TH without affecting DBH's expression. (cc – central canal). Scale bar – 50 µm in low magnification images and 10 µm in high magnification images. Sections from sub-postremal NTS.

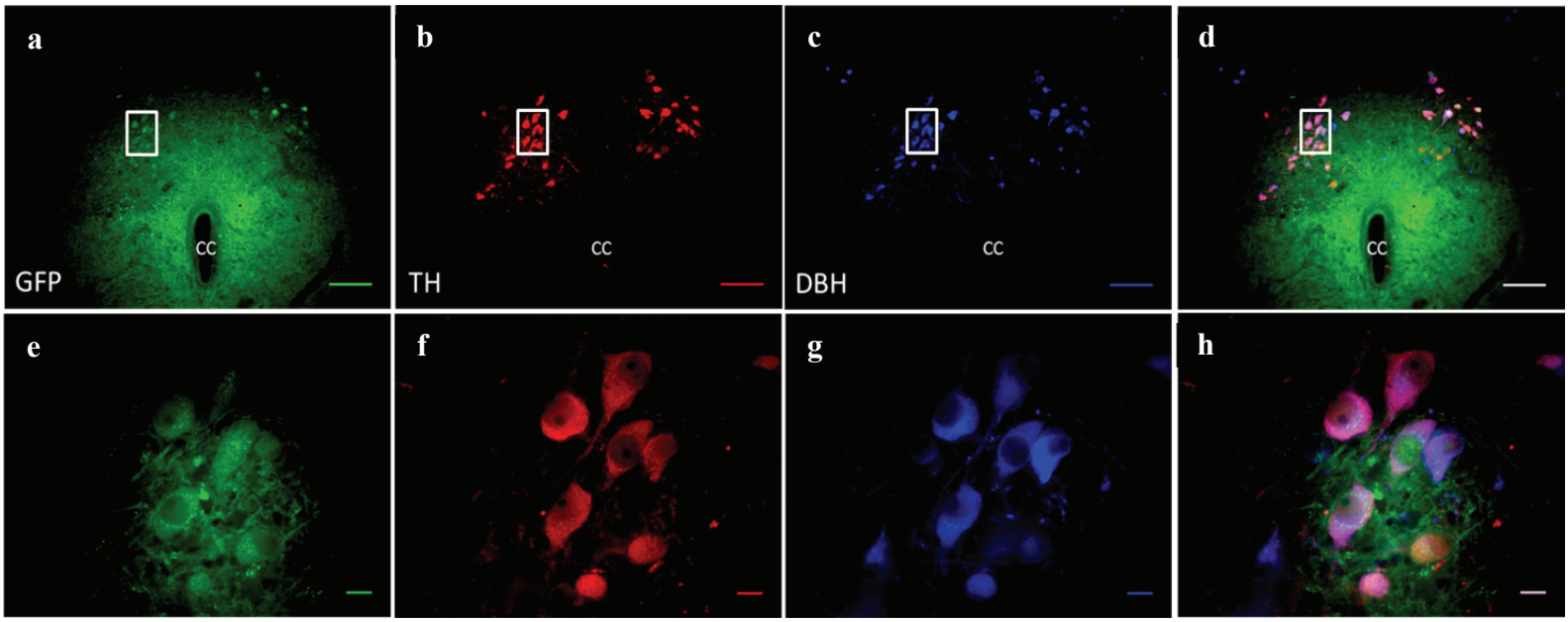

Figure 3. Scrambled virus does not affect the expression of TH in A2 neurons (a) GFP staining showing the AAV-Sc virus infected cells in the NTS. (b) Red colored Cy3 labeled A2 neurons expressing TH (c) AMCA labeled blue colored DBH positive cells. (d) Composite image of a,b and c. e, f, g and h are the high magnification images of the area in box of a, b, c and d respectively. Superimposed image of e, f and g in h showing mostly purple colored cells, where in both TH and DBH are intact in scrambled virus infected cells. (cc- central canal). Scale bar – 100 µm in low magnification images and 10 µm in high magnification images. Sections from caudal NTS

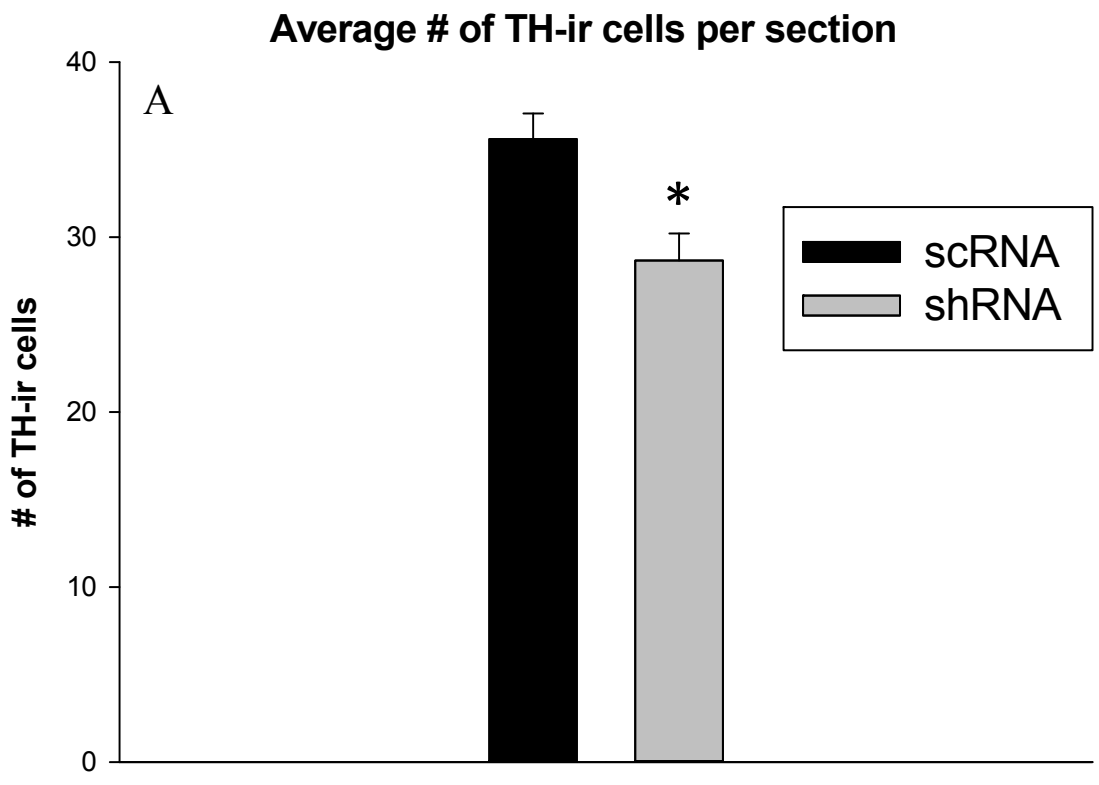
Average # of TH-ir cells per section
A
40
30
20
10
0
# of TH-ir cells
*
scRNA
shRNA

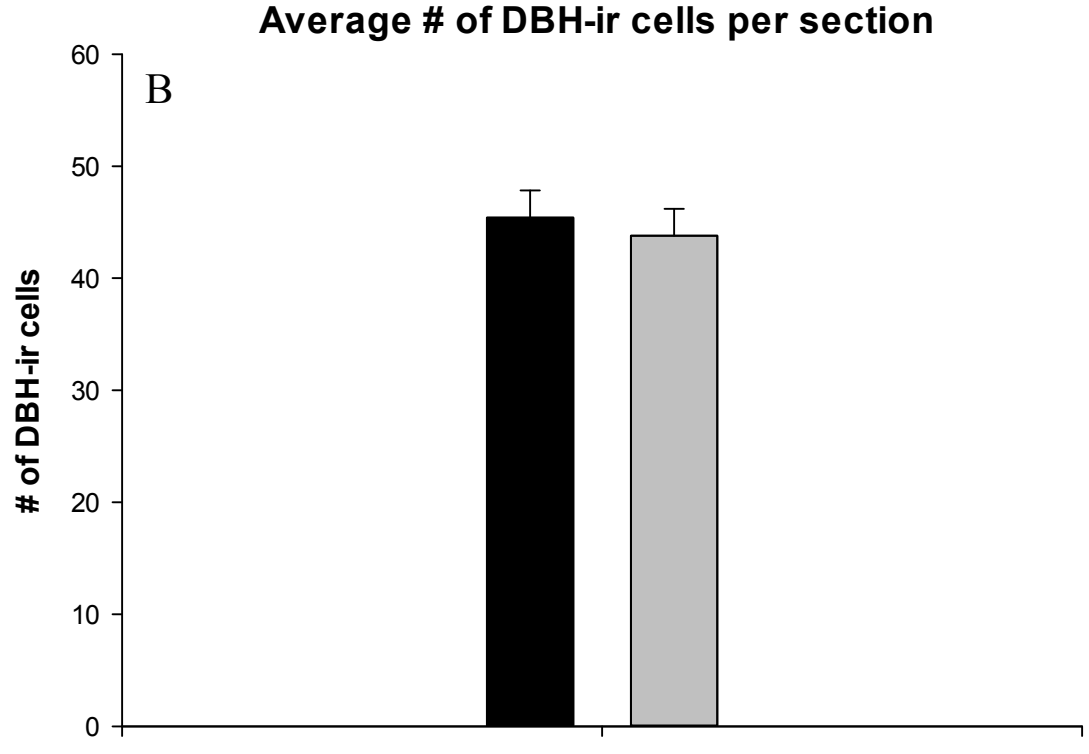
Average # of DBH-ir cells per section
B
60
50
40
30
20
10
0
# of DBH-ir cells

Figure 4. Cell counts for TH-ir showed significant reduction in the number of TH-ir neurons in the shRNA injected group without effecting DBH-ir A* *P*- value < 0.05 vs. scRNA. TH and DBH cell counts; n = 9 in shRNA and n=8 in scRNA

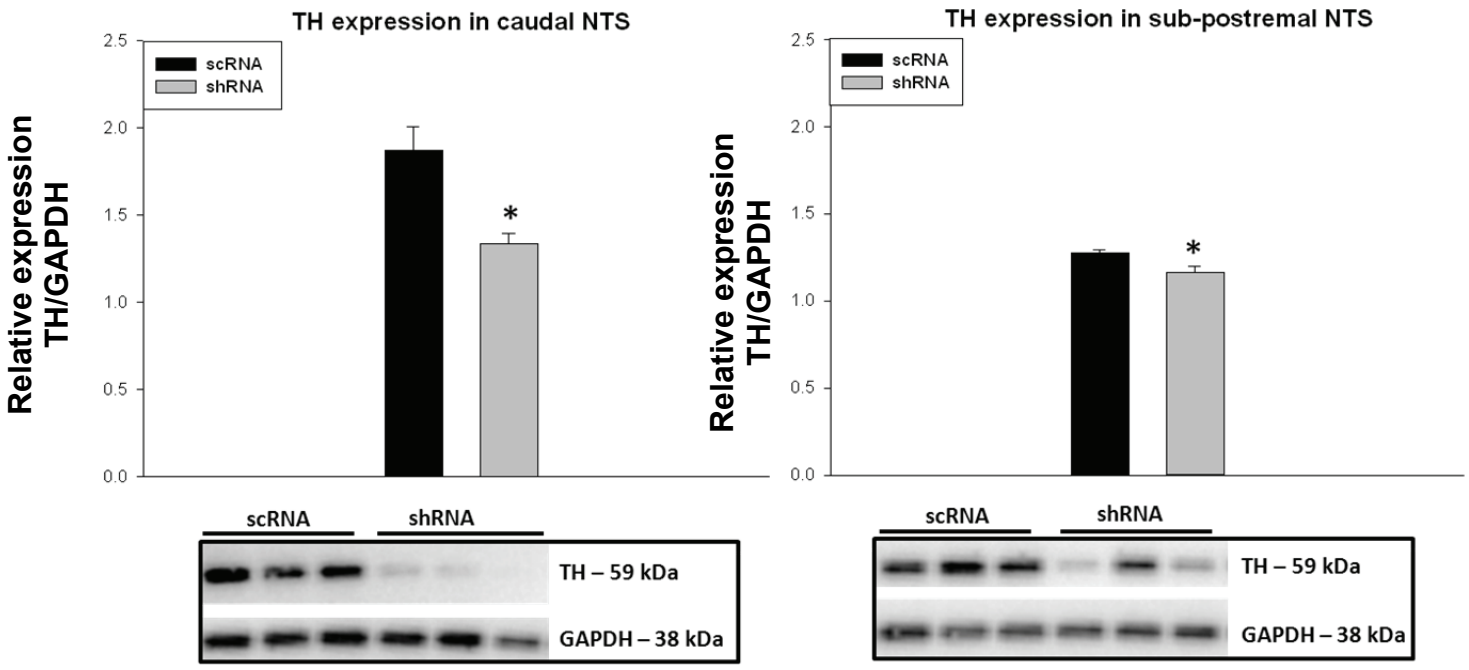

Figure 5. Western blot analysis shows a significant reduction of TH protein levels in caudal NTS (a) and sub-postremal NTS (b) of shRNA virus injected rats when compared to scRNA. TH expression was normalized using GAPDH. * *P*- value < 0.05 vs. scRNA. Caudal NTS: n = 6/group; Sub-postremal: n = 5 in shRNA and n = 6 in scRNA.

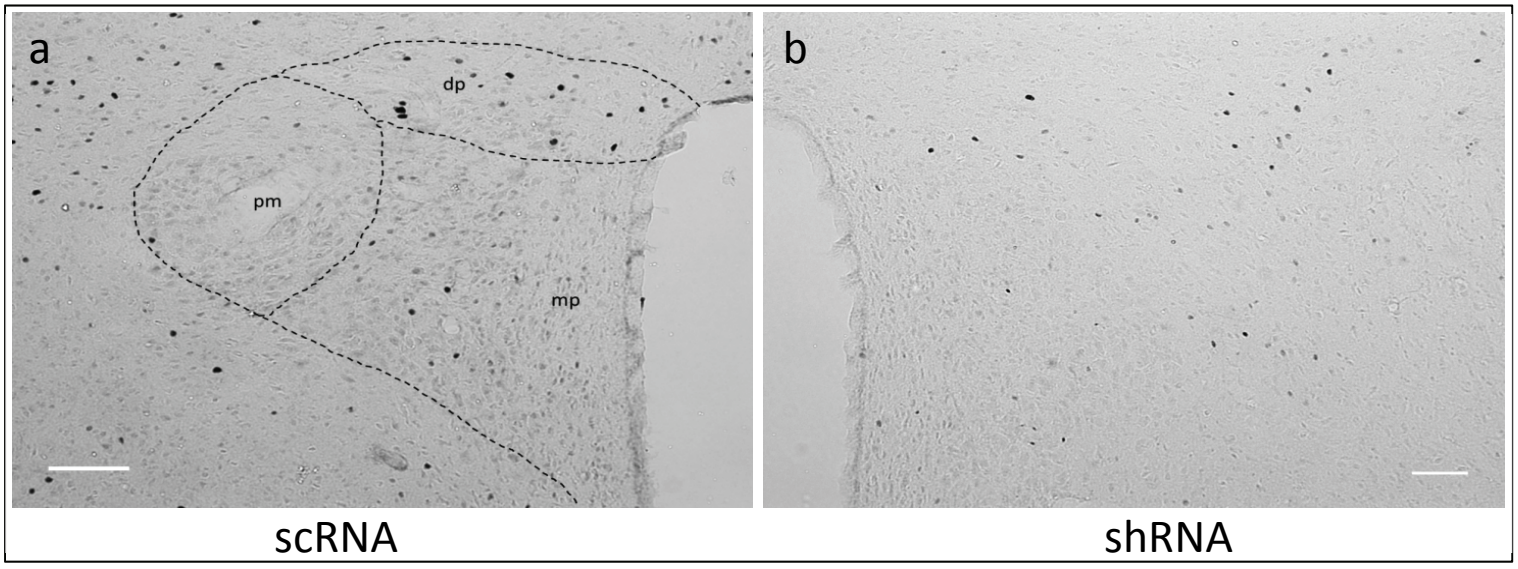

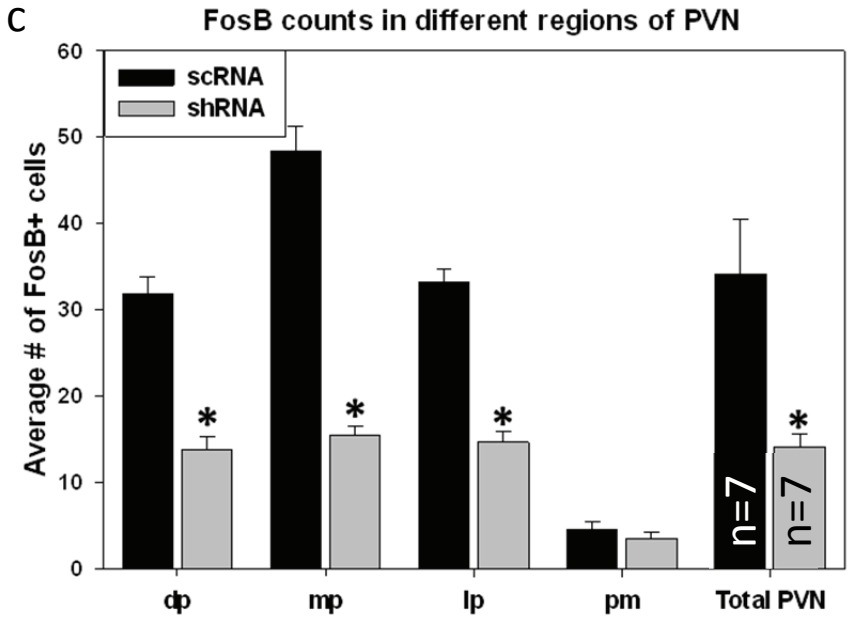

Figure 6. Representative digital images of FosB/ΔFosB staining on one side in PVN regions of scRNA (a) and shRNA (b) rats. Parvo cellular and magnocellular subdivisions are diagrammed in the scRNA (a). Image (c) indicates the mean no. of FosB/ΔFosB-positive cells counted in the different regions with in PVN. * *P*- value < 0.05 vs. scRNA; n= 8/group. dp, Dorsal parvocellular; mp, medial parvocellular; pm, posterior magnocellular; lp, lateral parvocellular (not shown in image (a), as it is found at different level of PVN), Scale bar = 100 µm.

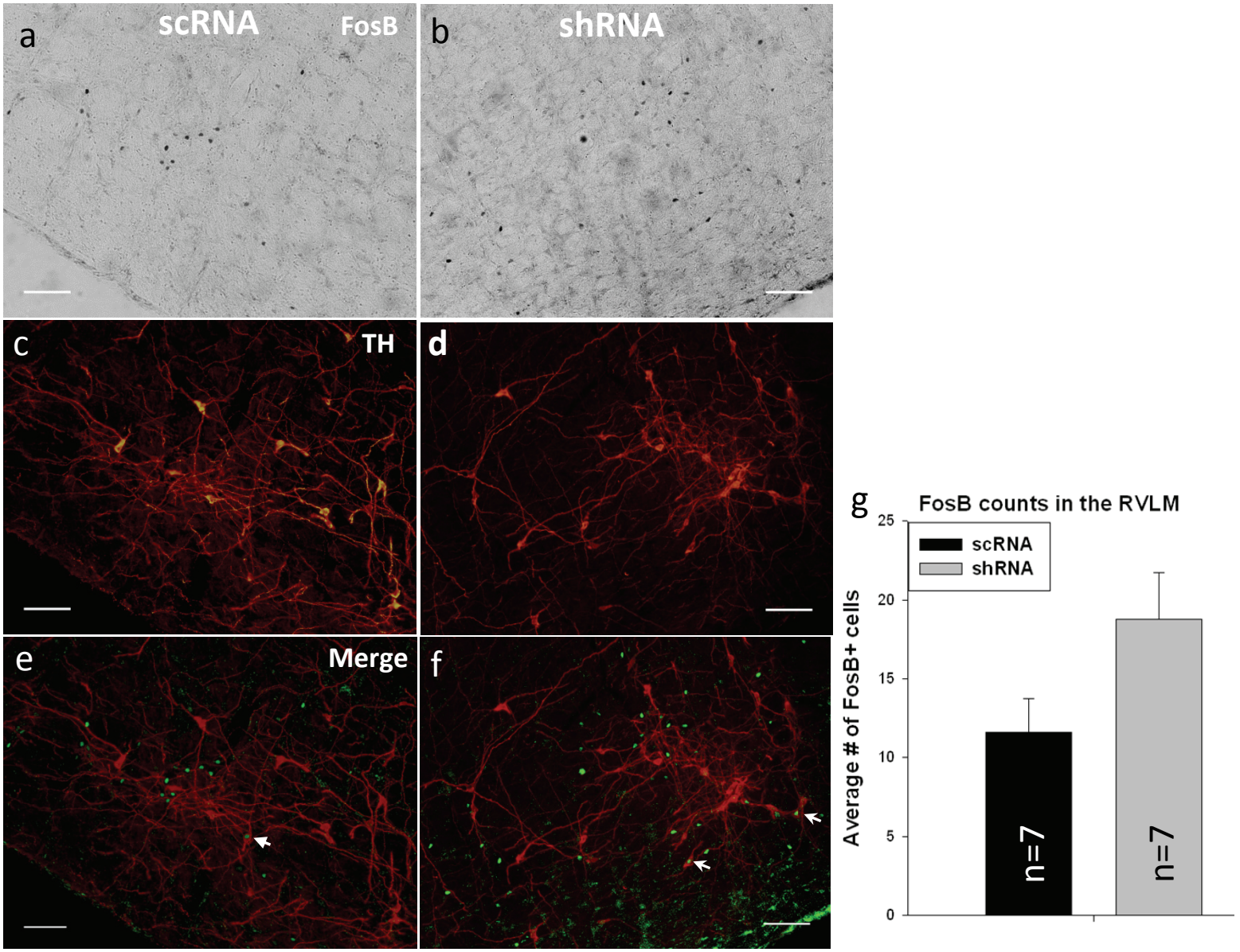

Figure 7. Representative digital images of FosB/ΔFosB staining on one side in RVLM region of scRNA (a) and shRNA (b). c and d are the TH images of scRNA and shRNA respectively, e and f are the colocalized images of FosB/ΔFosB and TH images of scRNA and shRNA respectively. (g) Indicates the mean no. of FosB/ΔFosB-positive cells counted in the RVLM. Arrows point at the TH- FosB/ΔFosB colocalization. n=7/group. Scale bar = 100 µm.

CHAPTER III

LASER CAPTURE MICRODISSECTION REVEALS ALTERATIONS IN mRNA LEVELS IN NTS A2 NEURONS FOLLOWING EXPOSURE TO CHRONIC INTERMITTENT HYPOXIA

Running Title: CIH-induced changes in mRNA levels in A2 neurons

Chandra Sekhar Bathina, T. Prashant Nedungadi, Steve W. Mifflin

Department of Integrative Physiology

Cardiovascular Research Institute

University of North Texas Health Science Center

To be submitted to Am J Physiol Regul Integr Comp Physiol

Abstract

Catecholaminergic A2 neurons in NTS are activated during stressors such as hypoxia and contribute to the increased mean arterial pressure (MAP) following exposure to chronic intermittent hypoxia (CIH), a model of arterial hypoxemia observed during sleep apnea. The aim of this study was to assess the effect of CIH on the mRNA levels of angiotensin-II (Ang-II) and glutamate receptor subunits in A2 neurons. Adeno-associated virus (AAV) vector mediated delivery of green fluorescent protein (GFP) labeled tyrosine hydroxylase promoter (AAV-GFP-TH) was used to label A2 neurons. 7 virus injected rats were exposed to 7 days CIH (alternating 10% O2 and 21% O2 from 8am to 4pm; from 4pm to 8am rats were exposed to 21% O2). Laser capture microdissection was performed to capture groups of 10 A2 neurons. Total RNA from these neurons was extracted and mRNA levels assessed by quantitative real time reverse transcription PCR and compared between the control and CIH rats using $2^{-\Delta\Delta ct}$ method. CIH decreased AngII AT1a receptor (p=0.002; control - 1.08 ± 0.13, n=7; CIH – 0.48 ± 0.07, n= 6) and AMPA receptor GluR2 subunit (p=0.03; control - 1.11 ± 0.24, n=7; CIH-0.52 ± 0.12, n= 6) and increased transcription factor FosB (p=0.03; control - 1.14 ± 0.25, n=7; CIH- 1.97 ± 0.25, n= 5) mRNA levels in the A2 neurons. CIH did not alter mRNA levels of GluR1, NR1, NR2 or delta FosB in A2 neurons. These results indicate that exposure to CIH selectively alters receptor subunit mRNAs in A2 neurons which could influence their responses to ligand and their role in the responses to CIH.

Introduction

The nucleus tractus solitarius (NTS) of the hind brain is the primary site where carotid chemoreceptor (CR) afferent fibers terminate in the central nervous system (CNS) (20) (79). Various phenotypically derived neuronal groups are found throughout the NTS (13, 22, 27, 52, 71) and among these groups are the noradrenergic A2 neurons (16, 67) which express tyrosine hydroxylase (TH), the rate-limiting enzyme in catecholamine synthesis (36, 54). A2 neurons are activated during stressors such as hypoxia (21, 77, 78). A2 neurons express immunoreactivity for the immediate early gene c-fos and it's more stable splice variant FosB following exposure to chronic intermittent hypoxia (CIH) in rats, an animal model to simulate hypoxemia occurring in sleep apnea patients (30, 40). Rats exposed to CIH exhibit increased blood pressure and sympathetic nerve activity, as do human sleep apnea patients (4, 8, 25, 40, 55, 86). Decreasing TH levels in A2 neurons reduces the CIH induced sustained elevation in mean arterial pressure (MAP) (4).

CR afferent fibers release the excitatory amino acid (EAA) glutamate in to the NTS (39, 80, 84). NTS neurons express EAA receptors like α-amino-3-hydroxy-5-methyl-4-isoxazole propionate (AMPA) and *N*-methyl-D-aspartate (NMDA) (80, 84). In addition, recent studies have found that icv infusion of the AngII AT1 receptor antagonist losartan reduces CIH-induced increases in MAP (41) and A2 neurons have been shown to express AngII AT1 receptors (83).

Previous studies have shown that CIH induces changes in the synaptic activation of NTS neurons (39) as well as changes in the responses to exogenous application of AMPA and NMDA (17). However, none of these studies have specifically focused on a phenotypically derived neuronal population, such as the A2 neurons. Our recent finding that reductions in TH in A2 neurons decrease CIH-induced sustained hypertension (4) leads us to propose that changes in EAA and/or

AngII AT1receptors in A2 neurons might contribute to the cardiovascular and respiratory responses to CIH. A novel technique was used to label A2 neurons using adeno-associated virus with TH promoter which enables analysis of mRNA in A2 neurons following CIH exposure.

Materials and Methods

Animals: Adult male Sprague-Dawley rats (250–350g, Charles River Laboratories, Inc., Wilmington, MA, USA) were provided with *ad libitum* food and water and were housed in a thermostatically regulated room (23°C) with 12 hour light: 12 hour dark cycle (12L: 12D, on at 7 AM, off at 7 PM). All experimental procedures were approved by the Institutional Animal Care and Use Committee (IACUC) guidelines of University of North Texas Health Science Center. Experimental procedures were performed after 1 week of acclimatization in the facility.

Adeno-associated virus (AAV): Adeno-associated virus with 2.5kb tyrosine hydroxylase (TH) promoter attached to green fluorescent protein (GFP) was used to label A2 neurons in NTS. The AAV are chimeric serotype AAV1/2 which have the AAV1 and AAV2 serotype proteins expressed on the surface of the virus in a 1:1 ratio and this serotype is a CNS-optimized serotype (31). The construct, AAV1/2-TH promoter-eGFP-WPRE-BGH-polyA was commercially synthesized (GeneDetect, New Zealand) based on the previously published sequences (64) at a titer 1.1x 10^{12} genomic particles/ml. The TH promoter in the constructs drives the over-expression of GFP, the woodchuck post-transcriptional regulatory element (WPRE) and the presence of a bovine growth hormone (BGH) polyadenylation sequence ensures high transcription following transduction.

NTS microinjections: 14 rats were injected with the viral construct. A standard surgical approach was used to expose the caudal medulla region (3, 19). Using a glass micropipette (tip diameter, 50μm), three 100nL injections of virus were performed with the help of pneumatic

picopump (PV 800, WPL, Sarasota, FL, USA) over a 5 minute period. To cover the NTS, the injections were performed at the calamus scriptorius and bilaterally at 0.5 mm rostral and 0.5 mm lateral to calamus.

Immunohistochemistry: As the virus is shown to cause maximal effect after 14 days of injection (33), brains from all microinjected rats were collected on the 21st day from injection. To assess if the GFP was selectively expressed in the A2 neurons, we performed immunohistochemistry for TH on brains of 4 virus injected rats. Rats were anesthetized with thiobutabarbital (100mg/kg i.p Inactin; Sigma, St. Louis, MO) on 21st day and perfused transcardially with phosphate buffered saline followed by 4% paraformaldehyde. Brains were then stored in 30% sucrose at 4°C after postfixing in paraformaldehyde for 1-2 hours. Three sets of 40-µm thick coronal sections of brain stem were collected using Leica cryostat (Leica Microsysytems, Wetzlar, Germany) and stored in cryoprotectant at -20°C until processed for immunohistochemistry. A set of sections were then processed with mouse anti-TH primary antibody (1: 1,000, MAB318; Millipore, Billerica, MA, USA) and a CY3-labeled donkey anti-mouse secondary antibody (1: 250, 715-165-150; Jackson ImmunoResearch, PA, USA).

Imaging and cell counts: Olympus IX-2 DSU confocal microscope (Olympus, Tokyo, Japan) equipped for epifluorescence was used to image TH immuno labeled and GFP labeled neurons in NTS. ImageJ software (v 1.44, NIH, Bethesda, MD, USA) was used to merge the TH and GFP images and also to count (4-5 sections/rat) the number of TH-immunoreactive neurons, GFP labeled neurons and TH+GFP labeled neurons (n=4). NTS regions between 300 µm caudal to obex extending rostrally 300–400 µm beyond the area postrema was used for cell counts. This area corresponds to - 13.2 to - 14.6 mm posterior to bregma according to the atlas of Paxinos and Watson (66).

Chronic intermittent hypoxia: 14 days after injection of virus rats (n=7) were transferred to a commercially available hypoxia chamber system where O_2 concentration was varied using a computerized system (Oxycycler, Biospherix, NY, USA). Rats were exposed to 7 days of CIH, as published earlier (4, 82). An O_2 concentration of 10% for 3 minutes in a 10 minute cycle was achieved by setting the cycles at 9% O_2 for 6 minutes and 21% O_2 for 4 minutes. CIH exposure of rats was done during the light phase to coincide with their sleeping period, from 8am to 4pm (8 hours). From 4pm-8am the rats were exposed to 21% O_2. Control rats (n=7) were housed in normal room air conditions. Following the last day of CIH exposure, the rats were euthanized and brains were collected for LCM of A2 neurons.

Laser capture microdissection (LCM) of GFP labeled A2 neurons: 14 microinjected rats (7 CIH and 7 controls) were used for LCM. Each rat was anesthetized with thiobutabarbital (100mg/kg i.p Inactin; Sigma, St. Louis, MO) and quickly decapitated. The brains were collected immediately and snap frozen in cold isopentane. 10 µm thick serial sections of brain stem at the level of subpostremal and commissural NTS (13.6 to 14.0 mm posterior to bregma) were collected and mounted on PEN membrane coated slides (catalogue no. LCM0522; Arcturus Bioscience, Mountain View, CA, USA) and used immediately for laser capture. An Arcturus Veritas Microdissection instrument (13553-00, version-c) that has an infrared capture laser and ultraviolet cutting laser functionality was used to laser capture the GFP labeled A2 neurons. The capture cap is coated with a thermal plastic film and when placed above the brain tissue mounted on PEN coated slide is melted by infrared laser at the region of interest. The ultraviolet laser is used to specifically cut the selected neurons of interest, allowing the collection of only A2 neurons on to the cap. 10 neurons per cap were collected from each rat and were transferred immediately to a 0.5 ml tube with 30 µl of ArrayPure Nano-Scale Lysis Solution with 5.0 g of

proteinase k (catalogue no. MPS04050; Epicentre Biotechnol Inc. Madison, WI, USA) and vortexed.

RNA extraction: The LCM protocol has been described in detail previously (6, 9, 57). All reactions were performed in RNAse free environment. Total RNA was extracted from each cap with 10 neurons collected per rat; with ArrayPure Nano-Scale RNA Purification Kit reagents (catalogue no. MPS04050; Epicentre Biotechnol Inc. Madison, WI, USA). For this, the cells in above mentioned solution was incubated for 15 min at 65–70°C and the protein was precipitated by addition of 18 µl of MPC Protein Precipitation reagent and centrifuging at 10,000g for 7 min at 4°C. The protein was then concentrated by adding 50 µl of isopropanol to the supernatant, followed by centrifugation at 10,000 g for 5 min at 4°C. The RNA pellet was air dried after discarding supernatant, followed by DNase treatment to remove any contaminating DNA. The RNA is concentrated one more time by addition of 20 µl each of 2X Nano-Scale Lysis Solution and MPC Protein Precipitation Reagent and centrifuging at 10,000 g for 5 min at 4°C followed by addition of 50 µl isopropanol and centrifuging at 10,000 g for 5 min at 4°C to pellet purified RNA. The resulting pellet is air dried after final rinsing with 70% ethanol and resuspended in 7 µl RNase free water supplemented with 1 µl of ScriptGuard RNase inhibitor (Epicentre Biotechnol Inc) before storing at -80°C.

RNA amplification: 3 µl per RNA sample was amplified to aminoallyl-aRNA with partial substitution of the canonical UTP nucleotide by aminoallyl-UTP, using TargetAmp 2-Round Aminoallyl-aRNA Amplification Kit materials (Epicentre Biotechnol Inc.) based on manufacturer's instructions as discussed previously (6). Nanodrop Spectrophotometer (Nanodrop 2000c Spectrophotometer; Thermo Fisher Scientific Inc., Waltham, MA, USA) was used to evaluate the concentration of the aminoallyl-aRNA from all the samples and contamination, if

any. Low 260/280 samples ratio were considered contaminated and not used for reverse transcription.

Quantitative reverse transcriptase-polymerase chain reactions (qRT-PCR): Aminoallyl-aRNA ~ 50 ng from the micro dissected A2 neurons was reverse-transcribed to cDNA using a Sensiscript RT kit (catalog no.205213; Qiagen Inc., Valencia, CA, USA) according to manufacturer's instructions. Forward and reverse primers for target genes (Table 1.) were obtained from Integrated DNA Technologies (Coralville, IA, USA) based on previously published sequences (14, 34, 57, 73). Each 25 µl of PCR sample consisted of 3 µl cDNA, 2 µl of forward and reverse primer mix (final concentration: 1 µM) for target genes (Table 1.), 12.5 µl of iQ SYBR Green Supermix (product no. 170-8880; Bio-Rad, Hercules, CA, USA) and 7.5 µl of RNase/DNase – free water. PCR reactions were performed in a Bio-RadiQTM5 iCycler system, with the cycle parameters: denaturation at 95°C for 3 min followed by 40 cycles of 1 min each (30 s at 94°C; followed by annealing and real-time quantitation for 30 s at 60°C for GluR1, GluR2, NR1, NR2A, AT1a, AT1b, FosB and ΔFosB, 55°C for TH and 1 min at 65°C for GAPDH). The mRNA levels were normalized using housekeeping gene, GAPDH. In each RT-PCR analysis, no template and RT controls were performed. Primer-dimers and nonspecific products were analyzed by generating melt curves. Target genes mRNA level in CIH animals was compared to controls based on Ct values using $2^{-\Delta\Delta Ct}$ method (45, 70) where in, the experimental group gene of interest's Ct value is normalized with the house keeping genes Ct value followed by normalization with the control group Ct values.

Statistical analysis: All data are presented as mean ± SE. Student t-test was conducted using SigmaPlot (SigmaPlot, SystatSoftware, Inc. San Jose, CA) to check for differences between control and CIH groups. $P \leq 0.05$ was considered statistically significant.

Results

AAV successfully labeled A2 neurons: Figure 1a demonstrates that the successful injection and transfection of viral constructs into NTS. Figure 1b shows the TH- immunoreactivity in the same section while Figure 1c shows colocalization, demonstrating that most of the GFP with in the NTS is colocalized in the TH-ir neurons. Figure 2 is a high magnification image of a unilateral side of NTS showing the precision with which the GFP is being expressed only in the TH-ir neurons. Analysis of average counts from 3 - 9 sections/rat in 4 rats injected with (AAV-GFP-TH) revealed that 85±3% of TH immunoreactive cells are GFP labeled and 91±3% of GFP labeled neurons are TH immunoreactive (Table 2).

LCM of A2 neurons: A representative images of laser capture microdissection of A2 neurons are shown in Figure 3. Figure 3a shows a low magnification image of a section of NTS with GFP localized in the NTS. Figure 3b labeled A2 neurons before capture and a bright field image of the same section in Figure 3c. Figure 3d and 3e displays the section after microdissecting the A2 neurons under fluorescence and bright field respectively, showing the specificity of the capture. The microdissected A2 neurons are collected on to a cap, as discussed above. Figure 3f and 3g represents the captured neurons on the cap under fluorescent and bright field, which also reveals that there was no random collection of tissue on the cap other than the A2 neurons.

qRT-PCR analysis of microdissected A2 neurons: We tested the effect of CIH on the NTS A2 neurons mRNA levels of TH, AngII receptor type1 subtypes AT1a and AT1b, ionotropic receptors; AMPA and NMDA receptor subunits GluR1 and GluR2; NR1 and NR2a respectively, in comparison to control rats. GAPDH was used as the house-keeping gene for all the genes of interest. AT1 receptor subtype AT1a (Figure 4b) and AMPA receptor subunit GluR2 (Figure 4g) mRNA levels decreased significantly following 7 days of CIH. FosB mRNA level increased

significantly (Figure 4d). The changes noticed in mRNA levels of TH (Figure 4a), AT1b (Figure 4c), ΔFosB (Figure 4e), GluR1 (Figure 4f), NR1 (Figure 4h) and NR2a (Figure 4i) were not significant ($P > 0.05$) when compared to control. Figure 4j and figure 4k display the relative fluorescence amplification curves and melt curves respectively of AT1a RT-PCR. Melt curves were generated for all the RT-PCR runs.

Western blot analysis from NTS punches: Following mRNA analysis of A2 neurons, we desired to analyze the changes in protein levels of the genes that displayed significant changes following CIH in A2 region, but, due technical difficulties of low protein concentrations from the microdissected A2 neurons, we did western blot analysis of the whole NTS punches at sub-postremal and caudal regions. The changes in TH protein levels were not significant in both caudal and sub-postremal NTS ($P > 0.05$) (Figure 5A and B). GluR1 and GluR2 protein level changes were not significant in the caudal NTS, however, there was a significant decrease ($P < 0.05$) in GluR1 protein levels and significant increase ($P < 0.05$) in GluR2 protein levels in sub-postremal NTS (Figure 5A and 5B)

Discussion

Attempts to determine the cellular alterations that accompany adaptations to chronic changes in physiological state are difficult in the NTS. Neurons with a variety of phenotypes and functions are mixed with no anatomical organization to enable reliable analysis of a specific group of cells. LCM enables analysis of mRNA levels in phenotypically-defined neurons (56, 58). The studies reported here used LCM to analyze mRNA levels in catecholaminergic NTS neurons following a chronic change in physiological state.

Intermittent hypoxia: Exposure to intermittent hypoxia, a model of the arterial hypoxemia that accompanies sleep apnea, increases blood pressure and sympathetic outflow (4, 40, 75). Both

remain elevated even during periods when the rats are not exposed to hypoxia. The persistent increase in blood pressure and sympathetic outflow depend upon chemoreceptor input to the CNS (24, 44). There is also a role for AngII AT1 receptors in the persistent increase in blood pressure and sympathetic outflow as systemic (26, 48) and icv (41) injections of losartan reduce CIH-induced increases in blood pressure. Several reports indicate that exposure to CIH is associated with alterations in NTS neuronal responses to excitatory synaptic inputs and exogenous application of excitatory amino acid agonists (17, 39).

A2 neurons: Noradrenergic neurons in caudal NTS (A2 neurons) play a role in a variety of homeostatic responses (69) and have been implicated in responses to stressors (68) (65). A2 neurons are activated during acute exposures to systemic hypoxia (21, 77, 78) and following CIH (40). A recent study from our lab reported that reductions in TH within hindbrain catecholaminergic neurons reduced the sustained increase in blood pressure observed following exposure to CIH (4), indicating that this aspect of the response to CIH is dependent upon A2 neurons.

Technical considerations Previous studies from our lab and others have shown that CIH induces alterations in the levels of several mRNAs and proteins in the NTS (21, 23, 30, 35). A limitation of these studies was that sample was obtained from punches of NTS which no doubt quantification levels of the gene or protein of interest from adjacent, non-relevant neurons as well as those receiving arterial chemoreceptor inputs. To determine the gene expression changes occurring only in the A2 neurons, we have used viral mediated GFP labeling of A2 neurons followed by LCM to selectively capture A2 neurons for analysis. Our recent publications have successfully demonstrated that the RNA extracted using LCM is good for gene analysis (56, 58).

LCM facilitates analysis of mRNA levels in phenotypically identified neurons (56, 58). Most uses of LCM involve a rapid immunohistochemical processing of tissue to characterize phenotype while maintaining neuronal viability (56, 58). The immunohistochemical protocols typically expose tissue to very high concentrations of primary and secondary antibodies for short periods of time. We used an adenoviral construct designed so that catecholaminergic neurons can be identified by the presence of GFP, eliminating the need for rapid immunohistochemical processing of the tissue. It also enables capture of neurons much sooner after sectioning of the brain as the time required for immunohistochemical processing of the tissue is eliminated. We used immunohistochemistry to verify that the viral vector was indeed generating GFP expression only in catecholaminergic neurons (Figures 1 and 2, Table 2). Neuronal levels of mRNA are dynamic. The present analysis cannot distinguish a change in mRNA level that results from altered transcription or a post-transcriptional alteration that alters message stability. Unfortunately, at this point we have been unable to measure protein in small groups of neurons.

Tyrosine hydroxylase TH levels within the carotid body (15) and dorso-medial medulla are increased following exposures to intermittent hypoxia (29). We found no difference in TH mRNA following exposure to CIH; however other aspects of enzyme function, such as activity, might be altered. Post-translational modifications such as phosphorylation can increase TH activity following CIH (29); however analyses of protein are necessary to determine if such changes occur in NTS after exposure to CIH. One downstream effect of activation of A2 neurons is the activation of the HPA-ACTH-corticosterone stress pathway. Following exposure to CIH, increased plasma CORT levels have been reported following sacrifice by decapitation (85). We have reported that exposure to CIH enhances the increase in plasma ACTH induced by a novel stressor such as restraint (46). These results suggest that the downstream effects of A2

neurons might not be associated with alterations in the TH content of A2 neurons, but rather the activity of a given neuron.

FosB and ΔFosB Neurons exhibit adaptations that lead to alterations in function in response to repeated exposures to a stressful stimulus. Studies to understand the molecular mechanisms that mediate these changes led to the discovery of the activator protein 1 (AP-1) family of transcription factors (5, 37). AP-1 transcription factors modulate gene expression during acute stress (72). Studies by Nestler group demonstrated that chronic, repeated stimuli can also modulate gene expression via AP-1 transcription factor activated by FosB and its more stable splice variant ΔFosB (10, 42, 61). Chronic, repetitive stimulation or stress induces expression of FosB/ ΔFosB, which have a longer time course and stable expression than the immediate early gene c-fos (32, 50, 60, 63). FosB/ΔFosB have been linked to neuronal adaptations and plasticity under conditions like drug addiction, epilepsy and long-term potentiation (11, 47, 50, 59, 60, 62, 63).

Using an antibody that does not distinguish FosB from ΔFosB, our group demonstrated that CIH induces FosB/ ΔFosB expression in A2 and non-catecholaminergic neurons of NTS (40) suggesting that NTS neurons may exhibit alterations in gene expression and function after exposure to CIH. We performed mRNA analysis for both FosB and ΔFosB in LCM captured A2 neurons. CIH induced increased mRNA levels of FosB and no change in ΔFosB levels in A2 neurons after exposure to CIH. ΔFosB mRNA levels are not elevated at times when other chronic Fos-related antigens (FRAs) are induced (Chen et al., 1995; Pennypacker et al., 1995), however recent work indicates that the chronic FRAs are products of the FosB gene. Induction of the chronic FRAs by repeated cocaine or electro-convulsive shock treatment is completely abolished in FosB knock-out mice (Hiroi et al., 1996, 1997). Nestler's group (1977)

demonstrated that the chronic FRAs are highly stable, modified forms of ΔFosB proteins. It is possible that FosB induces neuronal alterations following exposure to CIH.

Excitatory amino acid receptors Peripheral chemoreceptor afferents release glutamate in the caudal NTS region (53) which can then bind to NMDA and non-NMDA receptors. Neuronal Ca^{2+} influx can occur through ionotropic glutamatergic receptor channels like NMDA and α-amino-3-hydroxy-5-methyl-4-isoxazolepropionate receptor (AMPA). Significant expression of NMDA and AMPA receptors is found in the A2 neurons (80). Glutamate is found to modulate gene expression by inducing transcription factors and phosphorylation of jun proteins to bind to AP-1 sites through calcium calmodulin (CAM) kinase and microtubule-associated protein (Map) kinase pathway (72, 81). Thus, glutamate may play a role in long-term potentiation. Glutamate released from chemoreceptor afferents (53) might cause an increased Ca^{2+} concentration in A2 neurons to induce changes in message levels that facilitate the elevated AP and SNA induced by exposure to CIH.

GluR2 containing AMPA receptors exhibit low calcium permeability (7) and GluR2 mRNA levels are decreased in hypoxic condition (28). We hypothesized that A2 neurons might exhibit reduced GluR2 levels following exposure to CIH. Our results supported the hypothesis, as GluR2 levels in the A2 neurons decreased significantly in CIH rats. A2 neurons would then become more calcium permeable after CIH. As predicted by De Paula et al. (17), changes in receptor subunit composition might alter neuronal responses to glutamate following CIH (17). Moreover, there was no change in the mRNA levels of any NMDA receptor subunits, explaining the absence of any change in NMDA mediated currents in NTS neurons after CIH exposure (39). In contradiction to these studies, there were also findings where tractus-evoked excitatory post synaptic currents (EPSC's) decreased following CIH in NTS neurons (39); however this change

might be mediated by the recently reported dendritic pruning of afferent inputs to NTS neurons following exposure to CIH (2). Further studies using calcium imaging and electrophysiology of A2 and non-A2 neurons in this region will provide better insight into the physiological changes occurring at cellular level of these neurons.

AngII AT1 receptors Angiotensin AT1 receptors have been localized to the carotid body (1) and central sites involved in blood pressure and respiratory regulation (12, 49, 74, 83). The brain possesses an intrinsic renin-angiotensin system which can generate AngII (51). Circulating AngII also plays a role in BP regulation through AT1 receptors in the circumventricular organs of CNS which lack blood brain barrier near NTS (18, 76). The area postrema has been shown to have axonal projections to A2 neurons (67). Moreover, *in situ* hybridization studies have shown that there is a robust expression of AT1 receptor mRNA (AT1a and AT1b) in the NTS (43). The present study demonstrates that AT1a receptor mRNA is expressed in A2 neurons and there are changes occurring in AT1a receptor mRNA levels upon exposure to 7 day CIH. AT1a receptor mRNA has been shown to be the predominant AngII AT1 receptor subtype in the NTS (98%) and likely represent the site of action for angiotensin in the NTS (74). CIH-induced hypertension has been shown to be reduced by the AT1 receptor antagonist losartan administered systemically or during icv injections to selectively target hypothalamic AT1 receptors (41, 48, 86). It is difficult to discern the role that reductions in AT1a mRNA levels in A2 neurons might play in CIH-induced hypertension as reductions of AT1a mRNA in NTS are associated with an increase in baseline blood pressure in SHR (74) and in mice (12). Similarly, AngII microinjections into NTS have been shown to cause depressor and pressor effects (38, 49) depending upon a variety of experimental conditions.

Perspectives and Significance

This is the first study demonstrating gene changes occurring in a phenotypically derived population of A2 neurons following CIH. The novelty of this study is the AAV mediated labeling of the A2 neurons of NTS and their mRNA analysis following LCM capture. The changes in mRNA levels, if translated into protein, could impact the integration of excitatory inputs to A2 neurons and A2 neuronal function in a variety of stressful situations.

Acknowledgements

The authors gratefully acknowledge the expert technical assistance of Anuradha Rajulapati. This work was funded by HL80556.

Conflicts of Interest

None

References

1. **Allen AM**. Angiotensin AT1 receptor-mediated excitation of rat carotid body chemoreceptor afferent activity. *J Physiol* 510 (Pt 3): 773-781, 1998.

2. **Almado CE, Machado BH, and Leao RM**. Chronic intermittent hypoxia depresses afferent neurotransmission in NTS neurons by a reduction in the number of active synapses. *J Neurosci* 32: 16736-16746, 2012.

3. **Barraco RA, Janusz CJ, Polasek PM, Parizon M, and Roberts PA**. Cardiovascular effects of microinjection of adenosine into the nucleus tractus solitarius. *Brain Res Bull* 20: 129-132, 1988.

4. **Bathina CS, Rajulapati A, Franzke M, Yamamoto K, Cunningham JT, and Mifflin SW**. Knockdown of Tyrosine Hydroxylase in the Nucleus of the Solitary Tract Reduces Elevated Blood Pressure during Chronic Intermittent Hypoxia. *Am J Physiol Regul Integr Comp Physiol* 2013.

5. **Baum MJ, Brown JJ, Kica E, Rubin BS, Johnson RS, and Papaioannou VE**. Effect of a null mutation of the c-fos proto-oncogene on sexual behavior of male mice. *Biol Reprod* 50: 1040-1048, 1994.

6. **Briski KP, Nedungadi TP, and Koshy Cherian A**. Effects of hypoglycaemia on neurotransmitter and hormone receptor gene expression in laser-dissected arcuate neuropeptide Y/agouti-related peptide neurones. *J Neuroendocrinol* 22: 599-607, 2010.

7. **Burnashev N**. Calcium permeability of ligand-gated channels. *Cell Calcium* 24: 325-332, 1998.

8. **Carlson JT, Hedner J, Elam M, Ejnell H, Sellgren J, and Wallin BG**. Augmented resting sympathetic activity in awake patients with obstructive sleep apnea. *Chest* 103: 1763-1768, 1993.

9. **Carreno FR, Walch JD, Dutta M, Nedungadi TP, and Cunningham JT**. Brain-Derived Neurotrophic Factor-Tyrosine Kinase B Pathway Mediates NMDA Receptor NR2B Subunit Phosphorylation in the Supraoptic Nuclei Following Progressive Dehydration. *J Neuroendocrinol* 23: 894-905, 2011.

10. **Chao J, and Nestler EJ**. Molecular neurobiology of drug addiction. *Annu Rev Med* 55: 113-132, 2004.

11. **Chen J, Zhang Y, Kelz MB, Steffen C, Ang ES, Zeng L, and Nestler EJ**. Induction of cyclin-dependent kinase 5 in the hippocampus by chronic electroconvulsive seizures: role of [Delta]FosB. *J Neurosci* 20: 8965-8971, 2000.

12. **Chen Y, Chen H, Hoffmann A, Cool DR, Diz DI, Chappell MC, Chen AF, and Morris M**. Adenovirus-mediated small-interference RNA for in vivo silencing of angiotensin AT1a receptors in mouse brain. *Hypertension* 47: 230-237, 2006.

13. **Cone RD**. Anatomy and regulation of the central melanocortin system. *Nat Neurosci* 8: 571-578, 2005.

14. **Counts SE, McGuire SO, Sortwell CE, Crawley JN, Collier TJ, and Mufson EJ**. Galanin inhibits tyrosine hydroxylase expression in midbrain dopaminergic neurons. *J Neurochem* 83: 442-451, 2002.

15. **Czyzyk-Krzeska MF, Bayliss DA, Lawson EE, and Millhorn DE**. Regulation of tyrosine hydroxylase gene expression in the rat carotid body by hypoxia. *J Neurochem* 58: 1538-1546, 1992.

16. **Dahlstroem A, and Fuxe K**. Evidence for the Existence of Monoamine-Containing Neurons in the Central Nervous System. I. Demonstration of Monoamines in the Cell Bodies of Brain Stem Neurons. *Acta Physiol Scand Suppl* SUPPL 232:231-255, 1964.

17. **de Paula PM, Tolstykh G, and Mifflin S**. Chronic intermittent hypoxia alters NMDA and AMPA-evoked currents in NTS neurons receiving carotid body chemoreceptor inputs. *Am J Physiol Regul Integr Comp Physiol* 292: R2259-2265, 2007.

18. **Dempsey EW, and Wislocki GB**. An electron microscopic study of the blood-brain barrier in the rat, employing silver nitrate as a vital stain. *J Biophys Biochem Cytol* 1: 245-256, 1955.

19. **Doba N, and Reis DJ**. Acute fulminating neurogenic hypertension produced by brainstem lesions in the rat. *Circ Res* 32: 584-593, 1973.

20. **Donoghue S, Felder RB, Jordan D, and Spyer KM**. The central projections of carotid baroreceptors and chemoreceptors in the cat: a neurophysiological study. *J Physiol* 347: 397-409, 1984.

21. **Dumas S, Pequignot JM, Ghilini G, Mallet J, and Denavit-Saubie M**. Plasticity of tyrosine hydroxylase gene expression in the rat nucleus tractus solitarius after ventilatory acclimatization to hypoxia. *Brain Res Mol Brain Res* 40: 188-194, 1996.

22. **Dunn-Meynell AA, Routh VH, Kang L, Gaspers L, and Levin BE**. Glucokinase is the likely mediator of glucosensing in both glucose-excited and glucose-inhibited central neurons. *Diabetes* 51: 2056-2065, 2002.

23. **Durgam VR, Vitela M, and Mifflin SW**. Enhanced gamma-aminobutyric acid-B receptor agonist responses and mRNA within the nucleus of the solitary tract in hypertension. *Hypertension* 33: 530-536, 1999.

24. **Fletcher EC, Lesske J, Behm R, Miller CC, 3rd, Stauss H, and Unger T**. Carotid chemoreceptors, systemic blood pressure, and chronic episodic hypoxia mimicking sleep apnea. *J Appl Physiol* 72: 1978-1984, 1992.

25. **Fletcher EC, Lesske J, Qian W, Miller CC, 3rd, and Unger T**. Repetitive, episodic hypoxia causes diurnal elevation of blood pressure in rats. *Hypertension* 19: 555-561, 1992.

26. **Fletcher EC, Orolinova N, and Bader M**. Blood pressure response to chronic episodic hypoxia: the renin-angiotensin system. *J Appl Physiol* 92: 627-633, 2002.

27. **Geerling JC, Engeland WC, Kawata M, and Loewy AD**. Aldosterone target neurons in the nucleus tractus solitarius drive sodium appetite. *J Neurosci* 26: 411-417, 2006.

28. **Gorter JA, Petrozzino JJ, Aronica EM, Rosenbaum DM, Opitz T, Bennett MV, Connor JA, and Zukin RS**. Global ischemia induces downregulation of Glur2 mRNA and increases AMPA receptor-mediated Ca2+ influx in hippocampal CA1 neurons of gerbil. *J Neurosci* 17: 6179-6188, 1997.

29. **Gozal E, Shah ZA, Pequignot JM, Pequignot J, Sachleben LR, Czyzyk-Krzeska MF, Li RC, Guo SZ, and Gozal D**. Tyrosine hydroxylase expression and activity in the rat brain: differential regulation after long-term intermittent or sustained hypoxia. *J Appl Physiol* 99: 642-649, 2005.

30. **Greenberg HE, Sica AL, Scharf SM, and Ruggiero DA**. Expression of c-fos in the rat brainstem after chronic intermittent hypoxia. *Brain Res* 816: 638-645, 1999.

31. **Hauck B, Chen L, and Xiao W**. Generation and characterization of chimeric recombinant AAV vectors. *Mol Ther* 7: 419-425, 2003.

32. **Herdegen T, and Leah JD**. Inducible and constitutive transcription factors in the mammalian nervous system: control of gene expression by Jun, Fos and Krox, and CREB/ATF proteins. *Brain Res Brain Res Rev* 28: 370-490, 1998.

33. **Hommel JD, Sears RM, Georgescu D, Simmons DL, and DiLeone RJ**. Local gene knockdown in the brain using viral-mediated RNA interference. *Nat Med* 9: 1539-1544, 2003.

34. **Horii A, Smith PF, and Darlington CL**. Quantitative changes in gene expression of glutamate receptor subunits/subtypes in the vestibular nucleus, inferior olive and flocculus before and following unilateral labyrinthectomy in the rat: real-time quantitative PCR method. *Exp Brain Res* 139: 188-200, 2001.

35. **Huey KA, and Powell FL**. Time-dependent changes in dopamine D(2)-receptor mRNA in the arterial chemoreflex pathway with chronic hypoxia. *Brain Res Mol Brain Res* 75: 264-270, 2000.

36. **Kalia M, Fuxe K, and Goldstein M**. Rat medulla oblongata. II. Dopaminergic, noradrenergic (A1 and A2) and adrenergic neurons, nerve fibers, and presumptive terminal processes. *J Comp Neurol* 233: 308-332, 1985.

37. **Karin M, Liu Z, and Zandi E**. AP-1 function and regulation. *Curr Opin Cell Biol* 9: 240-246, 1997.

38. **Katsunuma N, Tsukamoto K, Ito S, and Kanmatsuse K**. Enhanced angiotensin-mediated responses in the nucleus tractus solitarii of spontaneously hypertensive rats. *Brain Res Bull* 60: 209-214, 2003.

39. **Kline DD, Ramirez-Navarro A, and Kunze DL**. Adaptive depression in synaptic transmission in the nucleus of the solitary tract after in vivo chronic intermittent hypoxia: evidence for homeostatic plasticity. *J Neurosci* 27: 4663-4673, 2007.

40. **Knight WD, Little JT, Carreno FR, Toney GM, Mifflin SW, and Cunningham JT**. Chronic intermittent hypoxia increases blood pressure and expression of FosB/DeltaFosB in central autonomic regions. *Am J Physiol Regul Integr Comp Physiol* 301: R131-139, 2011.

41. **Knight WD, Saxena A, Shell B, Nedungadi TP, Mifflin SW, and Cunningham JT**. Central losartan attenuates increases in arterial pressure and expression of FosB/DeltaFosB along the autonomic axis associated with chronic intermittent hypoxia. *Am J Physiol Regul Integr Comp Physiol* 305: R1051-1058, 2013.

42. **Koob GF, and Nestler EJ**. The neurobiology of drug addiction. *J Neuropsychiatry Clin Neurosci* 9: 482-497, 1997.

43. **Lenkei Z, Palkovits M, Corvol P, and Llorens-Cortes C**. Distribution of angiotensin type-1 receptor messenger RNA expression in the adult rat brain. *Neuroscience* 82: 827-841, 1998.

44. **Lesske J, Fletcher EC, Bao G, and Unger T**. Hypertension caused by chronic intermittent hypoxia--influence of chemoreceptors and sympathetic nervous system. *J Hypertens* 15: 1593-1603, 1997.

45. **Livak KJ, and Schmittgen TD**. Analysis of relative gene expression data using real-time quantitative PCR and the 2(-Delta Delta C(T)) Method. *Methods* 25: 402-408, 2001.

46. **Ma S, Mifflin SW, Cunningham JT, and Morilak DA**. Chronic intermittent hypoxia sensitizes acute hypothalamic-pituitary-adrenal stress reactivity and Fos induction in the rat locus coeruleus in response to subsequent immobilization stress. *Neuroscience* 154: 1639-1647, 2008.

47. **Madsen TM, Bolwig TG, and Mikkelsen JD**. Differential regulation of c-Fos and FosB in the rat brain after amygdala kindling. *Cell Mol Neurobiol* 26: 87-100, 2006.

48. **Marcus NJ, Li YL, Bird CE, Schultz HD, and Morgan BJ**. Chronic intermittent hypoxia augments chemoreflex control of sympathetic activity: role of the angiotensin II type 1 receptor. *Respir Physiol Neurobiol* 171: 36-45, 2010.

49. **Matsumura K, Averill DB, and Ferrario CM**. Angiotensin II acts at AT1 receptors in the nucleus of the solitary tract to attenuate the baroreceptor reflex. *Am J Physiol* 275: R1611-1619, 1998.

50. **McClung CA, Ulery PG, Perrotti LI, Zachariou V, Berton O, and Nestler EJ**. DeltaFosB: a molecular switch for long-term adaptation in the brain. *Brain Res Mol Brain Res* 132: 146-154, 2004.

51. **McKinley MJ, Albiston AL, Allen AM, Mathai ML, May CN, McAllen RM, Oldfield BJ, Mendelsohn FA, and Chai SY**. The brain renin-angiotensin system: location and physiological roles. *Int J Biochem Cell Biol* 35: 901-918, 2003.

52. **Mifflin SW**. Arterial chemoreceptor input to nucleus tractus solitarius. *Am J Physiol* 263: R368-375, 1992.

53. **Mizusawa A, Ogawa H, Kikuchi Y, Hida W, Kurosawa H, Okabe S, Takishima T, and Shirato K**. In vivo release of glutamate in nucleus tractus solitarii of the rat during hypoxia. *J Physiol* 478 (Pt 1): 55-66, 1994.

54. **Nagatsu T, Levitt M, and Udenfriend S**. Tyrosine Hydroxylase. The Initial Step in Norepinephrine Biosynthesis. *J Biol Chem* 239: 2910-2917, 1964.

55. **Narkiewicz K, and Somers VK**. The sympathetic nervous system and obstructive sleep apnea: implications for hypertension. *J Hypertens* 15: 1613-1619, 1997.

56. **Nedungadi TP, Carreno FR, Walch JD, Bathina CS, and Cunningham JT**. Region-specific changes in transient receptor potential vanilloid channel expression in the vasopressin

magnocellular system in hepatic cirrhosis-induced hyponatraemia. *J Neuroendocrinol* 24: 642-652, 2012.

57. **Nedungadi TP, Carreno FR, Walch JD, Bathina CS, and Cunningham JT**. Region specific changes in TRPV channel expression in the vasopressin magnocellular system in hepatic cirrhosis induced hyponatremia. *J Neuroendocrinol* 2011.

58. **Nedungadi TP, Dutta M, Bathina CS, Caterina MJ, and Cunningham JT**. Expression and distribution of TRPV2 in rat brain. *Exp Neurol* 237: 223-237, 2012.

59. **Nestler EJ**. Is there a common molecular pathway for addiction? *Nat Neurosci* 8: 1445-1449, 2005.

60. **Nestler EJ**. Molecular basis of long-term plasticity underlying addiction. *Nat Rev Neurosci* 2: 119-128, 2001.

61. **Nestler EJ**. Molecular mechanisms of drug addiction. *Neuropharmacology* 47 Suppl 1: 24-32, 2004.

62. **Nestler EJ**. Molecular neurobiology of addiction. *Am J Addict* 10: 201-217, 2001.

63. **Nestler EJ, Barrot M, and Self DW**. DeltaFosB: a sustained molecular switch for addiction. *Proc Natl Acad Sci U S A* 98: 11042-11046, 2001.

64. **Oh MS, Hong SJ, Huh Y, and Kim KS**. Expression of transgenes in midbrain dopamine neurons using the tyrosine hydroxylase promoter. *Gene Ther* 16: 437-440, 2009.

65. **Pardon MC, Ma S, and Morilak DA**. Chronic cold stress sensitizes brain noradrenergic reactivity and noradrenergic facilitation of the HPA stress response in Wistar Kyoto rats. *Brain Res* 971: 55-65, 2003.

66. **Paxinos G, Watson CR, and Emson PC**. AChE-stained horizontal sections of the rat brain in stereotaxic coordinates. *J Neurosci Methods* 3: 129-149, 1980.

67. **Rinaman L**. Hindbrain noradrenergic A2 neurons: diverse roles in autonomic, endocrine, cognitive, and behavioral functions. *Am J Physiol Regul Integr Comp Physiol* 300: R222-235, 2011.

68. **Ritter S, Dinh TT, and Li AJ**. Hindbrain catecholamine neurons control multiple glucoregulatory responses. *Physiol Behav* 89: 490-500, 2006.

69. **Sawchenko PE, and Swanson LW**. Central noradrenergic pathways for the integration of hypothalamic neuroendocrine and autonomic responses. *Science* 214: 685-687, 1981.

70. **Schmittgen TD, and Livak KJ**. Analyzing real-time PCR data by the comparative C(T) method. *Nat Protoc* 3: 1101-1108, 2008.

71. **Schwartz MW, Woods SC, Porte D, Jr., Seeley RJ, and Baskin DG**. Central nervous system control of food intake. *Nature* 404: 661-671, 2000.

72. **Schwarzschild MA, Cole RL, and Hyman SE**. Glutamate, but not dopamine, stimulates stress-activated protein kinase and AP-1-mediated transcription in striatal neurons. *J Neurosci* 17: 3455-3466, 1997.

73. **Schwendt M, and Jezova D**. Gene expression of two glutamate receptor subunits in response to repeated stress exposure in rat hippocampus. *Cell Mol Neurobiol* 20: 319-329, 2000.

74. **Shan Z, Zubcevic J, Shi P, Jun JY, Dong Y, Murca TM, Lamont GJ, Cuadra A, Yuan W, Qi Y, Li Q, Paton JF, Katovich MJ, Sumners C, and Raizada MK**. Chronic knockdown of the nucleus of the solitary tract AT1 receptors increases blood inflammatory-endothelial progenitor cell ratio and exacerbates hypertension in the spontaneously hypertensive rat. *Hypertension* 61: 1328-1333, 2013.

75. **Silva AQ, and Schreihofer AM**. Altered sympathetic reflexes and vascular reactivity in rats after exposure to chronic intermittent hypoxia. *J Physiol* 589: 1463-1476, 2011.

76. **Simpson JB**. The circumventricular organs and the central actions of angiotensin. *Neuroendocrinology* 32: 248-256, 1981.

77. **Soulier V, Cottet-Emard JM, Pequignot J, Hanchin F, Peyrin L, and Pequignot JM**. Differential effects of long-term hypoxia on norepinephrine turnover in brain stem cell groups. *J Appl Physiol* 73: 1810-1814, 1992.

78. **Soulier V, Dalmaz Y, Cottet-Emard JM, Kitahama K, and Pequignot JM**. Delayed increase of tyrosine hydroxylation in the rat A2 medullary neurons upon long-term hypoxia. *Brain Res* 674: 188-195, 1995.

79. **Torrealba F, and Claps A**. The carotid sinus connections: a WGA-HRP study in the cat. *Brain Res* 455: 134-143, 1988.

80. **Vardhan A, Kachroo A, and Sapru HN**. Excitatory amino acid receptors in commissural nucleus of the NTS mediate carotid chemoreceptor responses. *Am J Physiol* 264: R41-50, 1993.

81. **Xia Z, Dudek H, Miranti CK, and Greenberg ME**. Calcium influx via the NMDA receptor induces immediate early gene transcription by a MAP kinase/ERK-dependent mechanism. *J Neurosci* 16: 5425-5436, 1996.

82. **Yamamoto K, Eubank W, Franzke M, and Mifflin S**. Resetting of the sympathetic baroreflex is associated with the onset of hypertension during chronic intermittent hypoxia. *Auton Neurosci* 173: 22-27, 2013.

83. **Yang SN, Lippoldt A, Jansson A, Phillips MI, Ganten D, and Fuxe K**. Localization of angiotensin II AT1 receptor-like immunoreactivity in catecholaminergic neurons of the rat medulla oblongata. *Neuroscience* 81: 503-515, 1997.

84. **Zhang W, and Mifflin SW**. Excitatory amino-acid receptors contribute to carotid sinus and vagus nerve evoked excitation of neurons in the nucleus of the tractus solitarius. *J Auton Nerv Syst* 55: 50-56, 1995.

85. **Zoccal DB, Bonagamba LG, Antunes-Rodrigues J, and Machado BH**. Plasma corticosterone levels is elevated in rats submitted to chronic intermittent hypoxia. *Auton Neurosci* 134: 115-117, 2007.

86. **Zoccal DB, Bonagamba LG, Oliveira FR, Antunes-Rodrigues J, and Machado BH**. Increased sympathetic activity in rats submitted to chronic intermittent hypoxia. *Exp Physiol* 92: 79-85, 2007.

Table 1. Real-Time Quantitative-Reverse Transcriptase PCR primer sequences
GAPDH
Forward: 5’- CTCATGACCACAGTCCATGC - 3’
Reverse: 5’-TACATTGGGGGTAGGAACAC-3’
TH
Forward: 5’-TTTGAAAAAATTCACCA-3’
Reverse: 5’-GGCAATCTCTGCAATCAGCT-3’
AT1a
Forward: 5’- TTCTCAATCTCGCCTTGGCTGACT-3’
Reverse: 5’- AAGGAACACACTGGCGTAGAGGTT-3’
AT1b
Forward: 5’- CAAAAGGAGATGGGAGGTCA-3’
Reverse: 5’- AGCAGTTTGGCTTTGCAACT-3’
FosB
Forward: 5’- GTGAGAGATTTGCCAGGGTC-3’
Reverse: 5’- AGAGAGAAGCCGTCAGGTTG-3’
Δ FosB
Forward: 5’ – AGGCAGAGCTGGAGTCGGAGAT- 3’
Revers: 5’ – GCCGAGGACTTGAACTTCACTCG – 3’
GluR1
Forward: 5’- CAGATCGATATTGTGAACATCA -3’
Reverse: 5’- CCTGAAAGAGCATCTGGTAT -3’
GluR2

Forward: 5′-CGGGTAGGGATGGTTCAGTTT-3′

Reverse: 5′-TGGCTACCTCCAAATTGTCGAT-3′

NR1

Forward: 5′-GTTCTTCCGCTCAGGCTTTG-3′

Reverse: 5′-AGGGAAACGTTCTGCTTCCA-3′

NR2A

Forward: 5′-AGCCCCCTTCGTCATCGTA-3′
Reverse: 5′-GACAGGGCACCGTGTTCCT-3′

Table 2.		
	TH%	GFP%
Rat 1	78.5	95.8
Rat 2	83.6	86.2
Rat 3	87.1	83.5
Rat 4	91.8	96.5
Average	85.25	90.5
STDEV	5.62	6.62
SEM	2.8	3.3
TH % - Percentage of TH positive cells that are GFP labeled GFP % - Percentage of GFP labeled cells that are TH positive		
Analysis of 3 - 9 sections/rats in 4 rats revealed that 85±3% of TH immunoreactive cells to be GFP labeled and 91±3% of GFP labeled neurons to be TH immunoreactive.		

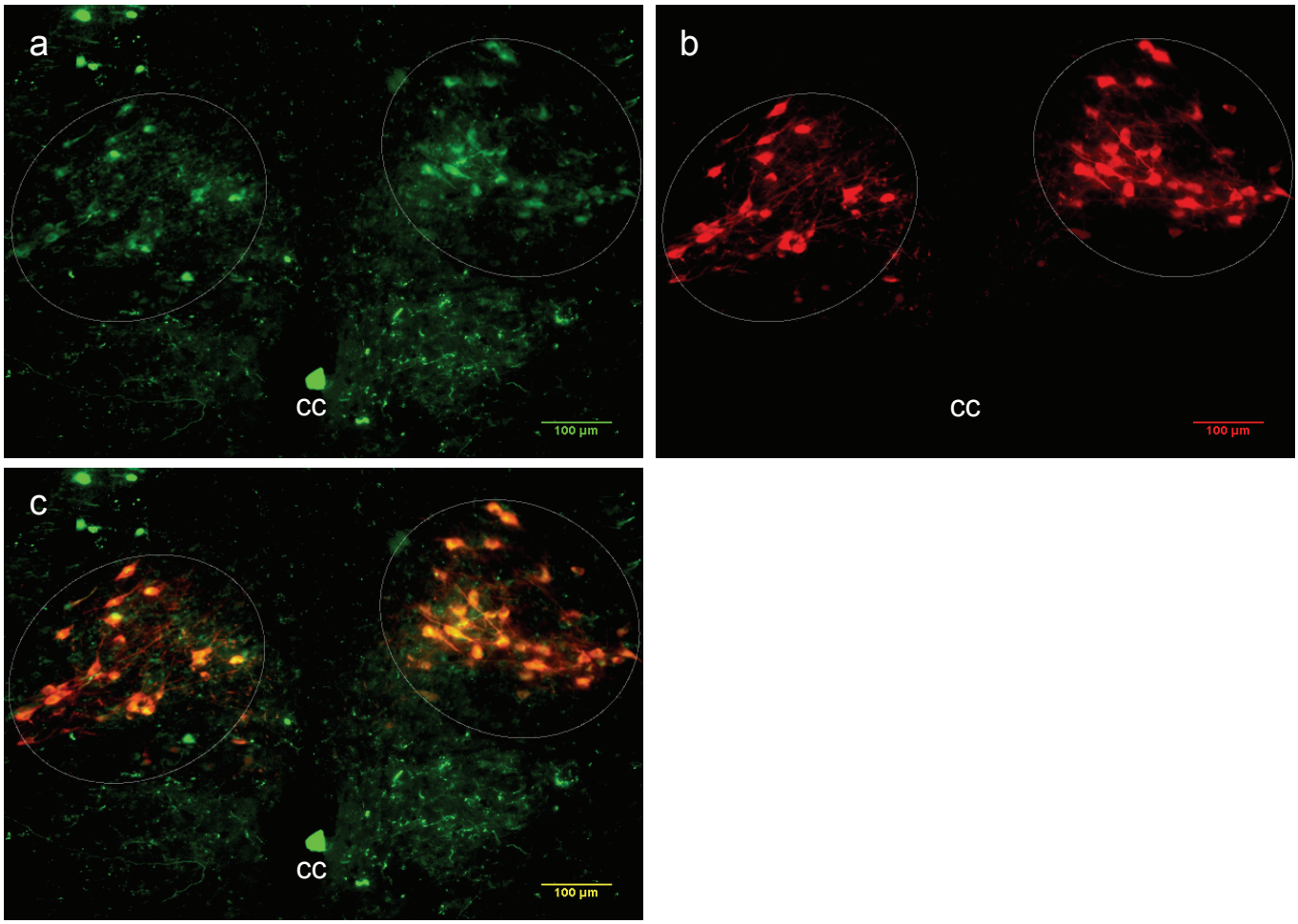

Figure 1. Labeling of A2 neurons bilaterally in the NTS by AAV-GFP-TH. (a) Neurons of NTS expressing GFP following virus injections (b) Cy3 labeled A2 neurons following immunohistochemistry for TH (c) superimposed image of a and b showing colocalization of GFP expression with TH positive cells. Circles mark the boundaries of NTS. (cc) central canal.

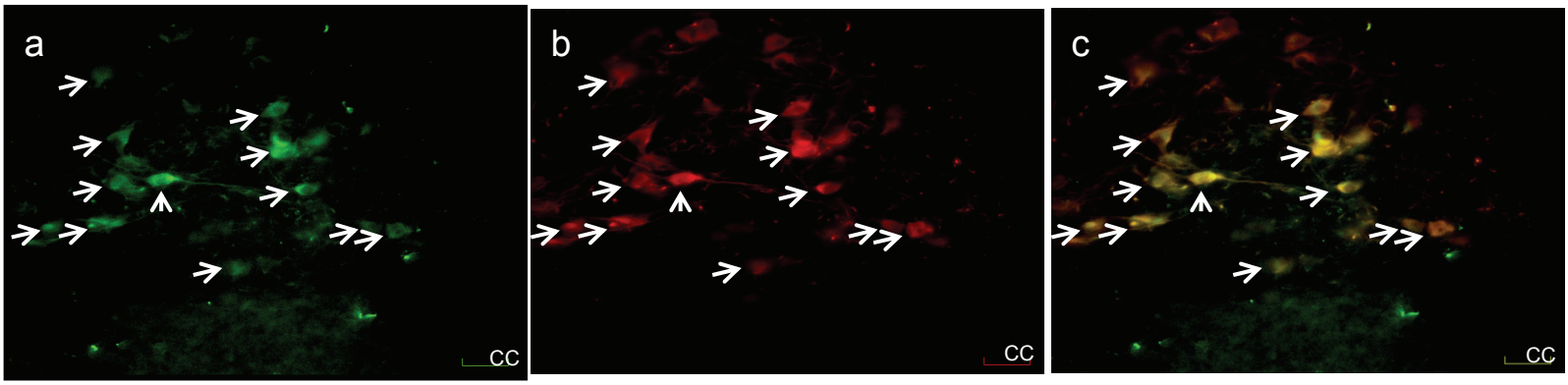

Figure 2. High magnification image of a unilateral side of NTS, showing the specificity of GFP expression in A2 neurons (a) GFP expression in cells of NTS. (b) Cy3 labeled A2 neurons expressing TH (c) Superimposed image of a and b showing the GFP expression to be mostly limited to TH expressing cells. Arrows point to individual neurons where the GFP colocalized with TH-ir. (cc) central canal. Scale bar – 50 μm.

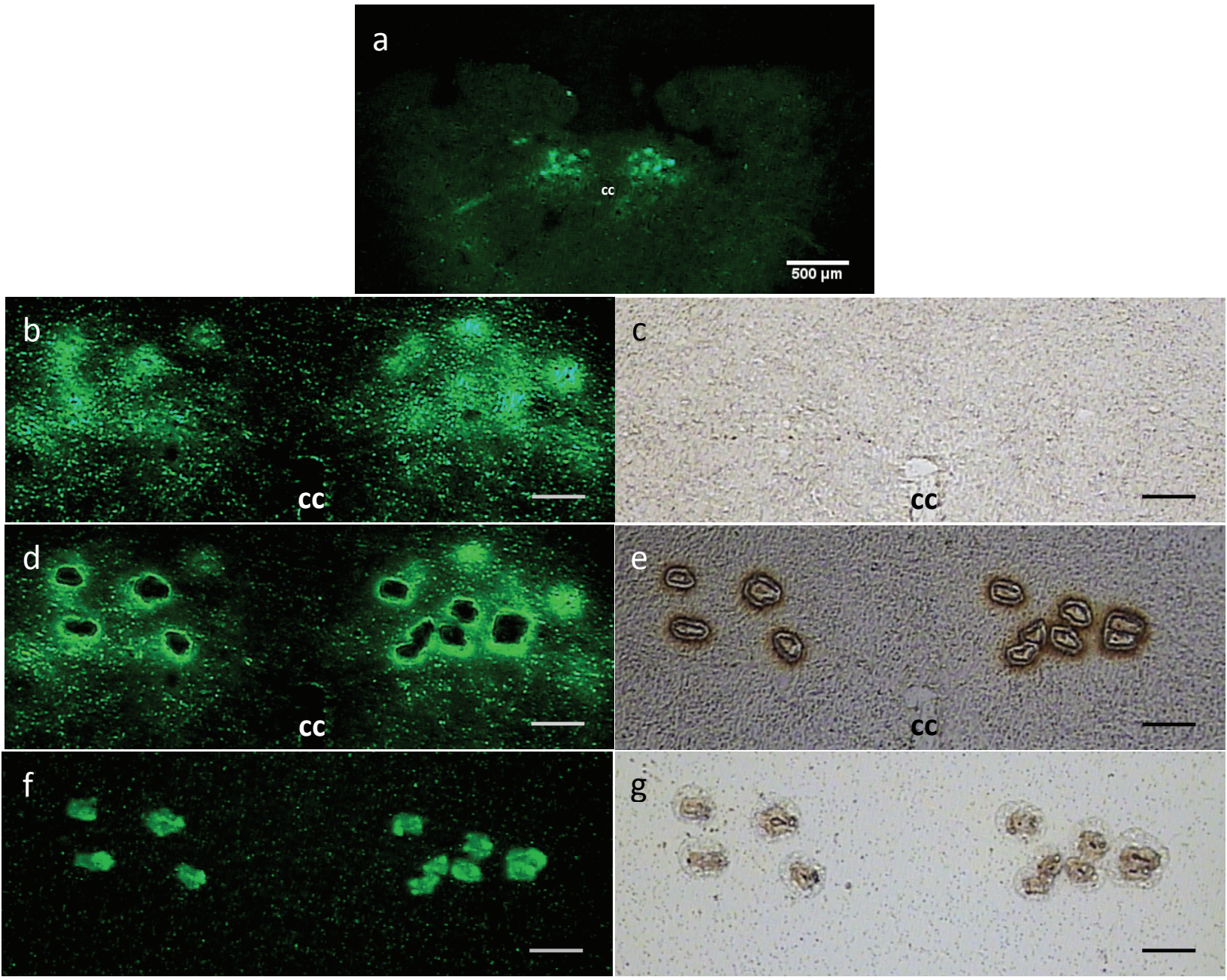

Figure 3. LCM of GFP labeled A2 neurons. a. Low magnification image of NTS showing the GFP localization to only NTS. b, d and f are the fluorescent images of A2 neurons before capture, after capture and captured cells on cap respectively. c, e and g are the bright field images of b, d and f respectively. (cc – central canal). Scale bar – 100 µm.

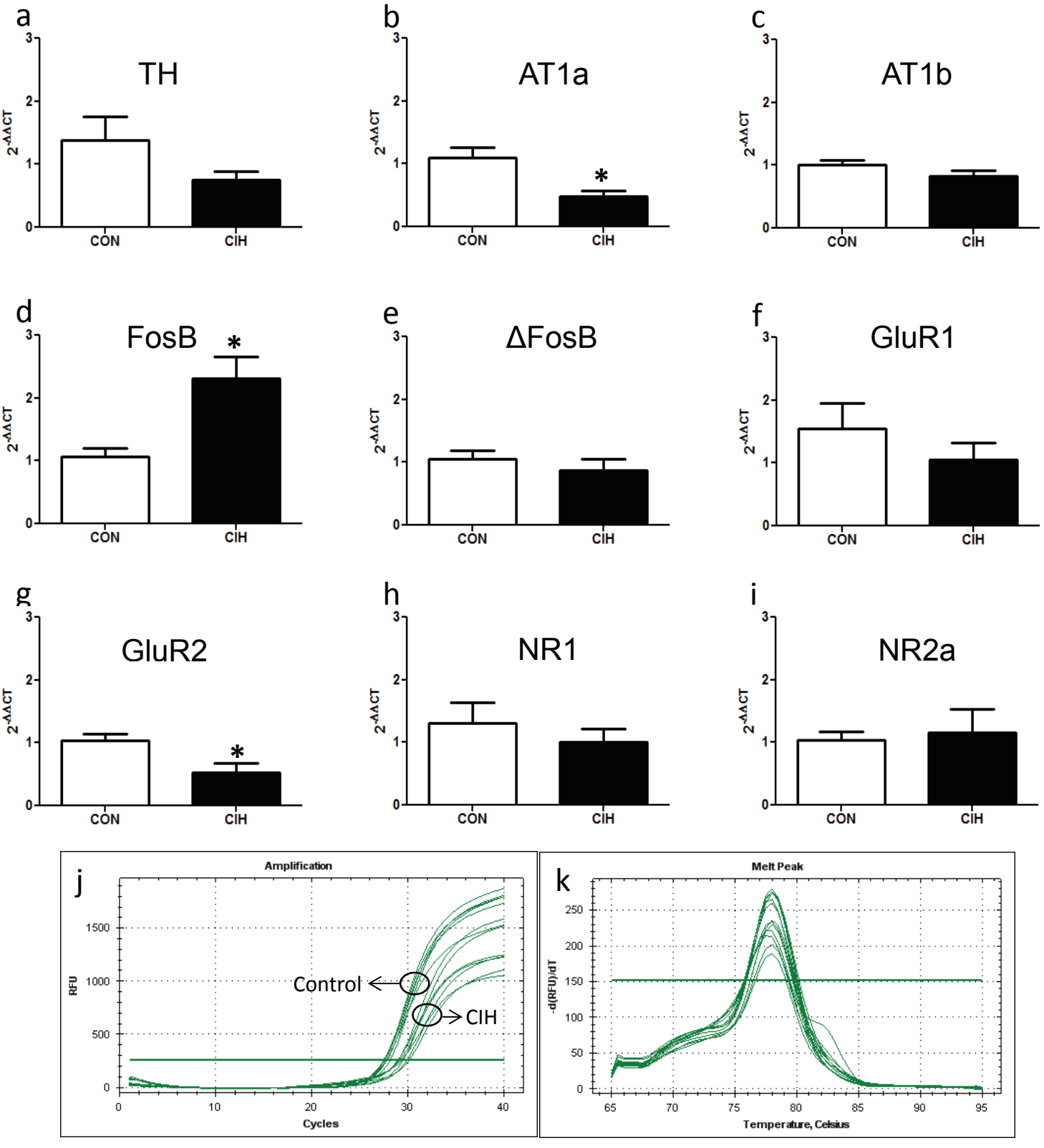
a
TH
b
AT1a
c
AT1b
d
FosB
e
ΔFosB
f
GluR1
g
GluR2
h
NR1
i
NR2a
2-ΔΔCT
CON
CIH
*
j
Amplification
RFU
Cycles
Control
CIH
k
Melt Peak
-d(RFU)/dT
Temperature, Celsius

Figure 4. mRNA expression of a) TH b) AT1a c) AT1b d) FOSB e) ΔFOSB, AMPA receptor subunits; f) GluR1 g) GluR2 and NMDA receptor subunits; h) NR1 i) NR2a, in LCM captured A2 neurons. j and k are the amplification curves and melt curves respectively of AT1a qPCR reactions. * $p < 0.05$ vs control

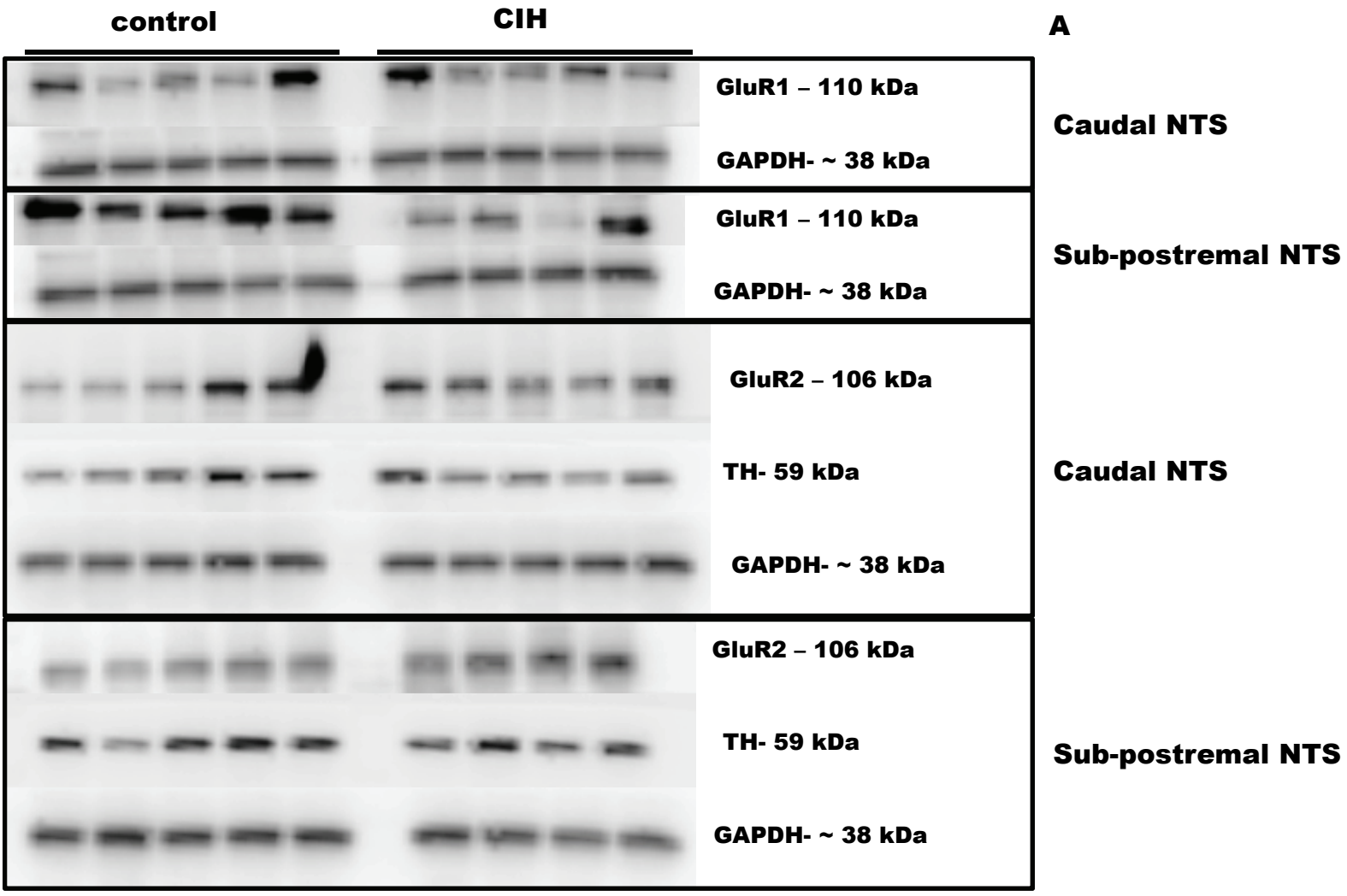
control
CIH
A
GluR1 – 110 kDa
GAPDH- ~ 38 kDa
Caudal NTS
GluR1 – 110 kDa
GAPDH- ~ 38 kDa
Sub-postremal NTS
GluR2 – 106 kDa
TH- 59 kDa
GAPDH- ~ 38 kDa
Caudal NTS
GluR2 – 106 kDa
TH- 59 kDa
GAPDH- ~ 38 kDa
Sub-postremal NTS

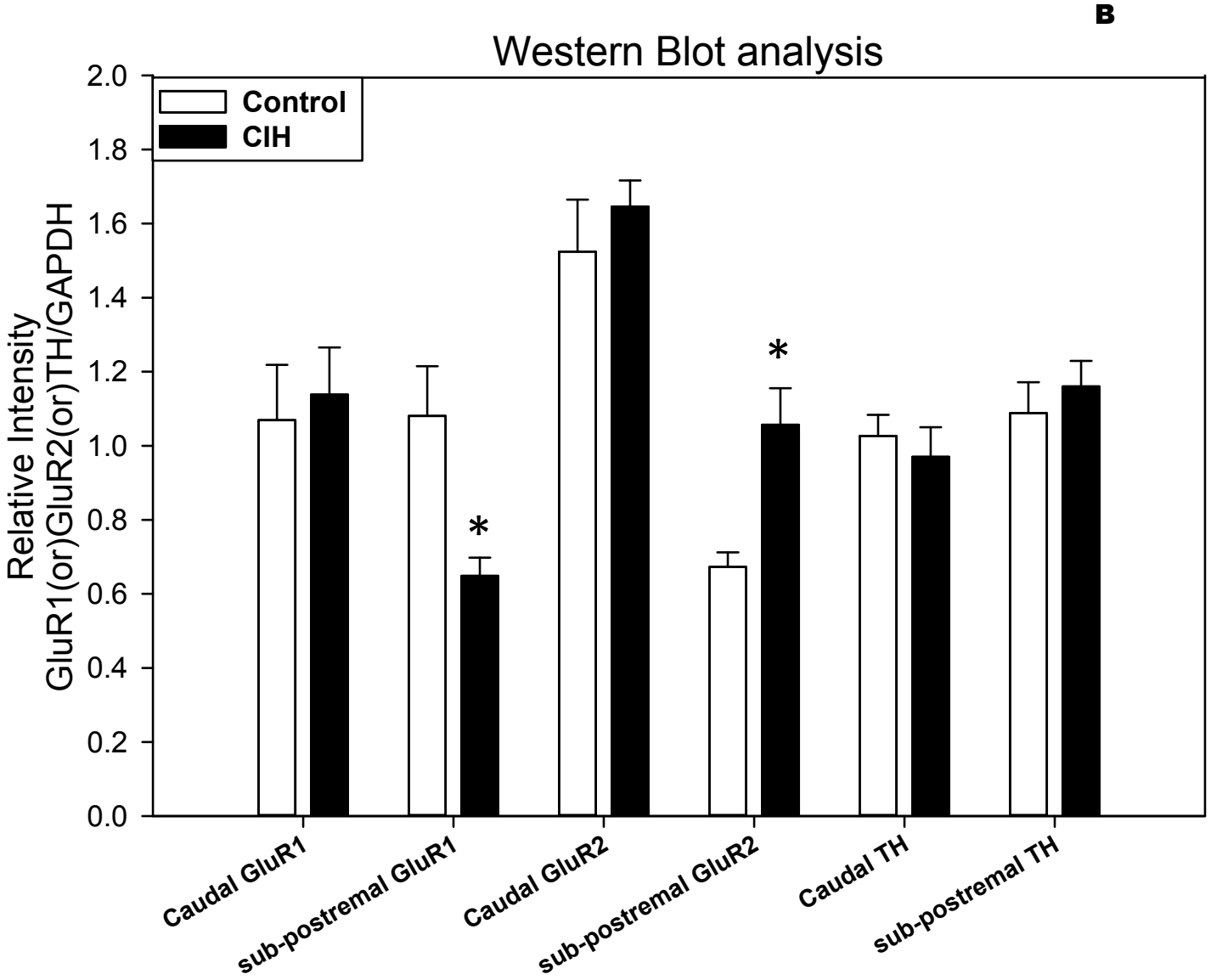

Figure 5. A) Westerns blots of GluR1, GluR2 and TH in the caudal and sub-postremal NTS of control and CIH (hypoxia) rats. B) Western blot analysis of GluR1, GluR2 and TH in caudal and sub-postremal NTS in control and CIH (hypoxia) rats. n= 5 in all groups except sub-postremal region of CIH group, where n=4. GAPDH levels were used to normalize the data. * *p*-value < 0.05 vs control

CHAPTER IV

NEURONS OF THE NUCLEUS OF THE SOLITARY TRACT DEMONSTRATE AMPA MEDIATED INCREASE IN INTRACELLULAR CALCIUM LEVELS FOLLOWING CHRONIC INTERMITTENT HYPOXIA

Running Head: NTS neurons and intermittent hypoxia

Chandra Sekhar Bathina and Steve Mifflin

Department of Integrative Physiology

Cardiovascular Research Institute

University of North Texas Health Science Center

Fort Worth, Texas – 76107

Abstract

Catecholaminergic (A2) neurons with in the nucleus of the solitary tract (NTS) are activated during CIH, a rodent model which simulates the hypoxemic conditions observed during sleep apnea. The activation is mediated through release of the neurotransmitter glutamate by chemoreceptor afferents. Glutamate acts through inotropic glutamate receptors like α-amino-3-hydroxy-5-methyl-4-isoxazole propionate (AMPA), N-methyl D-aspartate (NMDA) and kainate receptors. An attempt was made to test the hypothesis that A2 neurons exhibit increased calcium influx through AMPA receptors following CIH. A2 neurons were labeled through virus mediated delivery of GFP and fura-2AM mediated calcium imaging was conducted while applying AMPA, GFP and fura labeling did not colocalize. Therefore, the hypothesis was revised to test calcium influx of fura labeled NTS neurons following CIH and calcium imaging was conducted on NTS neurons. 30 μM AMPA application caused a 340/380 ratio change of 0.17 ± 0.01 (40 neurons from 5 rats) in control rats and this change was significantly higher 0.55 ± 0.13 (46 neurons from 4 rats) in CIH rats. The probability of neurons responding to AMPA application with increased calcium influx was considerably higher in CIH rats. AMPA receptor antagonist, CNQX treatment of the slices abolished AMAP induced changes in intracellular calcium in neurons from both control and CIH rats, demonstrating that the responses noticed after AMPA application were AMPA receptor mediated. Increases in intracellular calcium levels following 500 μM potassium chloride applications validate the fact that the neurons were viable. The results suggest that CIH induces alterations in NTS AMPA receptors, so that more neurons exhibit AMPA-induced increases in calcium.

Keywords: NTS neurons, Calcium imaging, AMPA receptors and Chronic intermittent hypoxia

Introduction

Sleep apnea (SA) condition is characterized by episodes where respiratory airflow ceases while sleeping resulting in hypoxemia. Chemoreceptor activation during apnea-induced hypoxemia during leads to increased SNA and increased AP (20, 44). Elevated SNA and AP persists even during the daytime, when the patients are not experiencing apneic episodes (3). SA is associated with cardiovascular disease and other metabolic problems (6). Many groups have used different animal models of intermittent hypoxia (2, 52) to simulate the hypoxemic conditions occurring in humans during SA to study the mechanism behind the elevated SNA and MAP during wakefulness in humans (18, 21, 24, 36)..

Arterial chemoreceptors activated by systemic hypoxia excite neurons in the nucleus of the solitary tract (NTS) which leads to elevated MAP (11, 23). Various phenotypic populations are found throughout the NTS and among those groups is catecholaminergic A2 neuronal group (28, 29, 37, 50, 53). The A2 neurons express tyrosine hydroxylase (TH) the rate limiting enzyme in catecholamine synthesis (31). A2 neurons are activated during stressors such as hypoxia (9, 45, 46) hypoglycemia (38), cold (35) and might undergo alterations during chronic exposure to stressor. This is consistent with the alterations noticed in α-amino-3-hydroxy-5-methyl-4-isoxazole propionate (AMPA) receptor subunit's mRNA and protein levels in the A2 neurons and NTS, respectively, following exposure to CIH (chapter III). Hypoxia is also shown to cause release of excitatory amino acid, glutamate from the chemoreceptor afferents into the NTS (22).

Glutamate released by chemoreceptor afferents act through NMDA (N-Methyl D-Aspartate) and non-NMDA receptors like AMPA. Glutamate can modulate gene expression by inducing transcription factors and phosphorylation of jun proteins to bind to AP-1 sites through calcium calmodulin (CAM) kinase and microtubule-associated protein (Map) kinase pathway (41, 51).

Previous studies from our lab have demonstrated that the AMPA mediated currents increase following CIH while NMDA mediated currents are reduced (7).It is hypothesized that glutamate acts through AMPA receptors to cause increase intracellular calcium levels in the NTS neurons to cause molecular alterations. We used AAV-GFP-TH promoter to label the A2 neurons and conducted membrane-permeant fura-2AM mediated calcium imaging of those labeled neurons and other NTS neurons after AMPA application.

Materials and Methods

Animals: Adult male Sprague-Dawley rats (250–350g, Charles River Laboratories, Inc., Wilmington, MA, USA) were used for conducting the experiments. Rats were provided with *ad libitum* food and water and were housed in a thermostatically regulated room (23°C) with 12 hour light: 12 hour dark cycle (12L: 12D, on at 7 AM, off at 7 PM). All experimental procedures were approved by the Institutional Animal Care and Use Committee (IACUC) guidelines of University of North Texas Health Science Center. Experimental procedures were performed after 1 week of acclimatization in the facility.

Adeno-associated virus (AAV): Adeno-associated virus with 2.5kb tyrosine hydroxylase (TH) promoter attached to green fluorescent protein (GFP) was used to label A2 neurons in NTS. The AAV are chimeric serotype AAV1/2 which have the AAV1 and AAV2 serotype proteins expressed on the surface of the virus in a 1:1 ratio and this serotype is a CNS-optimized serotype (13). The construct, AAV1/2-TH promoter-eGFP-WPRE-BGH-polyA was commercially synthesized (Catalog # GD1001-RV; GeneDetect, New Zealand) based on the previously published sequences (34) at a titer 1.1x 10^{12} genomic particles/ml. The TH promoter in the constructs drives the over-expression of GFP, the woodchuck post-transcriptional regulatory

element (WPRE) and the presence of a bovine growth hormone (BGH) polyadenylation sequence ensures high transcription following transduction.

NTS microinjections: 4 rats in the study were injected with the viral constructs. A standard surgical approach was used to expose the caudal medulla region (1, 8). Using a glass micropipette (tip diameter, 50μm), three 100nL injections of virus were performed with the help of pneumatic picopump (PV 800, WPL, Sarasota, FL, USA) over a 5 minute period. To cover the caudal NTS, the injections were performed at the calamus scriptorius and bilaterally at 0.5 mm rostral and 0.5 mm lateral to calamus.

Chronic intermittent hypoxia: Virus injected rats (n=2), after 14 days of injections and naïve rats (n=4) were transferred to a commercially available hypoxia chamber system where O_2 concentration was varied using a computerized system (Oxycycler, Biospherix, NY, USA). Rats were exposed to 7 days of CIH, as published earlier (52). An O_2 concentration of 10% for 3 minutes in a 10 minute cycle was achieved by setting the cycles at 9% O_2 for 6 minutes and 21% O_2 for 4 minutes. CIH exposure of rats was done during the light phase to coincide with their sleeping period, from 8am to 4pm (8 hours). From 4pm-8am the rats were exposed to 21% O_2. Control rats were housed in normal room air conditions. Following the last day of CIH exposure, the rats were euthanized and brains were collected.

Brain slice preparation: Both control (n=7; with 2 virus injected rats and 2 rats were used for CNQX study), CIH (n=6; with 2 virus injected rats and 2 rats were used for CNQX study) rats were anesthetized with isoflurane, following which brainstem was rapidly removed and placed in ice-cold, high-sucrose artificial cerebrospinal fluid that contains (in mM): 3 KCl,1 $MgCl_2$,1 $CaCl_2$,2 $MgSO_4$,1.25 NaH_2PO_4,26 $NaHCO_3$,10 glucose, and 206 sucrose, pH=7.4 while continuously bubbling with 95%O_2+5%CO_2. The brain stem was mounted in a vibrating

microtome; Vibrating blade microtome Leica VT1000 S (Leica Microsystems Inc; Buffolo Grove, IL, USA) to obtain horizontal slices (350µm thickness) using a sapphire knife (Delaware Diamond Knives; Wilmington, DE, USA). The brain slices were then incubated for at least 1 h in normal artificial cerebrospinal fluid (aCSF),that contains (in mM):124 NaCl,3 KCl,2 $MgSO_4$,1.25 NaH_2PO_4,26 $NaHCO_3$,10 glucose,and 2 $CaCl_2$, pH=7.4 while continuously bubbling with 95%O_2+5%CO_2.

Calcium imaging: Slices were then incubated for 50min with 10µM of Fura-2AM (F0888-1MG; Sigma-Aldrich; St. Louis, MO, USA) and 30µL of F127 (P2443; Sigma-Aldrich; St. Louis, MO, USA) (25%) at 40°C and then washed for 20min in aCSF bubbled with 95%O_2+5%CO_2. A single slice was transferred to the recording chamber on an upright epifluorescent microscope (E600FN; Nikon, Japan). The slice was held in place with a nylon mesh (203-776-064; Warner Instruments, Hamden, CT, USA) perfused with normal aCSF at a rate of 2.5 ml/min. Drug application of 30µM AMPA or 1mM KCl dissolved in aCSF solution was done using multi barrel patch pipette positioned close to the neuron so that injection (volume) occurred in the same direction as the flow of aCSF being perfused. Fluorescence of Fura-2AM was excited by epi-illumination with light provided by a 75 W Xenon lamp band-pass filtered alternatively at 340 or 380 nm. Emission light pass through a barrier filter (510 nm). Pairs of 340 and 380 nm images were acquired at intervals of 3s and analyzed off-line with NIS-Elements AR 3.2 (Nikon, Japan) software. All images were captured with a charge-coupled device (CCD) camera.

Statistical analysis: Data from different groups was presented as means±SE. Difference between groups was tested using unpaired t-test. A p value of < 0.05 was considered significant. A 340/380 ratio change of more than 0.08 was considered for analysis as neurons which showed no response to AMPA application were shown to have values below 0.08.

Results

Low fura and GFP colocalization: There were very low number of neurons (less than 1 in 100) in which there was colocalization of fura and GFP (Figure 2, 3 and 4). Therefore, we focused the calcium imaging on fura labeled NTS neurons.

Response of NTS neurons from control rats to AMPA application: Bath Application of 30 μM AMPA transiently on to the NTS neurons from control rats resulted in an increase in the intracellular calcium levels (Figure 5). The average change in the 340/380 ratio following the AMPA application was 0.17 ± 0.01(40 neurons form 5 rats) (Figure 9). Number of neurons showing a change in 340/380 ratio value above 0.08 were lower (40 out of 169 neurons studied; 23%) (Figure 6)

Response of NTS neurons from CIH exposed rats to AMPA application: 30 μM AMPA application caused a much more pronounced increase in the intracellular calcium levels in NTS neurons of CIH exposed rats, when compared to neurons of control rats (Figure 7). The average change in 340/380 ratio was also significantly higher in NTS neurons from CIH rats (0.55 ± 0.13; n=4) (Figure 9). The probability of neurons responding to AMPA were also higher in CIH rats and neurons with 340/380 ratio change above 0.08 were also higher in CIH rats (46 out of 114 neurons; 41%) (Figure 8).

CNQX treatment abolished the calcium influx seen with AMPA application: A set of slices from control as well as CIH rats were pretreated with 10 μM CNQX (AMPA receptor antagonist) to ascertain whether the prolonged increase in intracellular calcium levels noticed upon AMPA application were AMPA receptor mediated. CNQX pretreatment did not cause any response in NTS neurons following application of even 100 μM AMPA in control rats (94 neurons) and in CIH rats (114 neurons) (Figure 10 and 12) (n=2 in both groups). But, these

neurons responded to 500 μM potassium chloride (KCl) application almost similarly (control – 0.58 ± 0.02; n=8 neurons and CIH – 0.54 ± 0.07; n=12 neurons). Moreover, very few neurons (1 in control and 2 in CIH) had a 340/380 ratio change above 0.08 (Figure 11 and 13).

Discussion

A2 neurons have been shown to respond to stressors like hypoxia (9, 45, 46), hypoglycemia (38) and cold (35). A2 neurons with their projections to various sympatho-regulatory sites in CNS (37) might play an important role in the elevated MAP noticed in CIH rats. Same can be attributed to the NTS neurons in general. Studies showing that the persistent hypertension being abolished after TH knockdown (2) and changes in mRNA expression of AMPA receptor subunits following CIH, in NTS infer that molecular adaptations/alterations occurring in the A2 and NTS neurons could be one of the potential driving forces behind the persistent hypertension noticed in CIH rats. The initiation to this is the release of excitatory neurotransmitter, glutamate in the NTS region by the chemoreceptor afferents. Glutamate binds to the post synaptic ionotropic glutamate receptors which are tetrameric cation channels consisting of 3 distinct subtypes: AMPA, NMDA and kainate receptors (49). Among them AMPA receptors conduct the majority of fast, moment to moment synaptic transmission (26) in NTS neurons (7). So, attempts were made to perform calcium imaging studies on A2 neurons from slices of control normoxic rats and CIH rats. In this study, we utilized AAV-GFP-TH promoter to label the A2 neurons and conduct membrane-permeant fura-2AM mediated calcium imaging of those labeled neurons for changes in intracellular calcium levels. However, GFP and fura labeling was not colocalized, therefore, calcium imaging was performed on fura labeled NTS neurons. Cell culture studies have shown that early response to hypoxia in almost all cell types is an increase in intracellular calcium (Ca^{2+}) (47). This would cause a calcium signaling cascade in the cell to respond to the

hypoxia. This Ca^{2+} signaling has been seen mainly as a response system, mediated over short time intervals in response to hypoxia. However, recent experimental evidence shows that Ca^{2+} signaling can also exert an influence over much longer time intervals either by modulating gene expression or by exerting significant control on protein synthesis in endoplasmic reticulum (47). In neurons, Ca^{2+} entry can occur via ionotropic glutamatergic receptor channels like NMDA and α-amino-3-hydroxy-5-methyl-4-isoxazolepropionate receptor (AMPA). Significant expression of NMDA and AMPA receptors is found in the NTS neurons (50). Stimulated peripheral chemoreceptor afferents are found to release glutamate in the caudal NTS region (30). Glutamate acts through NMDA and non-NMDA receptors like AMPA. Glutamate is found to modulate gene expression by inducing transcription factors and phosphorylation of jun proteins to bind to AP-1 sites through calcium calmodulin (CAM) kinase and microtubule-associated protein (Map) kinase pathway (41, 51). This shows that glutamate may play a role in long-term alterations in neuronal function. Glutamate released from chemoreceptor afferents might cause an increased Ca^{2+} concentration in the NTS neurons and alter gene expression that contributes to the elevated AP seen during CIH.

TH immunohistochemistry of brains from AAV-GFP- TH injected rats has already demonstrated that the GFP expression is colocalized in A2 neurons (chapter III). Figure 2 and 3 demonstrate that fura labeling was not localized in GFP labeled neurons and neurons with GFP did not take up fura, respectively. Neurons with GFP and fura labeling (Figure 4) were very rare. The possible explanation for this anomaly could be that the GFP in the neurons is hindering the Fura-2AM uptake into the cell or possibly quenching fura fluorescence when both are inside the neuron.

NTS neurons from slices of control rats displayed moderate response to AMPA application (Figure 5), however, the amplitude of response and number of neurons responding to AMPA were very low (Figure 6). The CIH neurons responded with much larger amplitude calcium responses (Figure 7) and the number of neurons responding to the AMPA was considerably greater (Figure 8). This could be due to AMPA trafficking to the surface of neurons in response to hypoxia or glutamate (15, 25, 27, 33, 40, 42, 43) although the role of trafficking needs to be further studied. Post translational modifications at the receptor or sub-unit level (14, 19, 27) could also cause alterations in the response to the AMPA application following CIH. In contrary to the transient increases in intracellular calcium levels seen after AMPA application (16), we noticed a prolonged increase in calcium levels for longer durations after AMPA application. Similar responses were observed in earlier studies as well (12, 17). The reason for prolonged response could be due to the slowing of desensitization or enhanced channel conductance following CIH (32, 48).

To ensure that these responses were due to activation of AMPA receptor, antagonist studies were conducted using CNQX. 10 μM CNQX abolished all AMPA evoked responses in control and CIH rats (Figure 10 and 12). Moreover, number of neurons responding to AMPA was drastically decreased by CNQX treatment (Figure 11 and 13). Neuronal viability was also tested in the CNQX treated slices by applying 500 μM KCl, which resulted in all neurons showing an increase in intracellular calcium levels instantaneously. This establishes the fact that the prolonged responses noticed in NTS neurons of control and CIH rats were AMPA mediated and the responses were significantly greater in CIH neurons.

The results from specific aim 2 or (chapter III) made us hypothesize that, following CIH the A2 neurons would become more calcium permeable whereas the adjacent neurons of NTS be less

calcium permeable as the GluR2 mRNA is decreased in A2 neurons and GluR2 protein increased in NTS punches. Due to technical difficulties, calcium imaging of A2 and non A2 neurons of NTS was not performed and almost all neurons of NTS showed a similar response pattern to AMPA. Even though GluR1, the most calcium permeable subunit is decreased following CIH (chapter III) the most active, phosphorylated form of GluR1 (19) might have increased in the NTS neurons. Phosphorylation of GluR1 subunit is important in regulating GluR1- containing AMPA receptor trafficking to the surface (19). With the exception of GluR3, all the subunits of AMPA receptor have been shown to be phosphorylated by different kinases (4, 5, 10, 19, 27, 39). GluR2 phosphorylation causes AMPA receptor internalization (19). CIH might have reduced the GluR2 phosphorylation and promoted GluR1 phosphorylation to cause more AMPA receptor trafficking to the surface. Further studies are needed to quantify the phosphorylated forms of AMPA subunits to better understand the precise alterations that occur after CIH.

Perspectives and significance

This study shows that there is difficulty in colocalizing viral mediated GFP labeling with fura labeling. The calcium imaging studies suggest that almost all the NTS neurons display increased calcium influx following CIH which could cause alterations in their susceptibility, excitability and plasticity that might have a contribution to the elevation in SNA and MAP during CIH.

Grants

Funded by National institute of Health HL-088052

Conflict of Interest

None

References

1. **Barraco RA, Janusz CJ, Polasek PM, Parizon M, and Roberts PA**. Cardiovascular effects of microinjection of adenosine into the nucleus tractus solitarius. *Brain Res Bull* 20: 129-132, 1988.

2. **Bathina CS, Rajulapati A, Franzke M, Yamamoto K, Cunningham JT, and Mifflin SW**. Knockdown of Tyrosine Hydroxylase in the Nucleus of the Solitary Tract Reduces Elevated Blood Pressure during Chronic Intermittent Hypoxia. *Am J Physiol Regul Integr Comp Physiol* 2013.

3. **Carlson JT, Hedner J, Elam M, Ejnell H, Sellgren J, and Wallin BG**. Augmented resting sympathetic activity in awake patients with obstructive sleep apnea. *Chest* 103: 1763-1768, 1993.

4. **Chung HJ, Xia J, Scannevin RH, Zhang X, and Huganir RL**. Phosphorylation of the AMPA receptor subunit GluR2 differentially regulates its interaction with PDZ domain-containing proteins. *J Neurosci* 20: 7258-7267, 2000.

5. **Correia SS, Duarte CB, Faro CJ, Pires EV, and Carvalho AL**. Protein kinase C gamma associates directly with the GluR4 alpha-amino-3-hydroxy-5-methyl-4-isoxazole propionate receptor subunit. Effect on receptor phosphorylation. *J Biol Chem* 278: 6307-6313, 2003.

6. **Coughlin S, Calverley P, and Wilding J**. Sleep disordered breathing--a new component of syndrome x? *Obes Rev* 2: 267-274, 2001.

7. **de Paula PM, Tolstykh G, and Mifflin S**. Chronic intermittent hypoxia alters NMDA and AMPA-evoked currents in NTS neurons receiving carotid body chemoreceptor inputs. *Am J Physiol Regul Integr Comp Physiol* 292: R2259-2265, 2007.

8. **Doba N, and Reis DJ**. Acute fulminating neurogenic hypertension produced by brainstem lesions in the rat. *Circ Res* 32: 584-593, 1973.

9. **Dumas S, Pequignot JM, Ghilini G, Mallet J, and Denavit-Saubie M**. Plasticity of tyrosine hydroxylase gene expression in the rat nucleus tractus solitarius after ventilatory acclimatization to hypoxia. *Brain Res Mol Brain Res* 40: 188-194, 1996.

10. **Esteban JA, Shi SH, Wilson C, Nuriya M, Huganir RL, and Malinow R**. PKA phosphorylation of AMPA receptor subunits controls synaptic trafficking underlying plasticity. *Nat Neurosci* 6: 136-143, 2003.

11. **Fletcher EC, Lesske J, Behm R, Miller CC, 3rd, Stauss H, and Unger T**. Carotid chemoreceptors, systemic blood pressure, and chronic episodic hypoxia mimicking sleep apnea. *J Appl Physiol* 72: 1978-1984, 1992.

12. **Furukawa K, and Mattson MP**. The transcription factor NF-kappaB mediates increases in calcium currents and decreases in NMDA- and AMPA/kainate-induced currents induced by tumor necrosis factor-alpha in hippocampal neurons. *J Neurochem* 70: 1876-1886, 1998.

13. **Hauck B, Chen L, and Xiao W**. Generation and characterization of chimeric recombinant AAV vectors. *Mol Ther* 7: 419-425, 2003.

14. **Hayashi T, Rumbaugh G, and Huganir RL**. Differential regulation of AMPA receptor subunit trafficking by palmitoylation of two distinct sites. *Neuron* 47: 709-723, 2005.

15. **Hayashi Y, Shi SH, Esteban JA, Piccini A, Poncer JC, and Malinow R**. Driving AMPA receptors into synapses by LTP and CaMKII: requirement for GluR1 and PDZ domain interaction. *Science* 287: 2262-2267, 2000.

16. **Hermann GE, Nasse JS, and Rogers RC**. Alpha-1 adrenergic input to solitary nucleus neurones: calcium oscillations, excitation and gastric reflex control. *J Physiol* 562: 553-568, 2005.

17. **Itoh T, Beesley J, Itoh A, Cohen AS, Kavanaugh B, Coulter DA, Grinspan JB, and Pleasure D**. AMPA glutamate receptor-mediated calcium signaling is transiently enhanced during development of oligodendrocytes. *J Neurochem* 81: 390-402, 2002.

18. **Iturriaga R, Rey S, and Del Rio R**. Cardiovascular and ventilatory acclimatization induced by chronic intermittent hypoxia: a role for the carotid body in the pathophysiology of sleep apnea. *Biol Res* 38: 335-340, 2005.

19. **Jiang J, Suppiramaniam V, and Wooten MW**. Posttranslational modifications and receptor-associated proteins in AMPA receptor trafficking and synaptic plasticity. *Neurosignals* 15: 266-282, 2006.

20. **Kara T, Narkiewicz K, and Somers VK**. Chemoreflexes--physiology and clinical implications. *Acta Physiol Scand* 177: 377-384, 2003.

21. **Katayama K, Smith CA, Henderson KS, and Dempsey JA**. Chronic intermittent hypoxia increases the CO2 reserve in sleeping dogs. *J Appl Physiol* 103: 1942-1949, 2007.

22. **Kline DD, Ramirez-Navarro A, and Kunze DL**. Adaptive depression in synaptic transmission in the nucleus of the solitary tract after in vivo chronic intermittent hypoxia: evidence for homeostatic plasticity. *J Neurosci* 27: 4663-4673, 2007.

23. **Lesske J, Fletcher EC, Bao G, and Unger T**. Hypertension caused by chronic intermittent hypoxia--influence of chemoreceptors and sympathetic nervous system. *J Hypertens* 15: 1593-1603, 1997.

24. **Lin M, Ai J, Li L, Huang C, Chapleau MW, Liu R, Gozal D, Wead WB, Wurster RD, and Cheng ZJ**. Structural remodeling of nucleus ambiguus projections to cardiac ganglia following chronic intermittent hypoxia in C57BL/6J mice. *J Comp Neurol* 509: 103-117, 2008.

25. **Lissin DV, Gomperts SN, Carroll RC, Christine CW, Kalman D, Kitamura M, Hardy S, Nicoll RA, Malenka RC, and von Zastrow M**. Activity differentially regulates the surface expression of synaptic AMPA and NMDA glutamate receptors. *Proc Natl Acad Sci U S A* 95: 7097-7102, 1998.

26. **Lu W, and Roche KW**. Posttranslational regulation of AMPA receptor trafficking and function. *Curr Opin Neurobiol* 22: 470-479, 2012.

27. **Mammen AL, Kameyama K, Roche KW, and Huganir RL**. Phosphorylation of the alpha-amino-3-hydroxy-5-methylisoxazole4-propionic acid receptor GluR1 subunit by calcium/calmodulin-dependent kinase II. *J Biol Chem* 272: 32528-32533, 1997.

28. **Mifflin SW**. Arterial chemoreceptor input to nucleus tractus solitarius. *Am J Physiol* 263: R368-375, 1992.

29. **Mifflin SW**. Inhibition of chemoreceptor inputs to nucleus of tractus solitarius neurons during baroreceptor stimulation. *Am J Physiol* 265: R14-20, 1993.

30. **Mizusawa A, Ogawa H, Kikuchi Y, Hida W, Kurosawa H, Okabe S, Takishima T, and Shirato K**. In vivo release of glutamate in nucleus tractus solitarii of the rat during hypoxia. *J Physiol* 478 (Pt 1): 55-66, 1994.

31. **Nagatsu T, Levitt M, and Udenfriend S**. Tyrosine Hydroxylase. The Initial Step in Norepinephrine Biosynthesis. *J Biol Chem* 239: 2910-2917, 1964.

32. **Nicoll RA, Tomita S, and Bredt DS**. Auxiliary subunits assist AMPA-type glutamate receptors. *Science* 311: 1253-1256, 2006.

33. **O'Brien RJ, Kamboj S, Ehlers MD, Rosen KR, Fischbach GD, and Huganir RL**. Activity-dependent modulation of synaptic AMPA receptor accumulation. *Neuron* 21: 1067-1078, 1998.

34. **Oh MS, Hong SJ, Huh Y, and Kim KS**. Expression of transgenes in midbrain dopamine neurons using the tyrosine hydroxylase promoter. *Gene Ther* 16: 437-440, 2009.

35. **Pardon MC, Ma S, and Morilak DA**. Chronic cold stress sensitizes brain noradrenergic reactivity and noradrenergic facilitation of the HPA stress response in Wistar Kyoto rats. *Brain Res* 971: 55-65, 2003.

36. **Rey S, Tarvainen MP, Karjalainen PA, and Iturriaga R**. Dynamic time-varying analysis of heart rate and blood pressure variability in cats exposed to short-term chronic intermittent hypoxia. *Am J Physiol Regul Integr Comp Physiol* 295: R28-37, 2008.

37. **Rinaman L**. Hindbrain noradrenergic A2 neurons: diverse roles in autonomic, endocrine, cognitive, and behavioral functions. *Am J Physiol Regul Integr Comp Physiol* 300: R222-235, 2011.

38. **Ritter S, Dinh TT, and Li AJ**. Hindbrain catecholamine neurons control multiple glucoregulatory responses. *Physiol Behav* 89: 490-500, 2006.

39. **Roche KW, O'Brien RJ, Mammen AL, Bernhardt J, and Huganir RL**. Characterization of multiple phosphorylation sites on the AMPA receptor GluR1 subunit. *Neuron* 16: 1179-1188, 1996.

40. **Rongo C, and Kaplan JM**. CaMKII regulates the density of central glutamatergic synapses in vivo. *Nature* 402: 195-199, 1999.

41. **Schwarzschild MA, Cole RL, and Hyman SE**. Glutamate, but not dopamine, stimulates stress-activated protein kinase and AP-1-mediated transcription in striatal neurons. *J Neurosci* 17: 3455-3466, 1997.

42. **Shi S, Hayashi Y, Esteban JA, and Malinow R**. Subunit-specific rules governing AMPA receptor trafficking to synapses in hippocampal pyramidal neurons. *Cell* 105: 331-343, 2001.

43. **Shi SH, Hayashi Y, Petralia RS, Zaman SH, Wenthold RJ, Svoboda K, and Malinow R**. Rapid spine delivery and redistribution of AMPA receptors after synaptic NMDA receptor activation. *Science* 284: 1811-1816, 1999.

44. **Somers VK, Dyken ME, Clary MP, and Abboud FM**. Sympathetic neural mechanisms in obstructive sleep apnea. *The Journal of clinical investigation* 96: 1897-1904, 1995.

45. **Soulier V, Cottet-Emard JM, Pequignot J, Hanchin F, Peyrin L, and Pequignot JM**. Differential effects of long-term hypoxia on norepinephrine turnover in brain stem cell groups. *J Appl Physiol* 73: 1810-1814, 1992.

46. **Soulier V, Dalmaz Y, Cottet-Emard JM, Kitahama K, and Pequignot JM**. Delayed increase of tyrosine hydroxylation in the rat A2 medullary neurons upon long-term hypoxia. *Brain Res* 674: 188-195, 1995.

47. **Toescu EC**. Hypoxia sensing and pathways of cytosolic Ca2+ increases. *Cell Calcium* 36: 187-199, 2004.

48. **Tomita S, Adesnik H, Sekiguchi M, Zhang W, Wada K, Howe JR, Nicoll RA, and Bredt DS**. Stargazin modulates AMPA receptor gating and trafficking by distinct domains. *Nature* 435: 1052-1058, 2005.

49. **Traynelis SF, Wollmuth LP, McBain CJ, Menniti FS, Vance KM, Ogden KK, Hansen KB, Yuan H, Myers SJ, and Dingledine R**. Glutamate receptor ion channels: structure, regulation, and function. *Pharmacol Rev* 62: 405-496, 2010.

50. **Vardhan A, Kachroo A, and Sapru HN**. Excitatory amino acid receptors in commissural nucleus of the NTS mediate carotid chemoreceptor responses. *Am J Physiol* 264: R41-50, 1993.

51. **Xia Z, Dudek H, Miranti CK, and Greenberg ME**. Calcium influx via the NMDA receptor induces immediate early gene transcription by a MAP kinase/ERK-dependent mechanism. *J Neurosci* 16: 5425-5436, 1996.

52. **Yamamoto K, Eubank W, Franzke M, and Mifflin S**. Resetting of the sympathetic baroreflex is associated with the onset of hypertension during chronic intermittent hypoxia. *Auton Neurosci* 173: 22-27, 2013.

53. **Zhang W, and Mifflin SW**. Excitatory amino-acid receptors contribute to carotid sinus and vagus nerve evoked excitation of neurons in the nucleus of the tractus solitarius. *J Auton Nerv Syst* 55: 50-56, 1995.

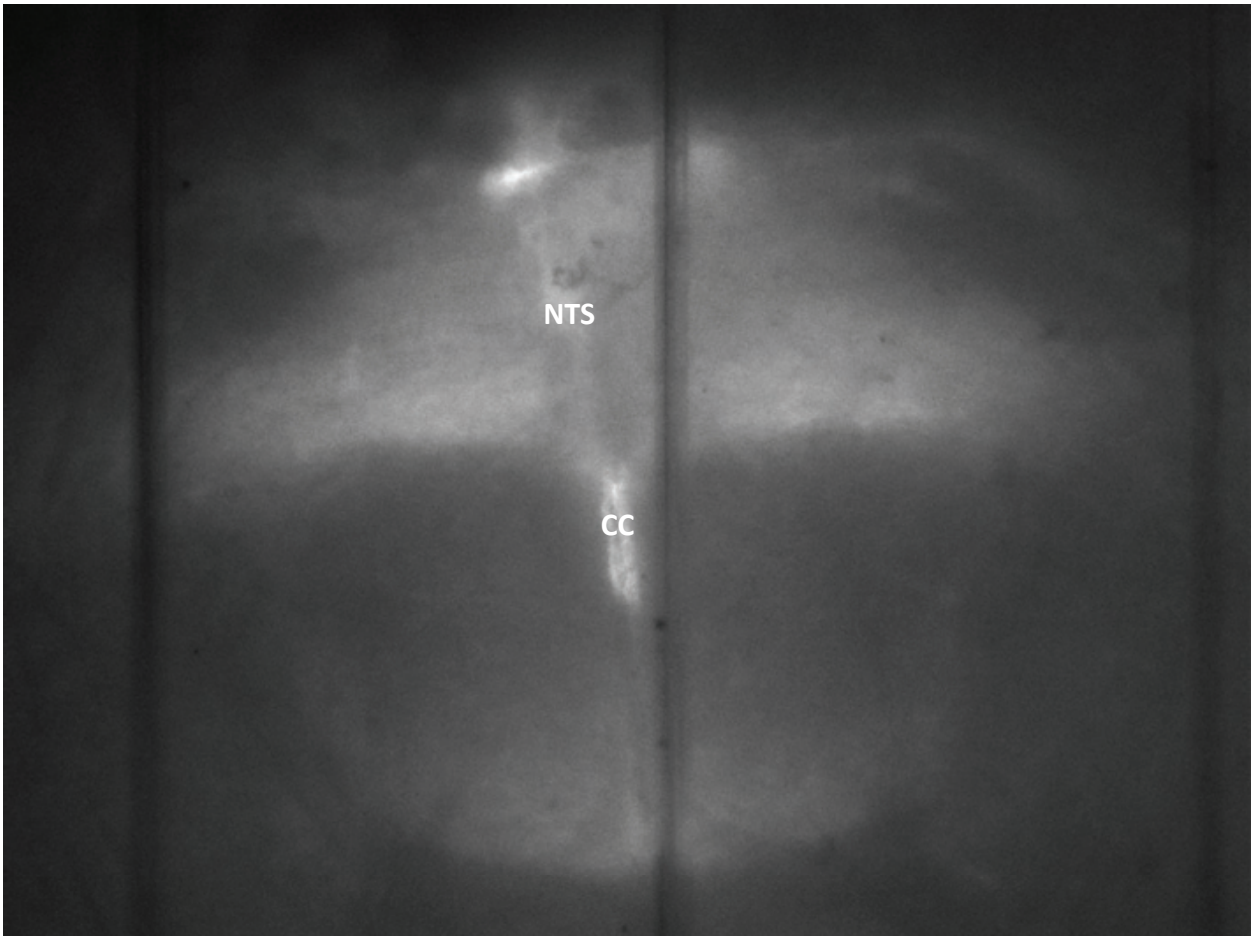

Figure 1. Visualization of NTS under the microscope. cc; central canal.

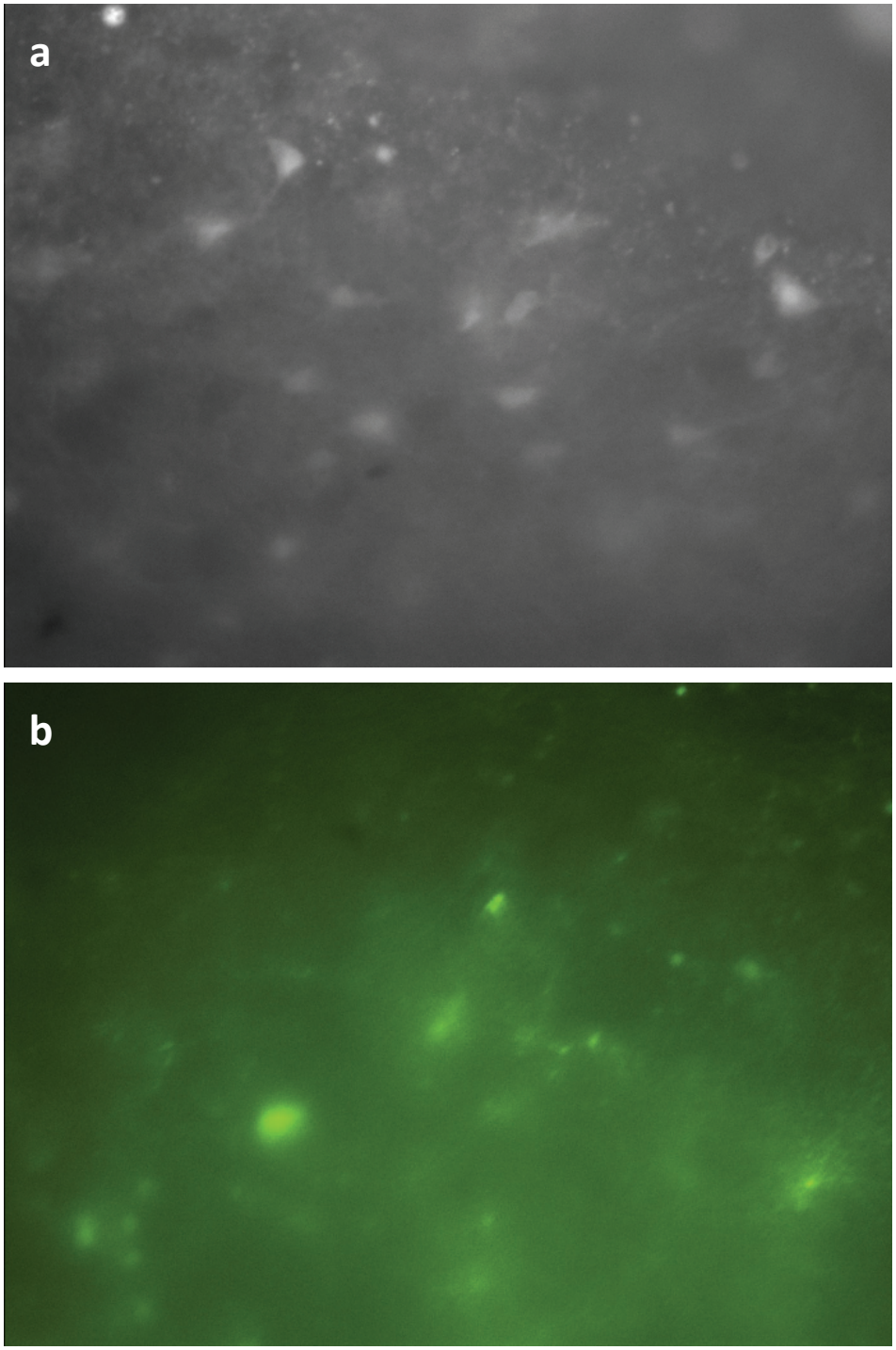

Figure 2. Fura labeling did not colocalize with GFP. a) Fura labeling b) GFP labeling

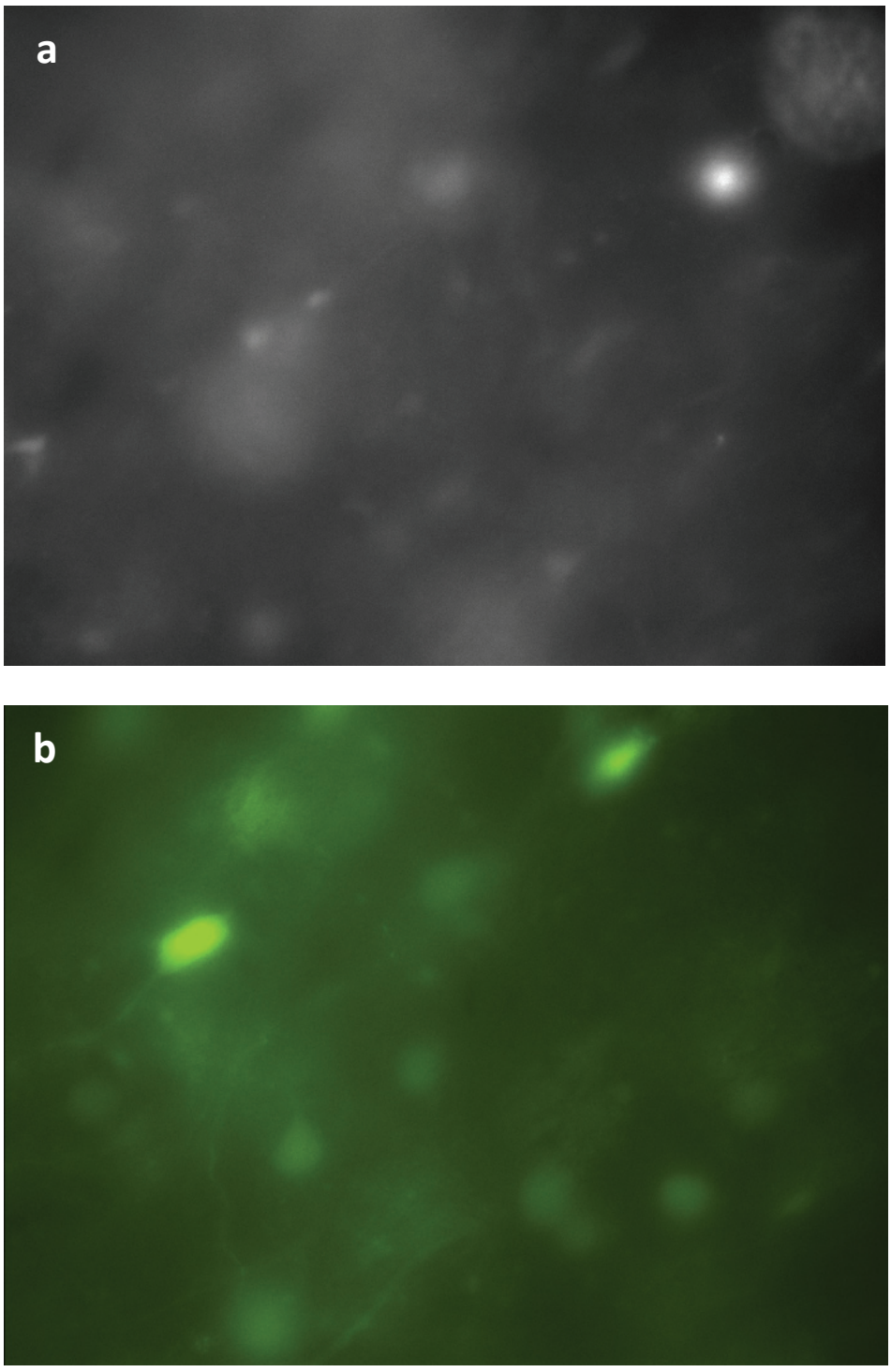

Figure 3. Fura labeling was not seen even in neurons with robust GFP labeling. a) Fura labeling. b) Good GFP labeling

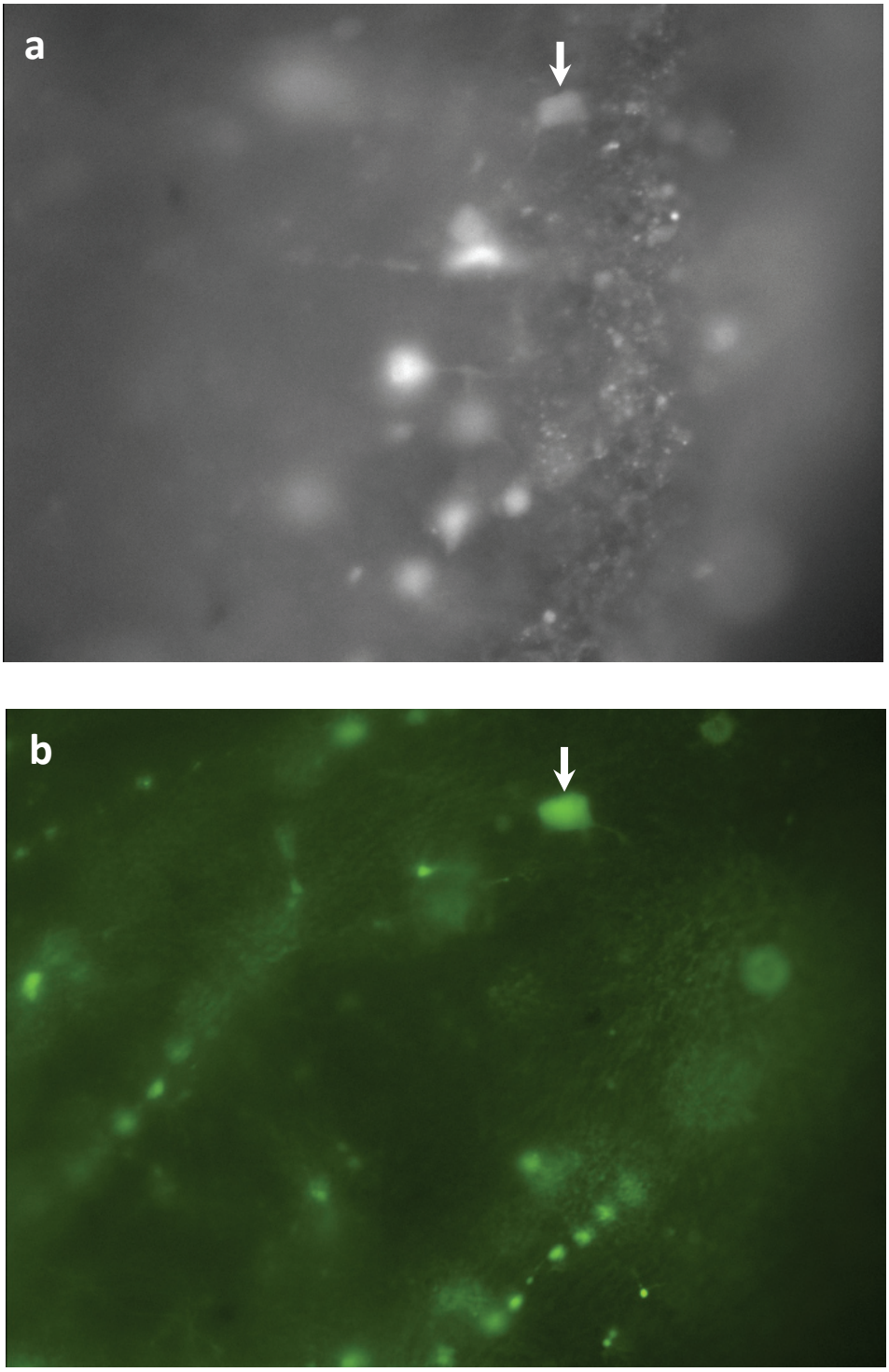

Figure 4. Fura and GFP colocalized neurons were rare. a) Fura labeling. b) GFP labeling. Arrows point to fura and GFP colocalized neuron.

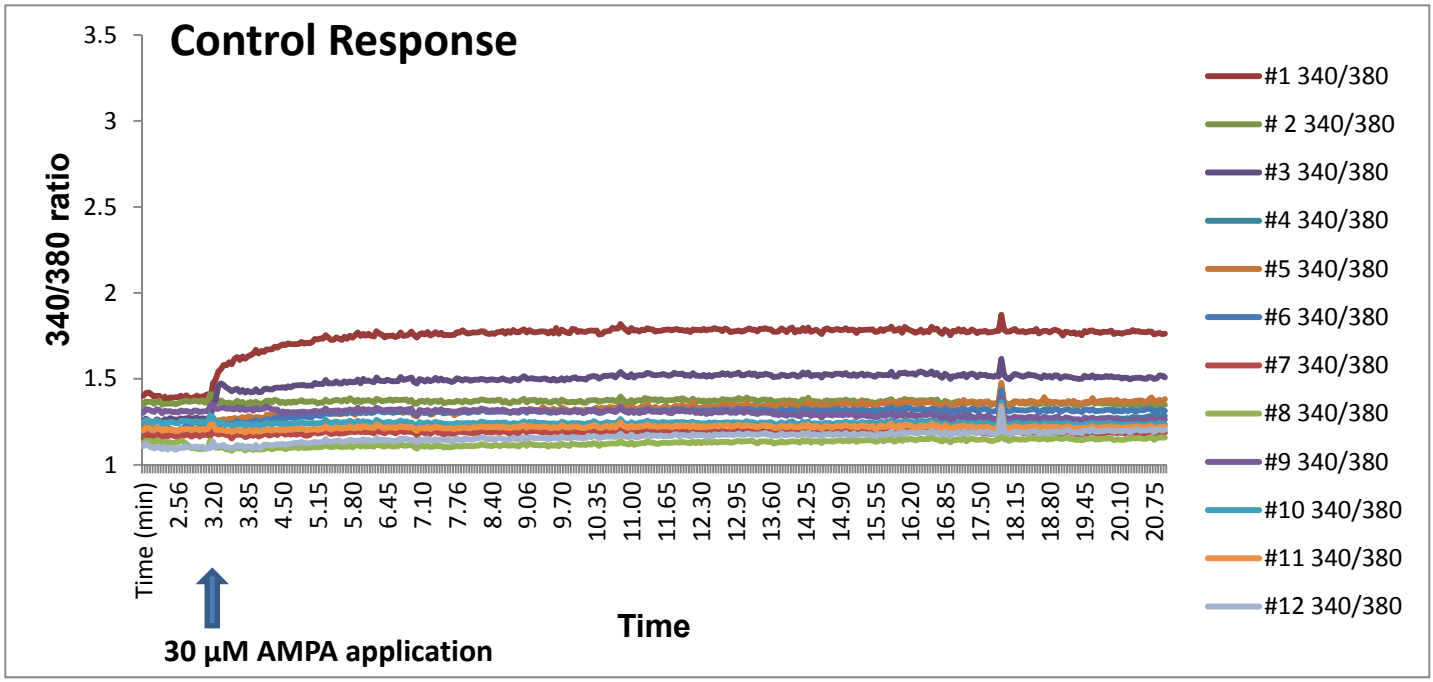

Figure 5. AMPA application caused moderate increase in intracellular calcium levels in neurons from control rats. 340/380 ratio trace from neurons of a control rat.

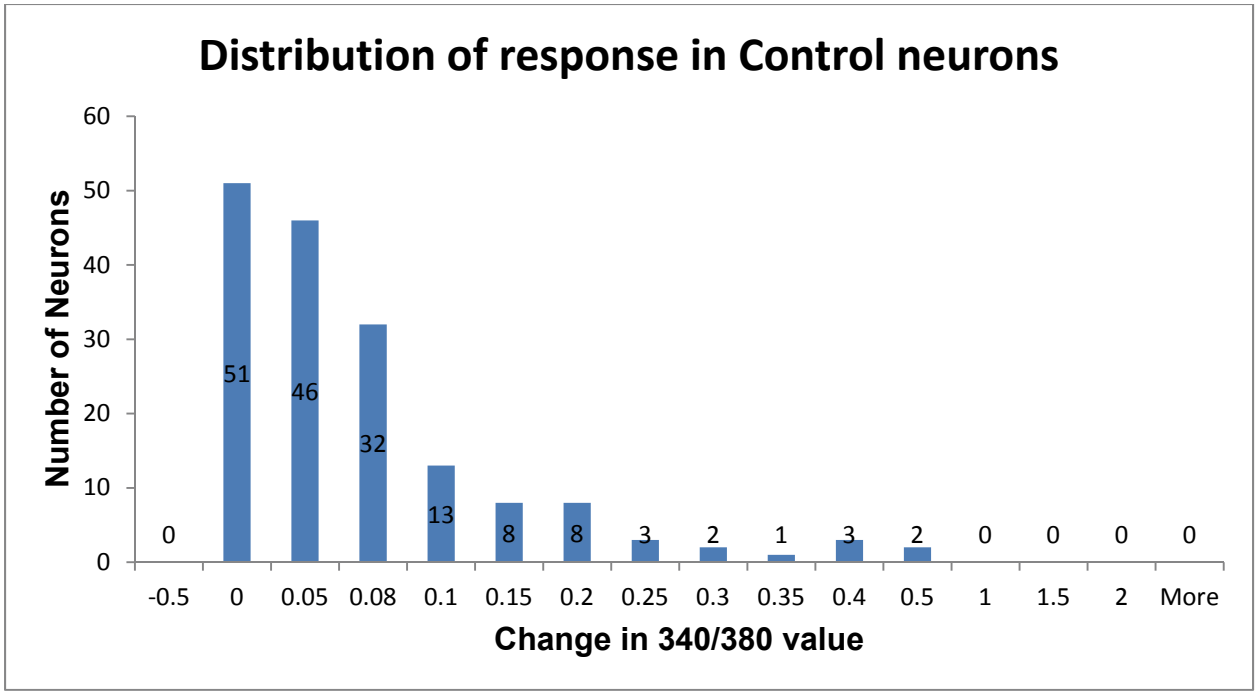

Figure 6. Graph showing the distribution of control neurons response to AMPA. It shows the number of neurons that showed a change in 340/380 ratio in a specific range.

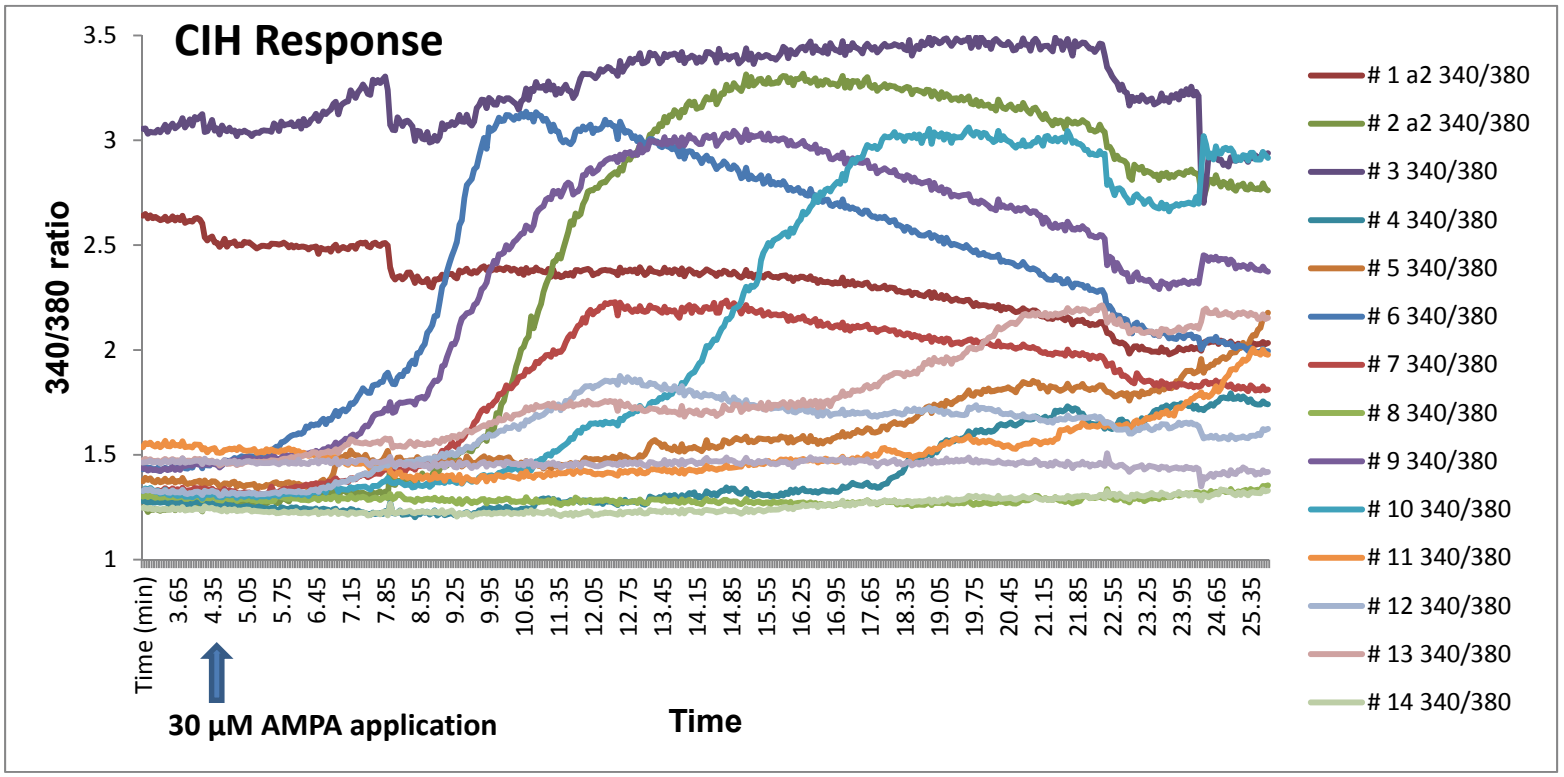

Figure 7. AMPA application caused profound increase in intracellular calcium levels in neurons from CIH rats. 340/380 ratio trace from neurons of a CIH rat.

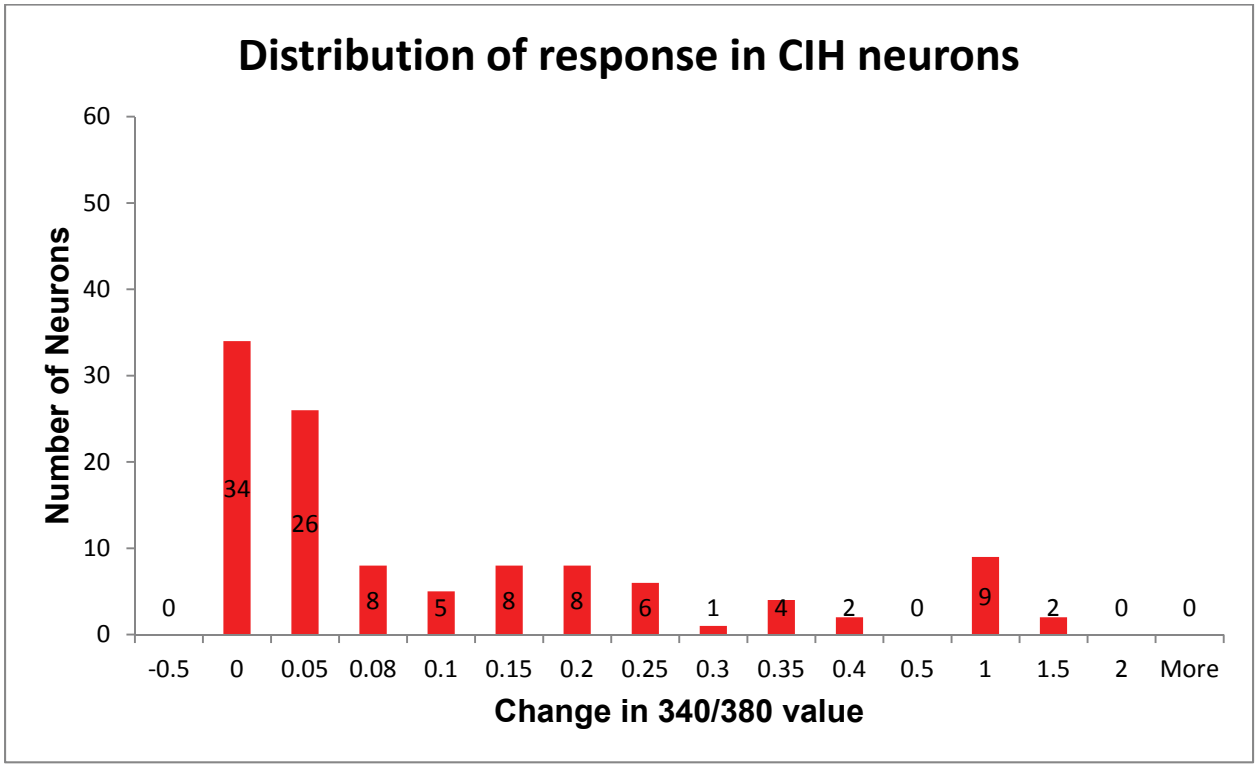

Figure 8. Graph showing the distribution of CIH neurons response to AMPA. It shows the number of neurons that showed a change in 340/380 ratio in a specific range.

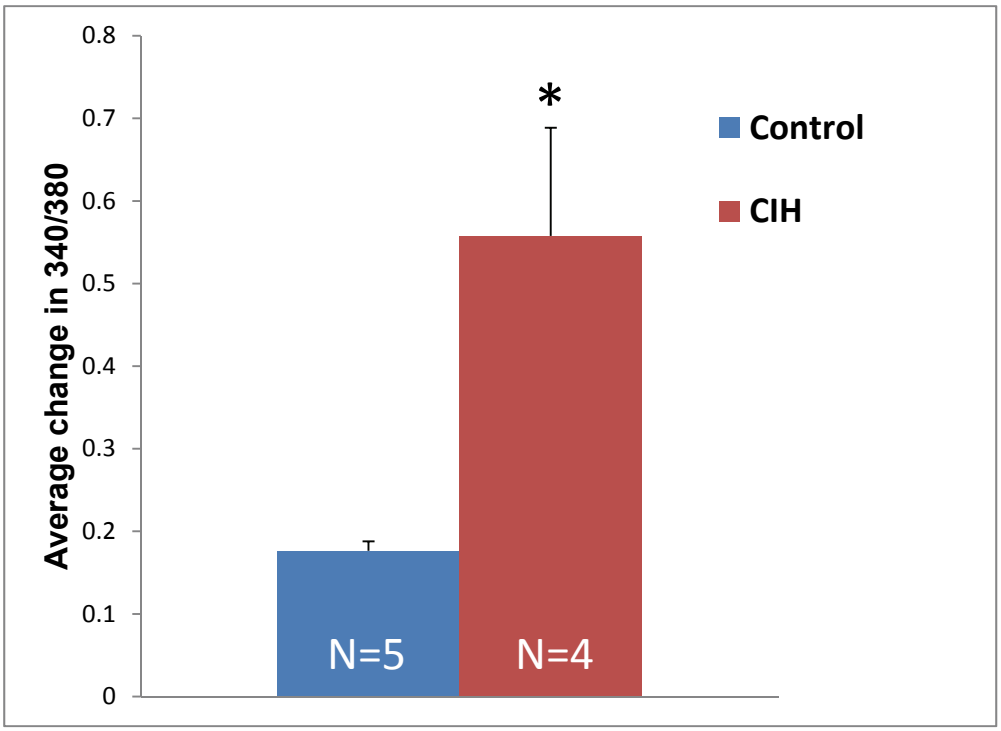

Figure 9. Graph showing the average change in the 340/380 ratio in neurons from control rats and CIH rats. *p< 0.05 vs control.

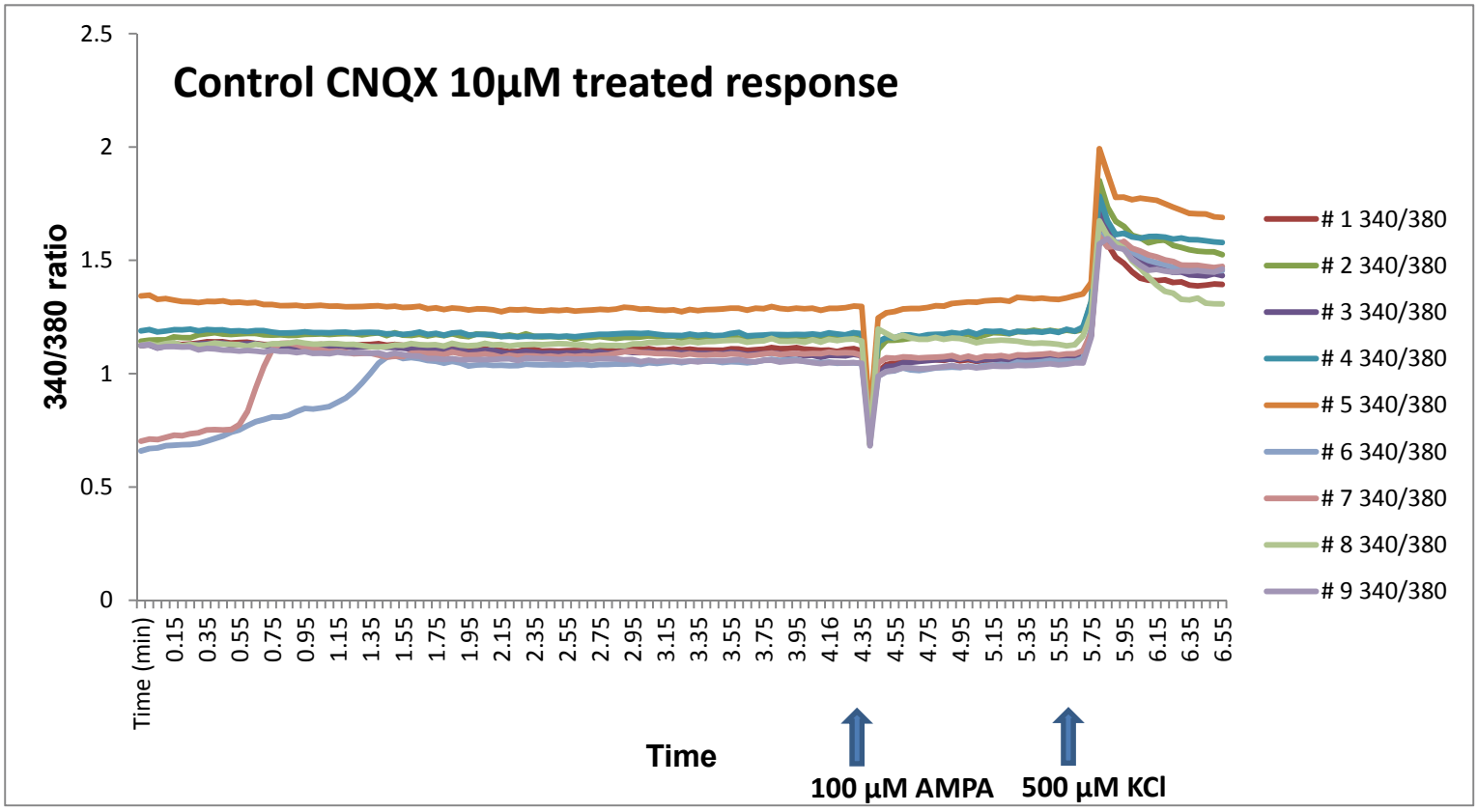

Figure 10. CNQX treatment of the slice abolished the response to AMPA in control rats. 340/380 ratio trace from neurons of a 10 µM CNQX treated slices from control rat.

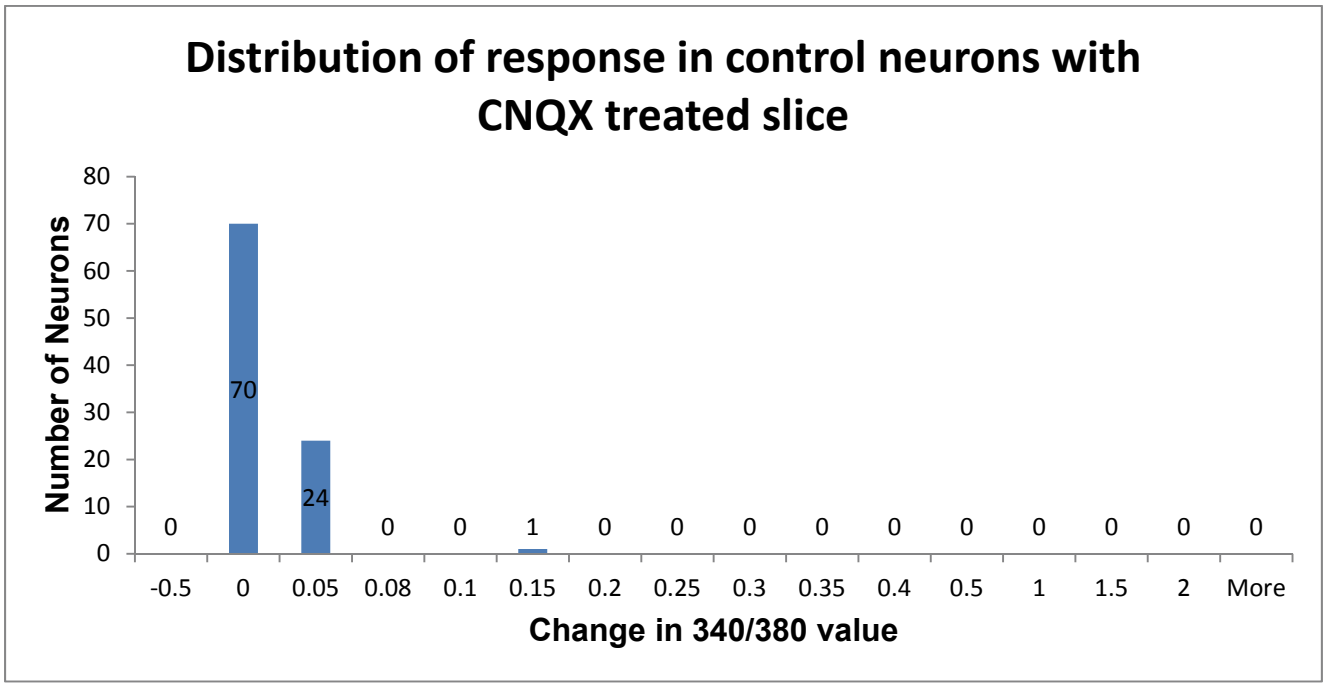

Figure 11. Graph showing the distribution of control neurons from CNQX treated slices response to AMPA. It shows the number of neurons that showed a change in 340/380 ratio in a specific range.

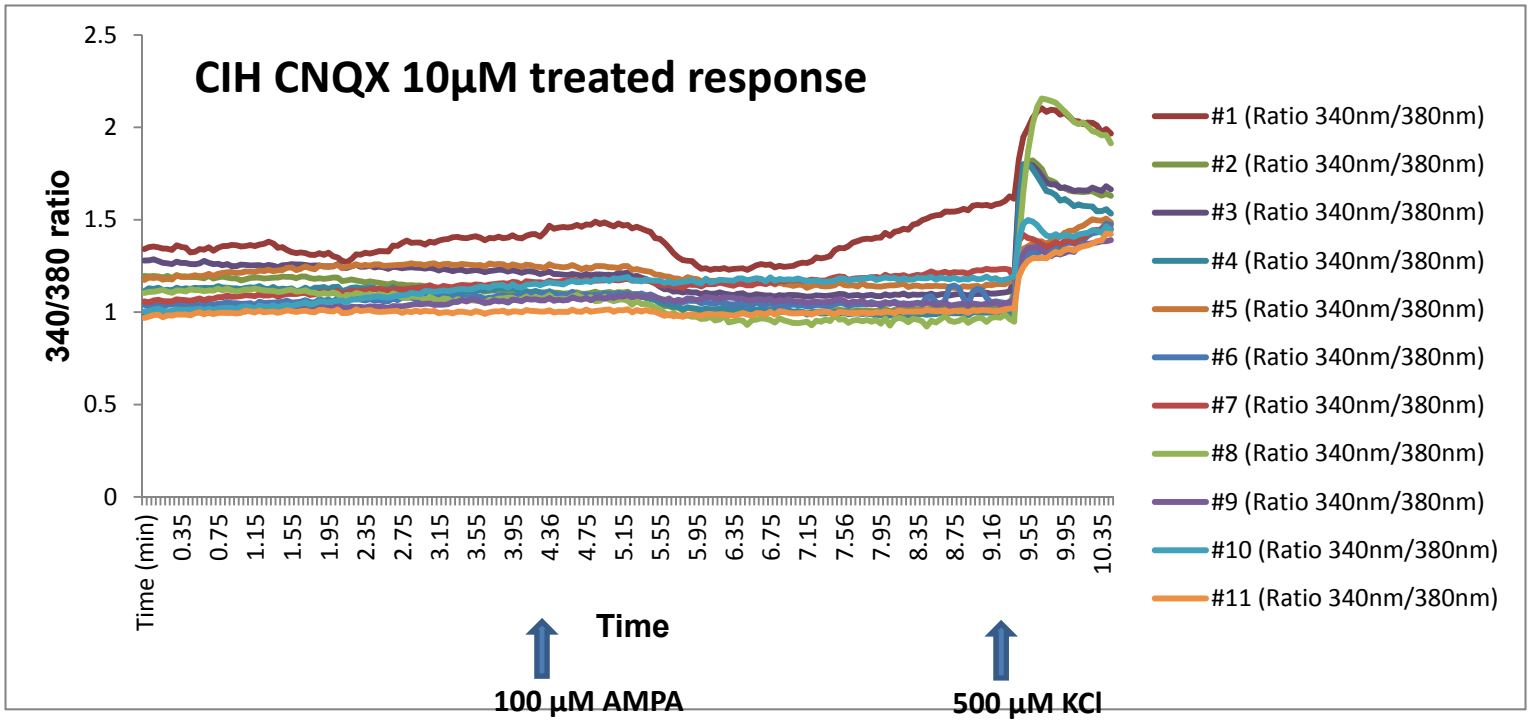

Figure 12. CNQX treatment of the slice abolished the response to AMPA in CIH rats. 340/380 ratio trace from neurons of a 10 µM CNQX treated slices from CIH rat.

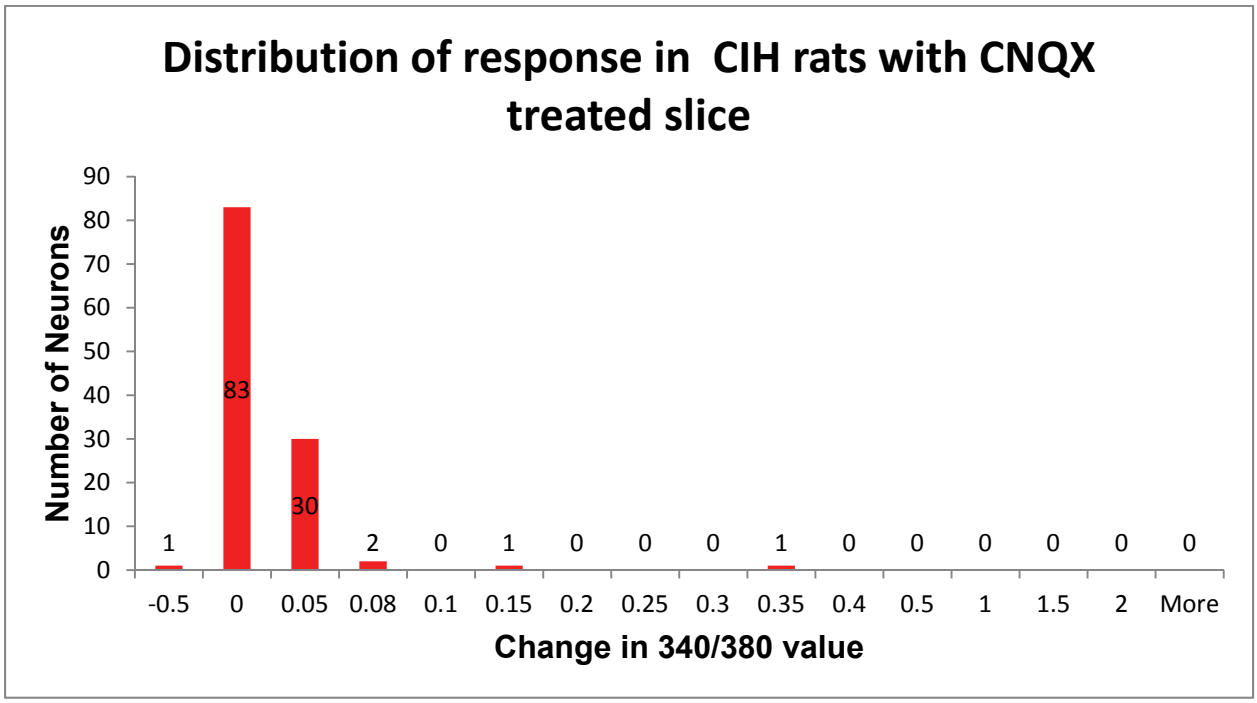

Figure 13. Graph showing the distribution of CIH neurons from CNQX treated slices response to AMPA. It shows the number of neurons that showed a change in 340/380 ratio in a specific range.

CHAPTER V

SUMMARY AND CONCLUSIONS

The purpose of this study was to ascertain the role of the A2 neurons of NTS in the cardiovascular and respiratory changes noticed in rats exposed to CIH. The summary of results from the 3 specific aims represented as chapters II, III and IV are;

1. It is possible to knockdown TH in NTS through AAV mediated technique.
2. TH knockdown in NTS reduces sustained hypertension observed during CIH.
3. Unlike previous studies where A2 ablation is thought to be the best approach to abolish stress induced hypertension, this study showed that partial reduction of only TH in NTS could abolish stress induced hypertension.
4. TH knockdown in NTS reduced the excitatory drive to the parvo cellular regions of PVN.
5. RVLM of brain stem might be playing an important role in light phase or phase of hypoxic exposure induced hypertension of CIH.
6. The A2 neurons might act through HPA axis or IML of spinal cord to cause hypertension during normoxic conditions of CIH.
7. GFP labeling of A2 neurons can be done by AAV mediated approach.
8. A2 neurons demonstrate an increase in FosB mRNA levels during CIH.
9. A2 neurons also show reduction in the mRNA levels of GluR2 subunit of AMPA receptor and angiotensin receptor AT1A following CIH.

10. Protein levels of AMPA receptor subunits GluR1 decreases and GluR2 increases in NTS after CIH.
11. GFP and fura coloclaization in NTS was not possible.
12. NTS neurons displayed increased calcium influx and responded more to AMPA following CIH.
13. There might be some post – translational modifications occurring in the AMPA receptor subunits in the NTS neurons during CIH to make them more calcium permeable.

Based on these results, the first and foremost conclusion is that the A2 neurons of the NTS play an important role in the sustained hypertension observed during CIH.

Our overall hypothesis can be accepted based on these results and the series of events occurring during CIH could be;

"Glutamate released from CR afferents due to hypoxemia during CIH can act through AMPA receptors on NTS neurons to increase calcium influx. This leads to molecular alterations. The resulting effect might be increased excitatory drive from the NTS neurons to the upstream nuclei, to act through different pathways and cause increased SNA which in turn could be responsible for sustained hypertension during CIH".

Proposals for further research

Overall, this research increased our understanding of the mechanisms behind the hypertension observed during CIH. However, there is scope for further studies that could be conducted from the results of this investigation. The following experiments are proposed:

1. Measuring the amount of neurotransmitter release at the upstream nuclei like PVN, MnPO and RVLM after TH knockdown in the NTS.
2. Corticosterone measurement in the TH-shRNA injected rats during CIH.
3. To determine if TH knockdown in NTS could decrease the SNA in CIH exposed rats.
4. To measure the angiotensin concentration in TH-shRNA injected rats.
5. Protein analysis of A2 neurons from CIH exposed rats to see if any changes in mRNA levels were also seen in their respective protein levels.
6. Protein analysis for phosphorylated forms of AMPA subunits in NTS of CIH exposed rats.
7. Retrograde labeling approach of A2 neurons to perform calcium imaging in A2 neurons.

CHAPTER VI

GENERAL DISCUSSION

In chapter II studies were conducted to examine the effect of TH knockdown on the sustained hypertension noticed during CIH in adult male Sprague-Dawley rats. The studies resulted in CIH induced sustained hypertension being eliminated by TH knockdown. There was also a moderate reduction in the sustained elevation in heart rate and a significant decrease in sustained increase in respiratory rate during the normoxic phase of CIH. Neuronal plasticity marker, FosB expression decreased in the PVN, presenting a potential pathway through which A2 neurons might mediate in the sustained hypertension during CIH. The RVLM did not display significant changes in FosB-ir. The IML of spinal cord and/or HPA axis might be part of the pathway through which the PVN might be acting (1).

The A2 neuron contribution to the CIH induced hypertension was evident from studies in chapter II. However, it was important to perform experiments to study the changes occurring at molecular level in the A2 neurons to understand the mechanisms behind CIH induced hypertension. Adeno-associated virus approach of labeling the A2 neurons and their analysis by laser capture microdissection was novel and adventurous. The results show that AAV mediated labeling was successful and there are certain molecular alterations occurring in A2 neurons during CIH. GluR2, the less calcium permeable AMPA subunit mRNA decreased in the A2 neurons which infer that these neurons might become more calcium permeable during CIH. However, protein analysis from NTS punches revealed an increase in the same GluR2 subunit and reduction in GluR1 sub-unit, the calcium permeable subunit of AMPA receptor. These results show that NTS neurons might display a varied calcium influx pattern by A2 and non-A2

neuronal groups following CIH. As A2 neurons have been shown to exhibit increased FosB-ir after CIH (6), increase in FosB mRNA levels was anticipated. Based on the existing literature, the reduction in angiotensin receptor AT1A mRNA following CIH is difficult to interpret.

Results from chapter III have made us hypothesize that A2 neurons can show an increased calcium influx following CIH and non-A2 neurons to exhibit less calcium influx. The colocalization of GFP labeled neurons with fura labeling was not seen probably due to GFP quenching fura or preventing fura uptake by the neurons. Calcium imaging of the NTS neurons revealed increased calcium influx following CIH upon AMPA treatment. The neurons analyzed likely included A2 and non A2 neurons. All neurons of NTS displaying a similar pattern of calcium influx after AMPA application was puzzling as it is different from what we anticipated. The possible reason for this trend could be that the AMPA receptor subunits of NTS neurons might be undergoing some post-translational modifications following CIH, which could lead to changes in trafficking and/or phosphorylation causing the calcium influx to go higher in all the neurons of NTS. Further studies to perform protein analysis for phosphorylated subunits of AMPA receptors are required to understand this increase in calcium influx in all NTS neurons following CIH.

Corticosterone assay from the urine samples displayed a significant reduction in the corticosterone of TH-shRNA injected rats (data not shown). This shows that A2 neurons also play a significant role in the HPA axis mediated hypertension during CIH (7). A2 neurons can also act through hypothalamic-pituitary-adrenal (HPA) axis as they are found to express glucocorticoid receptors (3, 4) and project to regions important in regulation of HPA axis function (8). Our group has shown that CIH sensitizes HPA axis reactivity (7) and since glucocorticoids have shown to increase arterial pressure in response to acute stress (9, 10), a

hyper-reactive stress response may also contribute to the CIH induced increase in MAP. CIH might activate the HPA axis resulting in increased circulating corticosterone which acts within the NTS through the glucocorticoid receptors to further augment neuronal responses to chemoreceptor activation. Exposure to CIH has been reported to increase the plasma corticosterone levels (11).

Based on these results, I propose the model shown in Figure 1. Systemic hypoxia during CIH will activate the chemoreceptors and CR afferents will release glutamate on to the NTS neurons, both A2 and non- A2 glutamatergic neurons. The released glutamate might be acting through AMPA receptors on these neurons to cause an increased discharge and possibly intracellular calcium levels. The calcium entering the neurons could cause molecular adaptations and vice-versa, further to increasing excitatory drive from these neurons to their respective downstream nuclei. A2 neurons might be playing an important role in the pathway 'A' through PVN, as these neurons do not project directly to RVLM (2, 5). The increased excitatory drive from A2 neurons could cause neuronal adaptations in the PVN to act through HPA axis leading to increased corticosterone release, which could act back on the A2 neurons to increase glutamatergic transmission and cause a positive feedback loop. PVN might also act through IML of spinal cord to cause an increased SNA. These 2 could be the pathways through which the A2 neurons might be playing a role in sustained hypertension during CIH. However, corticosterone might also be playing a role in the non-A2 neurons mediated pathway, 'B', increasing glutamatergic transmission from the non-A2 neurons. The pathway 'B' is where the excited non-A2 neurons might be directly acting on RVLM or the PVN acting on the RVLM increasing SNA to cause hypertension during light phase of CIH.

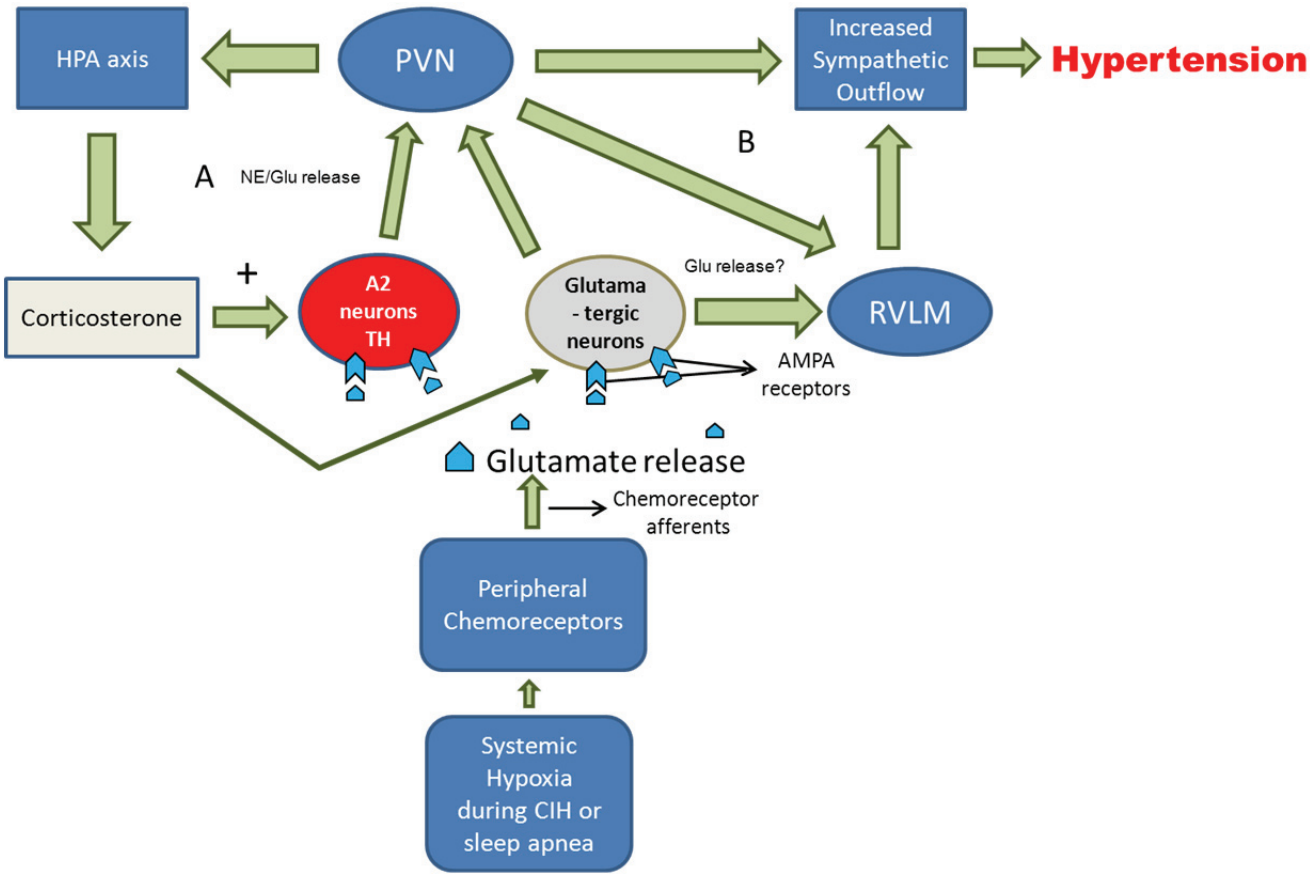

Figure 1. Overall conclusion

References

1. **Bathina CS, Rajulapati A, Franzke M, Yamamoto K, Cunningham JT, and Mifflin SW**. Knockdown of Tyrosine Hydroxylase in the Nucleus of the Solitary Tract Reduces Elevated Blood Pressure during Chronic Intermittent Hypoxia. Am J Physiol Regul Integr Comp Physiol 2013.

2. **Blessing WW, Hedger SC, Joh TH, and Willoughby JO**. Neurons in the area postrema are the only catecholamine-synthesizing cells in the medulla or pons with projections to the rostral ventrolateral medulla (C1-area) in the rabbit. Brain Res 419: 336-340, 1987.

3. **Fuxe K, Cintra A, Agnati LF, Harfstrand A, Wikstrom AC, Okret S, Zoli M, Miller LS, Greene JL, and Gustafsson JA**. Studies on the cellular localization and distribution of glucocorticoid receptor and estrogen receptor immunoreactivity in the central nervous system of the rat and their relationship to the monoaminergic and peptidergic neurons of the brain. J Steroid Biochem 27: 159-170, 1987.

4. **Harfstrand A, Fuxe K, Cintra A, Agnati LF, Zini I, Wikstrom AC, Okret S, Yu ZY, Goldstein M, Steinbusch H, and et al.** Glucocorticoid receptor immunoreactivity in monoaminergic neurons of rat brain. Proc Natl Acad Sci U S A 83: 9779-9783, 1986.

5. **Hirooka Y, Polson JW, Potts PD, and Dampney RA**. Hypoxia-induced Fos expression in neurons projecting to the pressor region in the rostral ventrolateral medulla. Neuroscience 80: 1209-1224, 1997.

6. **Knight WD, Little JT, Carreno FR, Toney GM, Mifflin SW, and Cunningham JT**. Chronic intermittent hypoxia increases blood pressure and expression of FosB/DeltaFosB in central autonomic regions. Am J Physiol Regul Integr Comp Physiol 301: R131-139, 2011.

7. **Ma S, Mifflin SW, Cunningham JT, and Morilak DA**. Chronic intermittent hypoxia sensitizes acute hypothalamic-pituitary-adrenal stress reactivity and Fos induction in the rat locus coeruleus in response to subsequent immobilization stress. Neuroscience 154: 1639-1647, 2008.

8. **Rinaman L**. Hindbrain noradrenergic A2 neurons: diverse roles in autonomic, endocrine, cognitive, and behavioral functions. Am J Physiol Regul Integr Comp Physiol 300: R222-235, 2011.

9. **Scheuer DA, Bechtold AG, Shank SS, and Akana SF**. Glucocorticoids act in the dorsal hindbrain to increase arterial pressure. Am J Physiol Heart Circ Physiol 286: H458-467, 2004.

10. **Scheuer DA, Bechtold AG, and Vernon KA**. Chronic activation of dorsal hindbrain corticosteroid receptors augments the arterial pressure response to acute stress. Hypertension 49: 127-133, 2007.

11. **Zoccal DB, Bonagamba LG, Antunes-Rodrigues J, and Machado BH**. Plasma corticosterone levels is elevated in rats submitted to chronic intermittent hypoxia. Auton Neurosci 134: 115-117, 2007.

APPENDIX A

MINERALOCORTICOID RECEPTOR IN THE NUCLEUS OF THE SOLITARY TRACT STIMULATES SALINE INTAKE DURING 4TH VENTRICULAR INFUSIONS OF ALDOSTERONE

Running Title: NTS and saline intake

Bhuvaneswari Koneru*, Chandra Sekhar Bathina*,

Brandon H. Cherry, Steve W. Mifflin

*These authors contributed equally to this work

Department of Integrative Physiology

Cardiovascular Research Institute

University of North Texas Health Science Center

Published in Am J Physiol Regul Integr Comp Physiol 306: R61–R66, 2014.

First published November 20, 2013; doi:10.1152/ajpregu.00434.2013.

Abstract

The purpose of this study was to determine if neurons within the NTS that express the mineralocorticoid receptor (MR) play a role in aldosterone stimulation of salt intake. Adult WKY rats received microinjections into the NTS of a short-hairpin RNA for the MR, to site-specifically reduce levels of the MR by RNA interference (shRNA; n=9), or scrambled RNA as a control (scRNA; n=8). After injection of the viral construct, aldosterone-filled osmotic mini-pumps were implanted subcutaneously and connected to a cannula extending into the 4th ventricle to infuse aldosterone at a rate of 25ng/h. Prior to and after surgeries, rats had *ad libitum* access to normal sodium (0.26%) rat chow and two graduated drinking bottles filled with either distilled water or 0.3M NaCl. Prior to surgeries, basal saline intake was 1.6ml ± 0.6ml in the scRNA group and 1.56ml ± 0.6ml in the shRNA group. 24 days post-surgery, saline intake was elevated to a greater extent in the scRNA group (5.9ml± 1.07ml) than in the shRNA group (2.41ml ± 0.6ml). Post-mortem immunohistochemistry revealed a significant reduction in the number of NTS neurons exhibiting immunoreactivity for MR in shRNA-injected rats (23 ± 1 cells/section) *vs.* scRNA-injected rats (33 ± 2 cells/section; p=.008). shRNA did not alter the level of HSD2 protein in the NTS as judged by the number of HSD2 immunoreactive neurons. These results suggest that 4th ventricular infusions of aldosterone stimulate saline intake and that this stimulation is at least in part mediated by hindbrain NTS neurons that express MR.

Key Words: Mineralocorticoid receptor, NTS, HSD2 neurons, sodium intake

Introduction

Sodium plays a very important role in maintaining electrolyte homeostasis (27). Sodium ingestion is often essential to restore lost body fluids. Excess sodium intake can lead to elevation in blood pressure and metabolic syndrome (3, 18). Many health organizations across the world suggest that hypertensive patients reduce their salt intake as a first line of defense in their anti-hypertensive therapy. Increased salt intake is also associated with oxidative stress (20). Furthermore, studies also show increased salt preference in heart failure patients, suggesting another link between salt intake and cardiovascular disease (9, 22).

The renin-angiotensin-aldosterone and vasopressin systems are important mechanisms by which the body maintains fluid and ion balance (12, 27). Aldosterone is released in response to falling concentrations of circulating sodium, as well as increased circulating concentrations of potassium and angiotensin II (7, 19). After being released, aldosterone binds the mineralocorticoid receptor (MR) to promote Na^+ and simultaneous water absorption and potassium excretion (6). This role of aldosterone in maintaining sodium balance was discovered long ago (23, 24), and in fact it was shown in the 1960's that high doses of aldosterone can increase sodium intake even in the absence of sodium deficiency (30).

The MR has equal affinity for mineralocorticoids such as aldosterone as it does for glucocorticoids such as cortisol and corticosterone (4, 13). 11-beta-hydroxysteroid dehydrogenase type II (HSD2) is an enzyme that catalyzes the conversion of active cortisol to inert cortisone (1). This conversion plays an important role in MR-expressing cells by preventing binding of cortisol (a glucocorticoid) to the MR and allowing aldosterone to bind in its place. Thus, co-expression of MR and HSD2 are the two key characteristics that define whether a cell is selective for aldosterone over corticosterone.

Despite numerous ongoing studies examining the mechanisms by which MR and aldosterone regulate renal function, the central mechanisms whereby aldosterone stimulates Na+ intake still remain unclear. Identifying the underlying neural circuitry responsible for modulating salt intake will aid in developing treatments that could specifically target key points in the regulatory cascades involved and prevent the deleterious cardiovascular effects of excess salt intake.

Previous studies have shown that MR is expressed in many CNS sites (5), but it is the presence of HSD2 that makes cells selective for aldosterone. Roland *et al.* in 1995, demonstrated that HSD2 mRNA is expressed in neurons within the nucleus tractus solitarius (NTS) (25). Adding to this, Geerling *et al.* in 2006 discovered a group of cells within the NTS which were immunoreactive for both MR and HSD2. These "HSD2 neurons" are situated in the NTS extending ventrally beneath the area postrema–an area with a diminished blood-brain barrier that allows easier influx of circulating aldosterone (14, 15).

It has been previously suggested that mechanisms driving the inhibition of salt appetite originate from the NTS. Right atrial stretch leads to activation of atrial mechanoreceptors and reduced salt intake, and NTS lesions increase salt intake (8, 21). Other studies have shown activation of HSD2 neurons in the NTS during sodium depletion, evidenced by increased immunoreactivity for c-fos—an early gene product of neuronal activation—suggesting a stimulatory role for these neurons during periods of sodium depletion (15). While these findings suggest that activation of NTS HSD2 neurons stimulates salt intake, a definitive role has yet to be established. An alternative hypothesis is that NTS HSD2 neurons function as part of a negative feedback circuit that inhibits or limits sodium intake. Therefore, the goal of this study was to determine if NTS HSD2 neurons play a role in the mediation/modulation of salt intake.

Materials and Methods

General: Rats (Wistar-Kyoto WKY, Charles River Laboratories, Inc., Wilmington, MA) were allowed to acclimatize for at least one week after arrival in the animal facility maintained at 23°c with 12hour light: 12hour dark cycle (12L:12D, on at 7 AM, off at 7 PM), before any surgical procedure was performed. All experimental procedures were approved by the Institutional Animal Care and Use Committee (IACUC) of the University of North Texas Health Science Center.

AAV microinjections: The adeno-associated viral vector with shRNA (short hairpin RNA) used to knock-down the MR (the construct sequence is AAV1/2-U6 Rat.Nr3c3/MR.shRNA terminator- CAG-EGFP-WPRE-BGH-polyA) and the scRNA (scrambled RNA, which acts as control) are commercially available (Catalog number: GD1009-RV; GeneDetect, New Zealand; previously cited by Xue *et al.*) (31). The U6 promoter drives expression of the shRNA and the CAG promoter drives expression of enhanced green fluorescent protein (EGFP). The CAG promoter consists of chicken β-actin promoter hybridized with the cytomegalovirus (CMV) immediate early enhancer sequence and is highly efficient in neurons. The Woodchuck post-transcriptional regulatory element (WPRE) and the presence of a bovine growth hormone (BGH) polyadenylation sequence ensure high transcription following transduction. Microinjections were performed in an aseptic environment as described previously (10, 29) to inject shRNA and scRNA into the NTS of WKY rats under 2% isoflurane anesthesia. To cover the rostral-caudal extent of NTS HSD2 neurons, three injections of the viral construct (100 nl; > 1 x 10^{12} genomic particles/ml) were injected 0.5 mm below the surface at calamus scriptorius and bilaterally at 0.5mm rostral and 0.5mm lateral to calamus. The NTS regions affected by these injection parameters have been shown to contain the highest number of HSD2 immunoreactive neurons (5,

14, 15). Importantly, although the AAV construct freely transfects any neurons in the regions encompassed by injections and drives GFP synthesis, the shRNA only acts to knock down MR in neurons that synthesize MR.

Osmotic mini-pumps: Immediately after injection of the AAV constructs and while still under isoflurane anesthesia, osmotic mini-pumps (Alzet model 2004, 0.25µl/h) were implanted into a small pocket under the skin at the base of the neck. The pumps were connected to the free end of a 23 gauge cannula that had been extended into in the 4th ventricle using stereotaxic coordinates then cemented into place with dental acrylic and jeweler's screws. Prior to implantation, pumps were filled with the MR receptor agonist aldosterone (Sigma, St.Louis, MO), dissolved in artificial cerebrospinal fluid (final concentration 100µg/ml). Infusions of aldosterone into the 4th ventricle occurred at a rate of 0.25µl/hr (25ng/hr).

Measurement of saline intake: Rats had *ad libitum* access to normal sodium (0.26%) rat chow. Two graduated glass bottles, one containing deionized water and one containing 0.3 M NaCl, were provided in the front of each cage and placed on opposite sides to prevent mixing of solutions. The position of the tubes was alternated every 24 h to control for placement preference and intake was measured to the nearest milliliter at noon every day.

Immunohistochemistry: To verify that the shRNA reduced MR levels in the NTS, rats were anesthetized with Inactin (100mg/kg IP, Sigma, St. Louis, MO) and transcardially perfused with 4% paraformaldehyde. Brains were removed and stored in 4% paraformaldehyde at 4°C for 1-2 hours, then transferred into 30% sucrose solution. Each hindbrain was sectioned (40 µm thick) coronally into 3 sets and stored at -20°C in a cryoprotectant solution until processed for immunohistochemistry. Different sets of serial sections were processed either for the MR (Primary antibody: rMR-1-18 1D5, provided by Dr. Elise Gomez-Sanchez; 1:500. Secondary

antibody: biotinylated anti mouse, Jackson immunoresearch laboratories Inc, PA; 1:1000.) or HSD2 (Primary antibody: Chemicon/Millipore, Billerica, MA. 1:20,000 and secondary antibody: biotinylated anti sheep, Jackson immunoresearch laboratories Inc, PA; 1:100). Tissue sections were incubated in primary antibody for 48 hrs at 4^{o}C after a series of washes with phosphate buffered saline (PBS), then for 2 hrs at room temperature with secondary antibody. At this point, sections were reacted with an avidin-peroxidase conjugate (Vectastain ABC kit, PK-4000; Vector labs, Burlingame, CA, USA) and PBS containing 0.04% 3, 3'–diaminobenzidine hydrochloride and 0.04% nickel ammonium sulfate for 10-11 min. The tissues were then mounted on gelatin coated slides and cover slipped with Permount mounting medium (Fisher Scientific, NJ)

Imaging and cell counts: An Olympus microscope (BX41) equipped with epifluorescence and Olympus DP70 digital camera and DP Manager Software (version 2.2.1., Olympus, Tokyo, Japan) was used to capture images of the MR and HSD2 immunostaining. ImageJ software (v 1.44, NIH, Bethesda, MD, USA) was used to count the number of MR or HSD2 positive cells from each rat and expressed as an average number per section.

Statistical analysis: All data are presented as mean ± SE. Differences between the group injected with shRNA and the one injected with scRNA over several days were determined by 2-way analysis of variance (ANOVA) with repeated measures on time. A Holm-Sidak *post hoc* test was performed to reveal any significant difference among mean values. Student t-test was conducted to compare the mean number of MR immunoreactive and HSD2 immunoreactive cells in the scRNA and shRNA groups. $P < 0.05$ was considered statistically significant.

Results

Prior to injections of the viral constructs into the NTS and implantation of 4th ventricular osmotic mini-pumps, the weights of shRNA-injected rats (n=9, 275±8 g) and scRNA-injected rats (n=8, 273±6 g) were not significantly different. Prior to sacrifice (28 days later) shRNA-injected rats still weighed approximately the same (323±6 g) as scRNA-injected rats (320±7 g) suggesting that the intake of sodium via the chow was not different between the 2 groups.

Figure 1 illustrates the mean saline intake values of shRNA-injected and scRNA-injected rats during the period of the study. Days 1-4 represent saline intake preceding NTS injections and implantation of the aldosterone-filled osmotic mini-pumps. Basal saline intake was low in both groups prior to surgery (1.6ml ± 0.6ml in the scRNA group and 1.56ml ± 0.6ml in the shRNA group). On the first post-surgical day (day 5) saline intake began to increase in both groups indicating that the 4^{th} ventricular infusion of aldosterone was stimulating saline intake. Saline intake remained elevated for the duration of the study in the scRNA-injected rats. However, the aldosterone stimulated saline appetite began to fall one week post-surgery in the shRNA–injected rats and remained lower than saline intake in the scRNA –injected rats for the duration of the study. Furthermore, this increased saline intake in scRNA compared to shRNA was sustained 24 days post-surgery (5.9ml± 1.07ml in the scRNA group and 2.41ml ± 0.6ml in the shRNA group).

Two-way ANOVA revealed significant difference in saline intake both as a function of group (shRNA *vs.* scRNA, $p<.001$) and as a function of time ($p<.001$). Post-hoc analysis (Holm-Sidak) revealed that in scRNA-injected rats, there was a significant increase in saline intake following implantation of the osmotic mini-pump compared to control (day 4), except on days 5,6,7,10,11,18,19 & 27 ($p<.05$). In shRNA injected rats, there was no significant increase in

saline appetite compared to control on any day following implantation of the osmotic mini-pump. Water intake was not different between the groups.

Figure 2A depicts the robust difference in mean saline intake between scRNA-injected rats *vs.* those injected with shRNA during the period from 14-21 days after microinjections and osmotic minipump implantation. Figure 2B shows that the mean water intake of scRNA- and shRNA-injected groups during this same period after the microinjections and osmotic minipump implantation was not significantly different. Figure 2C illustrates the absence of any difference in total fluid intake between shRNA- and scRNA-injected groups during this time.

Immunohistochemistry was performed to visualize the reduction in apparent amount of MR within the NTS following shRNA injection (Figure 3). GFP expression and immunofluorescence (Figure 3A) marked a successful transfection of NTS neurons with the viral constructs, and MR immunoreactivity was predominantly nuclear (Figure 3C and 3D). The number of cells showing immunoreactivity for MR was greater in scRNA-injected brains *vs.* shRNA-injected brains (33 ± 2 cells/section and 23 ± 1 cells/section, respectively; p=.008). This significantly decreased number of MR immunoreactive neurons in shRNA-injected brains demonstrates the efficacy of the virus in successfully knocking down the MR.

Since HSD2 and MR are co-localized within the NTS (HSD2 neurons) (14, 15), we counted neurons demonstrating immunoreactivity for HSD2 in both the scRNA- and shRNA-injected groups (Figure 3E and 3F), and observed no difference between groups. This suggests that the observed reduction in MR immunoreactivity following injections of the shRNA constructs was not due to neurotoxicity. Figure 3B shows the comparison of NTS neurons per section exhibiting MR immunoreactivity (left bar graph; $p<0.05$) and HSD2-immunoreactivity (right bar graph) in rats injected with scRNA and rats injected with shRNA.

Discussion:

Stimulation of salt intake is understood to originate primarily from the structures of the hypothalamus and forebrain, whereas inhibition of salt intake is proposed to arise from a pathway between the NTS and parabrachial nucleus, which can be activated by right atrial stretch (8). The findings by Geerling and Loewy describing NTS neurons that contain both MR and HSD2 in 2006 (14, 15) generated a great deal of interest in how these neurons may play a role in the stimulation of salt intake (14). However this evidence is correlative and not demonstrative. They demonstrated that reductions in dietary sodium induced the expression of c-fos in NTS HSD2 neurons, while re-establishing access to dietary sodium reduced c-fos expression in NTS HSD2 neurons to basal levels (15). These changes in activity are consistent with a role for HSD2 neurons in the stimulation of salt intake during periods of sodium depletion. However, such responses are also consistent with a negative feedback system that serves to suppress sodium intake during periods when salt intake is increased.

To test the hypothesis that NTS neurons play a role in mediating stimulated saline intake we utilized shRNA to reduce the amount of MR in these cells, then stimulated saline intake by infusing aldosterone at the rate of 25ng/hr into the 4th ventricle. RNA-interference using viral-mediated shRNA delivery can reduce protein levels in a region of interest. shRNA integrates into the cell's nucleic acid and silences genes in a sequence specific manner at the mRNA level by forming a RNA-induced silencing complex (RISC) after being cleaved into small interference RNA (siRNA) by ribonuclease III enzyme. The mechanism of shRNA-mediated gene silencing has been discussed in detail in a previous publication (28). Unlike, knockout models which are limited by developmental defects and lack of regional specificity, shRNA delivery through AAV can result in in vivo reduction of a selective gene in a precise region. Many groups, including

ours, have successfully demonstrated the advantage and specificity of shRNA (2, 17, 26, 32). Since cerebrospinal fluid flows rostral to caudal within the central ventricular system, the effects of 4th ventricular infusion should be restricted to the hindbrain. Our data indicate that increased saline intake during 4th ventricular infusions of aldosterone can be attributed to activation of the MR within the NTS, which lie near enough to the 4th ventricle for adequate diffusion of the drug, and also in an area which has an incomplete blood brain barrier (16).

Based upon the functional anatomical studies of Geerling and Loewy cited previously, we feel the neurons most likely to mediate the increased saline intake stimulated by 4th ventricular infusions of aldosterone are the NTS HSD2 neurons. However, it is important to consider that while the majority of NTS neurons that contain MR also contain HSD2, not all MR-containing NTS neurons contain HSD2. While non-HSD2 neurons would not be likely to respond to physiological levels of aldosterone due to occupancy of the MR by corticosterone, we cannot exclude the possibility that they may participate in the responses to 4th ventricular infusions of aldosterone.

A recent study by Formenti *et al.* support our results—they showed that 4th ventricular infusions of aldosterone increased the saline intake in Wistar Hanover rats in a dose-dependent fashion (11). The increase in the saline intake they observed after aldosterone infusion in their study is quite higher (~40ml in response to infusion of aldosterone at the rate of 25ng/hr) than what we observed in the scrambled group (~6ml in response to infusion of aldosterone at the rate of 25ng/hr). They also reported decreased water intake in aldosterone-treated (10ng/hr) and vehicle-treated groups on 6th day after the minipump implantation, which was absent in our current study following a higher dose of aldosterone. One potential explanation for this discrepancy in water intake could be the difference in animal strain used. Also, Formenti *et al*. used a higher rate of

infusion (2µl/hr) with low concentration of aldosterone (5µg/ml), while we used a higher concentration of aldosterone (100µg/ml) at a low rate of infusion (0.25µl/hr). Despite their higher rate of infusion, the amount of aldosterone accessible to the target neurons was higher in our study (0.25 ug/hr) than in the study of Formenti *et al*. (.01ug/hr). Therefore, at this time there is not an obvious explanation for the difference between the two studies.

The initial increase in saline intake observed following aldosterone infusion is similar between both experimental groups in our study. During the period of time when the shRNA is reported to have begun exerting its effects (i.e. 14-21 days post-injection), saline intake of the shRNA-injected group dropped significantly compared to the scRNA-injected group. Water intake did not differ between the two groups 14-21 days post-op, but the saline intake of shRNA-injected group was reduced. This demonstrates that the shRNA-mediated MR knockdown altered saline intake independently. Reducing NTS MR expression by this method did not exert any apparent effect on basal saline intake, however we noted that basal saline intake is very low in WKY (and in the Sprague-Dawley, unpublished observations, 2012).

MR knock-down in the NTS did not appear to modulate food intake, as weight gain during the protocol was not different in shRNA-injected rats *vs.* scRNA- injected rats. The expression of GFP in the NTS offered assurance that successful transfection was achieved in the desired region. shRNA knock-down reduced the number of cells with MR immunoreactivity by 27%, but did not alter the number of cells with HSD2 immunoreactivity. Since MR and HSD2 are co-localized in most NTS HSD2 neurons, this suggests that the viral constructs had no obvious neurotoxic effects.

Conclusion

Reductions in the expression of MR within the rostral-caudal NTS do not appear to alter basal saline intake. However, infusion of aldosterone into the 4th ventricle evokes a prompt and dramatic increase in saline appetite that is suppressed by shRNA knock-down of MR. These viral constructs do not appear to exhibit any neurotoxicity, as the shRNA does not alter the number of HSD2 immunoreactive neurons. Since HSD2 and MR are co-localized in the NTS, these results indicate a reduction in MR level that is acting to reduce the increased saline appetite stimulated by 4th ventricular infusions of aldosterone.

Perspectives

Infusion of aldosterone into the 4th ventricle evoked a prompt and significant increase in saline appetite. Injection of a viral construct to reduce the expression of MR within the NTS attenuated the increase in saline appetite stimulated by 4th ventricular infusions of aldosterone. The constructs did not appear to have any toxicity as the shRNA did not alter the number of HSD2 immunoreactive neurons and HSD2 and MR are co-localized in the NTS. These results suggest that HSD2 neurons in the NTS are responsible for increased saline intake following stimulation by aldosterone.

Sources of funding

This work was supported by funds provided by the Dept. of Integrative Physiology, UNTHSC.

Conflicts of Interest/Disclosures

None

References:

1. **Amelung D, Hubener HJ, Roka L, and Meyerheim G**. Conversion of cortisone to compound F. *J Clin Endocrinol Metab* 13: 1125-1126, 1953.

2. **Bathina CS, Rajulapati A, Franzke M, Yamamoto K, Cunningham JT, and Mifflin SW**. Knockdown of Tyrosine Hydroxylase in the Nucleus of the Solitary Tract Reduces Elevated Blood Pressure during Chronic Intermittent Hypoxia. *Am J Physiol Regul Integr Comp Physiol* 2013.

3. **Baudrand R, Campino C, Carvajal C, Olivieri O, Guidi G, Faccini G, Vohringer P, Cerda J, Owen G, Kalergis A, and Fardella C**. High sodium intake is associated with increased glucocorticoid production, insulin resistance and metabolic syndrome. *Clin Endocrinol (Oxf)* 2013.

4. **Beaumont K, and Fanestil DD**. Characterization of rat brain aldosterone receptors reveals high affinity for corticosterone. *endocrinology* 113: 2043-2051, 1983.

5. **Chao HM, Choo PH, and McEwen BS**. Glucocorticoid and mineralocorticoid receptor mRNA expression in rat brain. *Neuroendocrinology* 50: 365-371, 1989.

6. **Cuthbert AW, and Painter E**. Mechanism of action of aldosterone. *Nature* 222: 280-281, 1969.

7. **Davis JO, Urquhart J, and Higgins JT, Jr.** The effects of alteration of plasma sodium and potassium concentration on aldosterone secretion. *J Clin Invest* 42: 597-609, 1963.

8. **De Gobbi JI, Menani JV, Beltz TG, Johnson RF, Thunhorst RL, and Johnson AK**. Right atrial stretch alters fore- and hind-brain expression of c-fos and inhibits the rapid onset of salt appetite. *J Physiol* 586: 3719-3729, 2008.

9. **de Souza JT, Matsubara LS, Menani JV, Matsubara BB, Johnson AK, and De Gobbi JI**. Higher salt preference in heart failure patients. *Appetite* 58: 418-423, 2012.

10. **Dias AC, Vitela M, Colombari E, and Mifflin SW**. Nitric oxide modulation of glutamatergic, baroreflex, and cardiopulmonary transmission in the nucleus of the solitary tract. *Am J Physiol Heart Circ Physiol* 288: H256-262, 2005.

11. **Formenti S, Bassi M, Nakamura NB, Schoorlemmer GH, Menani JV, and Colombari E**. Hindbrain mineralocorticoid mechanisms on sodium appetite. *Am J Physiol Regul Integr Comp Physiol* 304: R252-259, 2013.

12. **Funder JW**. Central effects of mineralocorticoids on blood pressure: new answers, new questions. *J Hypertens* 20: 1715-1716, 2002.

13. **Funder JW, Pearce PT, Smith R, and Smith AI**. Mineralocorticoid action: target tissue specificity is enzyme, not receptor, mediated. *Science* 242: 583-585, 1988.

14. **Geerling JC, Engeland WC, Kawata M, and Loewy AD**. Aldosterone target neurons in the nucleus tractus solitarius drive sodium appetite. *J Neurosci* 26: 411-417, 2006.

15. **Geerling JC, Kawata M, and Loewy AD**. Aldosterone-sensitive neurons in the rat central nervous system. *J Comp Neurol* 494: 515-527, 2006.

16. **Geerling JC, and Loewy AD**. Aldosterone in the brain. *Am J Physiol Renal Physiol* 297: F559-576, 2009.

17. **Hommel JD, Sears RM, Georgescu D, Simmons DL, and DiLeone RJ**. Local gene knockdown in the brain using viral-mediated RNA interference. *Nat Med* 9: 1539-1544, 2003.

18. **Karppanen H, and Mervaala E**. Sodium intake and hypertension. *Prog Cardiovasc Dis* 49: 59-75, 2006.

19. **Kotchen TA**. Effects of potassium on renin and aldosterone. *Arch Mal Coeur Vaiss* 77 Spec No: 87-91, 1984.

20. **Kushiro T, Fujita H, Hisaki R, Asai T, Ichiyama I, Kitahara Y, Koike M, Sugiura H, Saito F, Otsuka Y, and Kanmatsuse K**. Oxidative stress in the Dahl salt-sensitive hypertensive rat. *Clin Exp Hypertens* 27: 9-15, 2005.

21. **Ogihara CA, Schoorlemmer GH, Colombari E, and Sato MA**. Changes in sodium appetite evoked by lesions of the commissural nucleus of the tractus solitarius. *Braz J Med Biol Res* 42: 561-566, 2009.

22. **Parrinello G, Torres D, and Paterna S**. Salt and water imbalance in chronic heart failure. *Intern Emerg Med* 6 Suppl 1: 29-36, 2011.

23. **Rice KK, and Richter CP**. Increased sodium chloride and water intake of normal rats treated with desoxycorticosterone acetate. *Endocrinology* 33: 106-115, 1943.

24. **Richter CP**. Increased salt appetite in adrenalectomized rats. *American Journal of Physiology* 115: 155-161, 1936.

25. **Roland BL, Li KX, and Funder JW**. Hybridization histochemical localization of 11 beta-hydroxysteroid dehydrogenase type 2 in rat brain. *Endocrinology* 136: 4697-4700, 1995.

26. **Salahpour A, Medvedev IO, Beaulieu JM, Gainetdinov RR, and Caron MG**. Local knockdown of genes in the brain using small interfering RNA: a phenotypic comparison with knockout animals. *Biol Psychiatry* 61: 65-69, 2007.

27. **Skott O**. Body sodium and volume homeostasis. *Am J Physiol Regul Integr Comp Physiol* 285: R14-18, 2003.

28. **Sliva K, and Schnierle BS**. Selective gene silencing by viral delivery of short hairpin RNA. *Virol J* 7: 248, 2010.

29. **Vitela M, and Mifflin SW**. gamma-Aminobutyric acid(B) receptor-mediated responses in the nucleus tractus solitarius are altered in acute and chronic hypertension. *Hypertension* 37: 619-622, 2001.

30. **Wolf G**. Effect of Deoxycorticosterone on Sodium Appetite of Intact and Adrenalectomized Rats. *Am J Physiol* 208: 1281-1285, 1965.

31. **Xue B, Beltz TG, Yu Y, Guo F, Gomez-Sanchez CE, Hay M, and Johnson AK**. Central interactions of aldosterone and angiotensin II in aldosterone- and angiotensin II-induced hypertension. *Am J Physiol Heart Circ Physiol* 300: H555-564, 2011.

32. **Xue B, Beltz TG, Yu Y, Guo F, Gomez-Sanchez CE, Hay M, and Johnson AK**. Central interactions of aldosterone and angiotensin II in aldosterone- and angiotensin II-induced hypertension. *Am J Physiol Heart Circ Physiol* 300: H555-564, 2011.

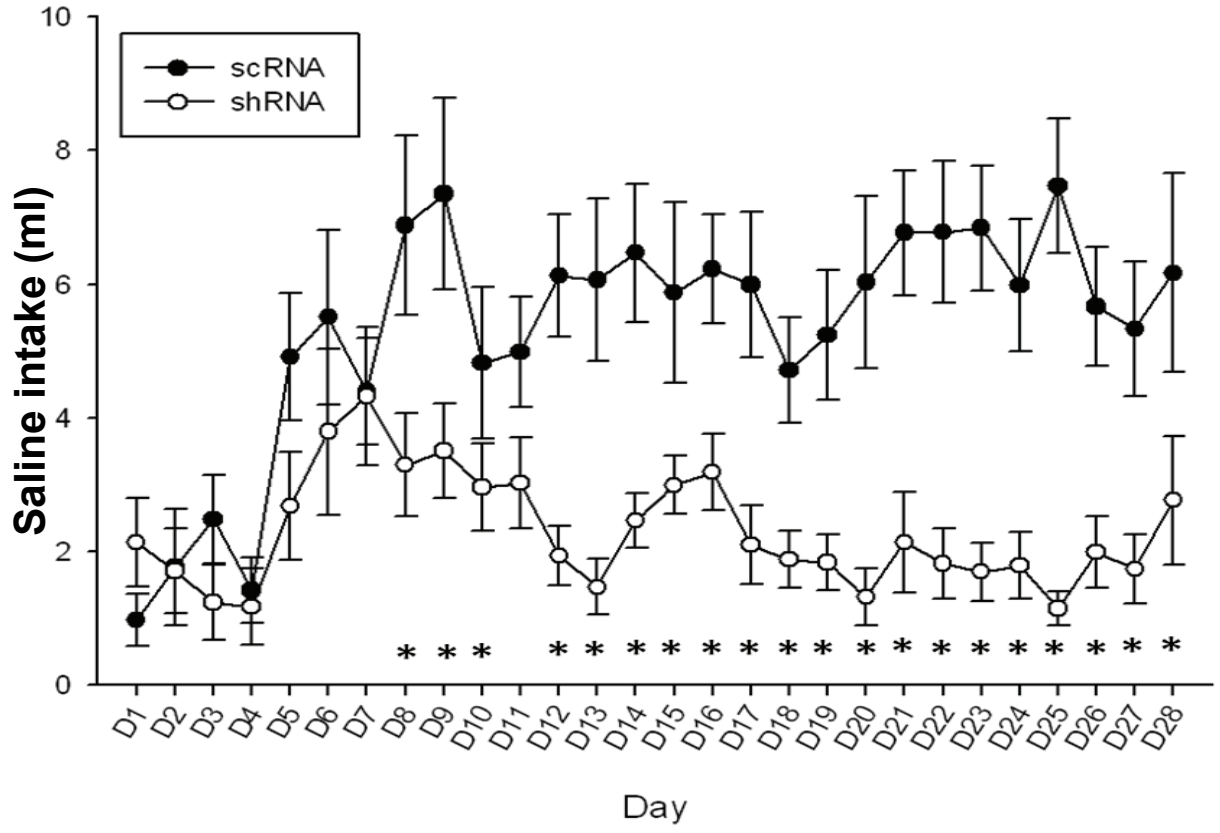

Figure 1: Saline intake before and after injections of viral constructs into the NTS

Days 1-4 represent saline intake prior to NTS injections of viral vectors and implantation of aldosterone-filled osmotic mini-pumps. Following implantation of the osmotic mini-pump there was a significant increase in saline intake in the scRNA group (n=8) compared to control while in shRNA group there is no significant change in saline intake. Comparing scRNA to shRNA injected rats, the saline intake of scRNA injected groups was significantly more than shRNA injected group after surgeries. Asterisks indicate the days on which the saline intake between the two groups was significantly different. ($p<0.05$)

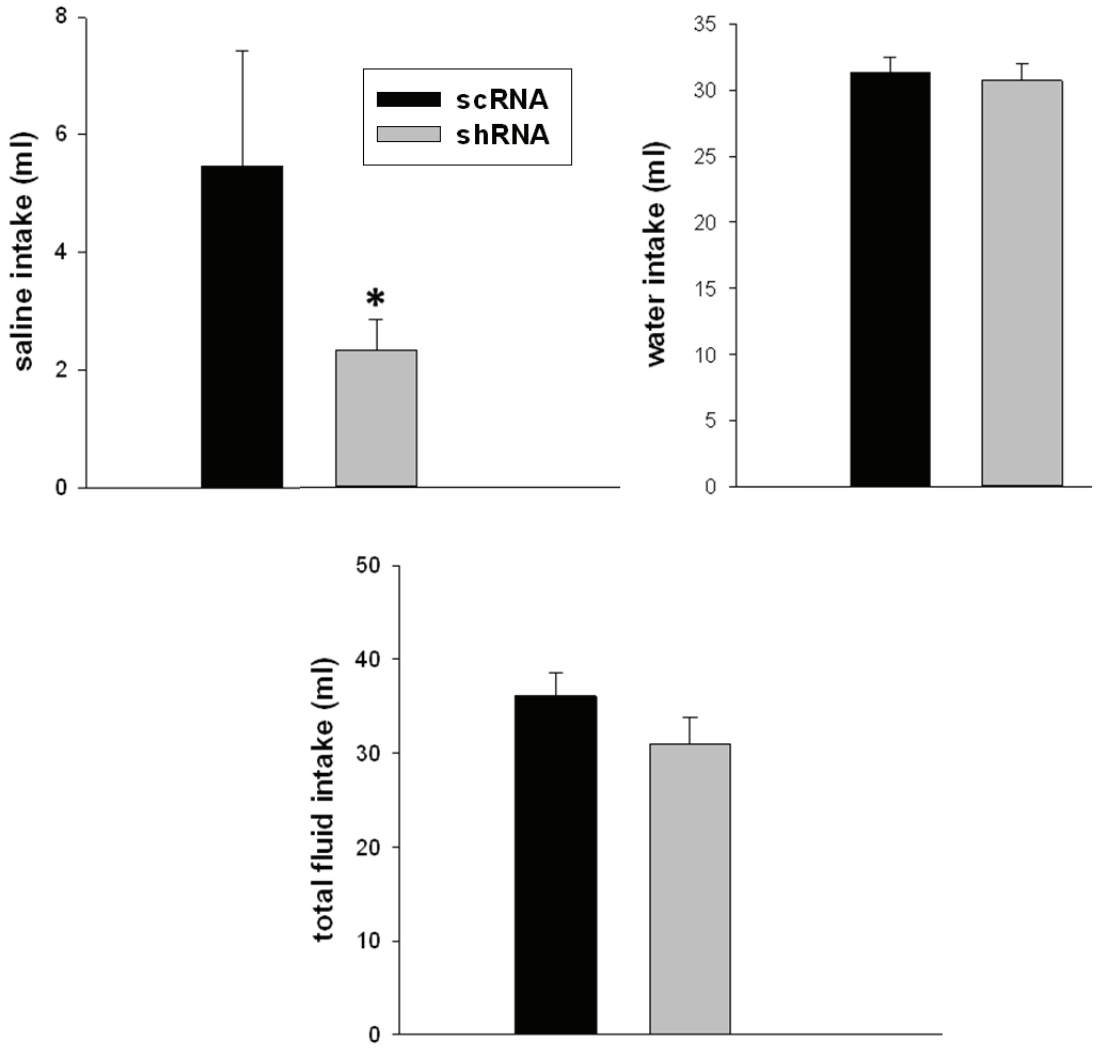
saline intake (ml)
8
6
4
2
0
scRNA
shRNA
*
water intake (ml)
35
30
25
20
15
10
5
0
total fluid intake (ml)
50
40
30
20
10
0

Figure 2: Saline and water intake comparison between scRNA and shRNA injected groups 14 days after mini-pump implants and virus injections

A. Mean values of saline intake of scRNA and shRNA injected groups after mini-pump implantation. The shRNA injected group has significantly lower saline intake.
B. Mean values of water intake of scRNA and shRNA injected groups after mini-pump implantation. There was no significant difference between the two groups.
C. Total fluid intake of scRNA and shRNA injected groups after mini-pump implantation. There was no significant difference between the two groups

Values are expressed as mean ± Standard error. Asterisk indicate $p<0.05$.

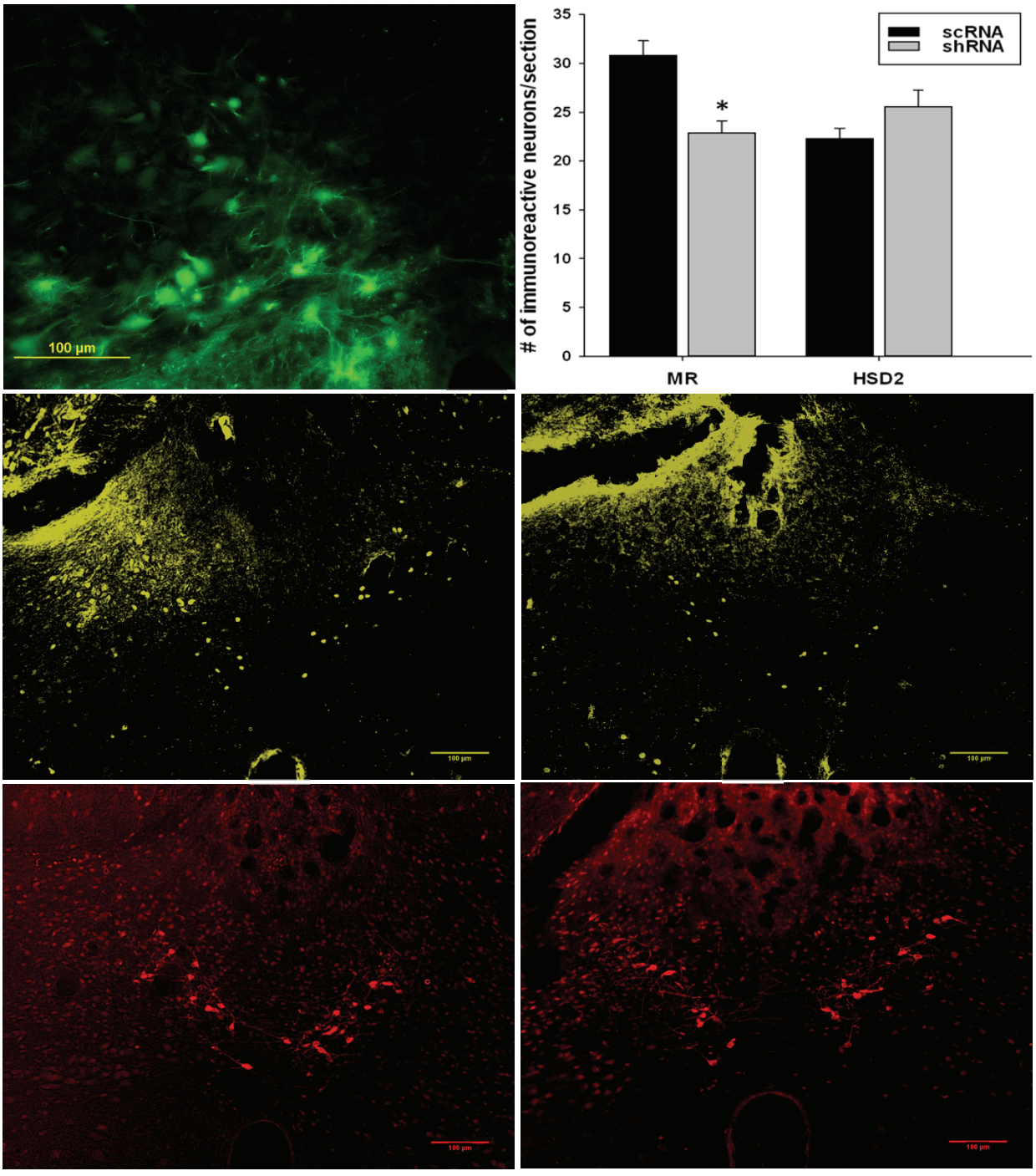
100 µm
# of immunoreactive neurons/section
35
30
25
20
15
10
5
0
scRNA
shRNA
*
MR
HSD2

Figure 3: Expression of GFP (A), MR (C and D) and HSD2 (E and F) immunoreactivity in NTS of respective groups.

A. Expression of GFP in the NTS of a scRNA injected rat, indicating successful transfection of neurons with the viral construct.

B. Mean number of MR immunoreactive (left bar graph) and HSD2-immunoreactive (right bar graph) NTS neurons per section in scRNA and shRNA injected rats.

C. Section showing pseudo yellow colored MR immunoreactive neurons in the NTS of a scRNA injected rat. The majority of MR immunoreactivity is nuclear.

D. Section showing pseudo yellow colored MR immunoreactive neurons in the NTS of a shRNA injected rat. Number of MR immunoreactive neurons were less when compared to image in C.

E. Section showing pseudo red colored HSD2 immunoreactive neurons in the NTS of a scRNA injected rat. They lie in same region as neurons demonstrating MR immunoreactivity.

F. Section showing pseudo red colored HSD2 immunoreactive neurons in the NTS of a shRNA injected rat

cc = central canal; scale bars = 100 μm. Asterisk denotes $p < 0.05$.